Moonlighting and mimicry: Identification and functional characterization of a SAM-dependent methyltransferase responsible for methylation of EF-Tu in *Pseudomonas aeruginosa*

Joshua Phillip Owings
Baltimore, MD

Bachelor of Arts, St. Mary's College of Maryland, 2006
Master of Biological and Physical Sciences, University of Virginia, 2012

A Dissertation presented to the Graduate Faculty of the University of Virginia in Candidacy for the Degree of Doctor of Philosophy

Department of Microbiology, Immunology, and Cancer Biology
University of Virginia
July 2014

Joanna B. Goldberg

David Brautigan

Dean Kedes

Robert Nakamoto

Abstract

Phosphorylcholine (ChoP) is a charged molecule that, in humans, is the major recognition component of platelet activating factor (PAF) by its cognate receptor, platelet activating factor receptor (PAFR). ChoP-like molecules have been detected on the surfaces of numerous respiratory pathogens where they confer persistence related phenotypes mediated through an increase in adhesion. *Pseudomonas aeruginosa* is a Gram-negative opportunistic pathogen which is often associated with nosocomial pneumonia. Previously, in *P. aeruginosa* a ChoP-like modification was detected using ChoP-specific antibodies on surface exposed elongation factor-Tu (EF-Tu), a normally cytoplasmic protein involved in protein chain elongation. Here we identify a gene, *eftM*, which is required for the modification of EF-Tu. To our surprise, mass spectrometry analysis of modified EF-Tu revealed the modification was not ChoP but rather trimethyl-lysine at amino acid residue 5. This trimethyl-lysine acts as a structural mimic of ChoP and confers similar phenotypes to *P. aeruginosa* as ChoP does to other respiratory pathogens. Bioinformatic analysis of EftM showed amino acid sequence similarity to *S*-adenosylmethionine (SAM)-dependent methyltransferases. We confirmed biochemically that EftM is able to bind SAM and used it to directly methylate lysine 5 of EF-Tu both *in vivo* and *in vitro*. Mass spectrometry analysis of products from these reactions confirmed that EF-Tu is trimethylated at lysine 5. *In vivo*, *P. aeruginosa* methylates EF-Tu only at temperatures closer to ambient, 25°C, and not at body temperature, 37°C. We show that this temperature-dependent methylation phenotype is not due to differences in transcription of *eftM*. The methyltransferase activity of the laboratory *P. aeruginosa* strain PAO1 EftM is slightly higher at 25°C compared to 37°C, while the rate of

degradation of EftM expressed in *P. aeruginosa* is significantly decreased at 25°C compared to 37°C allowing for a longer half-life of the protein. The difference in the rate of degradation suggested an increase in protein stability at 25°C and was confirmed by heat pre-treatment of EftM *in vitro*. Pre-incubation of EftM at 37°C abolished methyltransferase activity while methyltransferase activity was retained when the enzyme was pre-incubated at 25°C. In the absence of evidence for transcriptional regulation of this phenomenon, these results may suggest that the *in vivo* temperature-dependent phenotype is due to differences in the steady state levels of the EftM protein at different temperatures.

In this work, we have discovered a modification that mimics a known bacterial adhesin in respiratory pathogens. It is possible that the ChoP-like modification seen in other respiratory pathogens is actually trimethyl-lysine, the addition of which could be mediated by a methyltransferase similar to EftM. The identification and characterization of EftM could have broad implications for both basic and applied biology. These include the potential identification of a novel export pathway of a normally cytoplasmic protein and insight into the bacterial regulation of protein synthesis. Additionally, the enzyme responsible for the methylation of EF-Tu may be a good target for novel therapeutics to prevent the establishment of respiratory infections.

Dedication

For my parents, Gary and Ginette Owings, w**h**o provided me with a wonderful education and never let me give up when the times got t**o**ugh. For my father, Robert Lewis Hirschfeld, who I kn**o**w has been guiding me since his passing and whose scientific spirit lives on in me. For all of my grandparent**s** (George, Fernande, Wayne, and Phyllis) who have all had a huge impact on my life by teaching me the true meaning of determination, spoiling me to no end, and supporting me in all that I have done. Lastly, to my entire family both Hirschfelds and Owings, I thank you for putting up with me being a perpetually broke student. I love all of you very much and would not be where I am today without everything each of you has done for me. This achievement belongs to all of you as much as it does to me.

Acknowledgements

I would like to thank my mentor Joanna Goldberg for the enormous amount of support she has provided me over the last seven years. She has been a great mentor, colleague, and friend that has provided me with excellent training and advice in all aspects of my life. She truly cares about all of her students and it has been a pleasure to become a part of her scientific family. In regards to her scientific family, I would also like to thank both past and present Goldberg lab members: Erica Kintz for convincing me that the Goldberg lab was the right place for me, Mike Davis for politely answering probably thousands of questions over the years, Preston Garcia and George Liechti for making sure there was never a dull moment in lab, Brian Hall for all of the farm parties and bike help, Heath Damron for all of his scientific advice and doing his best to both get me into and keep me out of trouble, Beth McKenney, Dina Moustafa, and Laura Gonyar for being excellent lab mates and some of the nicest people I know, and Mariette Barbier for laying the groundwork for my entire project. As for recent members, I can hardly overstate how much all of the recent members have been involved in my life both personally and professionally. Sarah "Cutie Patoutie" Fankhauser, Jeff "Maverick" Meisner, Sam "Lil' Sis" Prezioso, and John "Lab Police" Varga have all been amazing lab mates and kept me sane during my time here in Atlanta. I also need to thank my current and past committee members: David Brautigan, Alison Criss, Ian Glomski, Dean Kedes, and Bob Nakomoto. If only I had listened to everything that was brought up during my qualifying exam maybe I would have finished up everything a little sooner.

It would be remiss not to mention the plethora of friends I have met along this journey both in Charlottesville and Atlanta. To my Atlanta friends, I want to thank you for not letting me quit…even though I was closer than most people think. To all of my Charlottesville friends, I want to say that the last 7 years have been some of the most fun and fulfilling of my life. I want to single out Lindsay Yowell in particular for being the best roommate and friend anyone could ever ask for. You and the Brown Dog have been through all of the best and worst times of my life for the last 7 years. You have listened to WAY too many of my scientific practice talks, helped me with photoshop, made sure I was always having a fun time and of course Killer was always there to give me kisses and snuggle (as evidenced by the numerous pictures of me and her "napping" together).

Lastly, I want to than my wonderful and talented girlfriend Jessica Jaglois who has put up with me throughout this whole process for the last three years. I'm very lucky to have you in my life and can't wait to ride your coat tails when you are a famous reporter. All in all, I can't wait to see what the future brings as Dr. Owings!

Table of Contents

Abbreviations

CF – Cystic Fibrosis

CFTR – Cystic Fibrosis Transmembrane Conductance Regulator

ChoP – Phosphorylcholine

CRP – C-Reactive Protein

DMG – Dimethyl Glycine

EF-Tu – Elongation Factor Tu

Fn - Fibronectin

GDP – Guanosine diphosphate

GTP – Guanosine triphosphate

GB – Glycine Betaine

LPS – Lipopolysaccharide

LOS – Lipooligosaccharide

NHS – Normal Human Serum

PAF – Platelet Activating Factor

PAFR – Platelet Activating Factor Receptor

PC – Phosphatidylcholine

SAM – *S*-adenosylmethionine

SM – Sphingomyelin

TLR – Toll-like Receptor

TNF – Tumor Necrosis Factor

Chapter One

Introduction

Pseudomonas aeruginosa: Pathogenesis and virulence factors

Pseudomonas aeruginosa is a Gram-negative, environmental bacterium that causes opportunistic infections in patients with compromised immune systems such as those with cancer, HIV, cystic fibrosis (CF), and serious burn. It primarily infects the respiratory tract of these patients, and ranks as the second most common cause of ventilator-associated pneumonia in the United States. *P. aeruginosa* is the leading cause of morbidity and mortality in patients with CF (3), the most common autosomal recessive genetic disease in Caucasians caused by dysfunction of the CF transmembrane conductance regulator (CFTR) in the airway epithelium, leaving patients susceptible to infection (3). Infections of CF patients by *P. aeruginosa* generally arise as recurring acute infections that eventually become clonally derived chronic infections (4). By age 3, 97% of children with CF are chronically colonized with *P. aeruginosa*; these infections are extremely difficult to treat due to their natural resistance to many antibiotics (3, 5). This resistance is due to many factors including the low permeability of its outer membrane, multidrug efflux pumps, the presence of antibiotic inactivating enzymes, as well as hypermutator phenotypes which allow the bacteria to accumulate mutations very quickly (6-8).

The *P. aeruginosa* genome encodes a host of virulence factors which contribute to its pathogenicity. These virulence factors include flagella and type 4 pili, a type 3 secretion system, quorum sensing systems, secreted proteases and other factors, and lipopolysaccharide (LPS) (9). When the bacteria transition from an acute to chronic

infection, a plethora of virulence factors are down-regulated while other factors are up-regulated including alginate and adaptation to a biofilm mode of growth, all of which presumably allow the bacterium to evade the host immune system. This clinically important pathogen has a relatively large genome, 6.22 to 6.91 Mb (8), compared to other bacterial pathogens. This large complex genome contains many genes of unknown and unique function, which is likely due to selective pressure to adapt to its usual niches as an environmental bacterium (10). Included in the genome are a vast number of metabolic genes, including a large number of regulatory proteins that provide the *P. aeruginosa* with an incredible level of metabolic flexibility, affording it the ability to survive in extreme conditions (8, 10).

Many of these virulence factors can play a role in the first steps to a successful infection, which include gaining entry to a host and adhering to a target tissue, allowing colonization of the host. Bacteria have developed various means to facilitate adherence to their target tissues, such as the use of adhesins (11). Some of the most well-characterized adhesins that *P. aeruginosa* possesses are pili/fimbria, flagella, type III secretion systems, LPS, and other molecules which recognize various host surface molecules (11). Host molecules such as fibronectin (Fn), a ubiquitous eukaryotic extracellular matrix glycoprotein, are recognized by many types of bacteria to facilitate adhesion and invasion (12, 13). The known host receptor platelet activating factor receptor (PAFR) recognizes the expression of phosphorylcholine (ChoP) on bacterial surface structures. This host mimicry facilitates adhesion and invasion of the airway epithelium by these pathogens (14-19).

Phosphorylcholine (ChoP) in pathogens

ChoP is a zwitterionic molecule at neutral pH that is a common modification found in eukaryotic cells. It is linked to lipids to form phosphatidylcholine (PC), a phospholipid that is a major component of the eukaryotic plasma membrane (Figure 1.1). ChoP is also a major component of the host molecule platelet activating factor (PAF) (20, 21). PAF is a glycerophospholipid produced by many cell types in humans, including platelets, endothelial cells, macrophages and neutrophils (Figure 1.1). It plays an important role in proinflammatory responses to bacterial infections mediated through its binding to PAFR which is expressed on many different cell types (22). PAF binds to its cognate receptor via an exposed ChoP moiety which induces stimulation and degranulation of granulocytes, monocytes, and macrophages, as well as the release of inflammatory cytokines and toxic oxygen metabolites (23).

Recently, it has been appreciated that a large number of human pathogens express ChoP moieties on various surface structures. ChoP was first discovered to be associated with the teichoic and lipoteichoic acids of the *Streptococcus pneumoniae* cell wall (24). This discovery led to further study of this epitope on other microbes and subsequent detection of ChoP on a range of both Gram-positive and Gram-negative bacteria, as well as numerous eukaryotic pathogens including protozoa, fungi, and filarial nematodes. In most of these organisms, the ChoP moiety is associated with structural glycans or glycolipids (25, 26). The first exception to this was found in pathogenic *Neisseria*, *N. meningitidis* and *N. gonorrhoeae*, which express ChoP on their pili (fimbriae) (26, 27).

Their commensal counterparts also express ChoP but it is linked to their lipopolysaccharide (LPS) (27), providing evidence that ChoP can have distinct properties based upon the structure that is modified (27, 28). The mechanism for this difference in function has yet to be elucidated. More recently, ChoP has been found on another protein, outer membrane porin D, in the pathogen *Acinetobacter baumannii* where the modification facilitates similar functions to those seen in other respiratory pathogens as described below (29).

Costs and benefits of ChoP modification

The prevalence of ChoP on a large number of respiratory pathogens is striking, leading to the possibility that it may be a common motif used by these pathogens to survive in the respiratory tract. *Haemophilus influenzae* is an excellent model organism to study ChoP due to the genetically-tractable phase-variation in expression of ChoP on its lipooligosaccharide (LOS). *H. influenzae* ChoP expression is regulated by multiple tandem repeats of 5'-CAAT-3' in the 5' region of the choline kinase gene *licA*, allowing the bacteria to quickly adapt to the environment; the same genetic regulation of ChoP is seen in commensal *Neisseria* (1, 27, 30). Isogenic mutants of ChoP$^+$ strains can be made by deleting *licD*, a ChoP transferase, rendering the strain ChoP$^-$. *In vitro* studies have shown that ChoP$^+$ variants of *H. influenzae* adhere to epithelial cells better than isogenic ChoP$^-$ mutants. Furthermore, this ability to adhere can be competitively inhibited by the addition of PAFR antagonists or PAF itself (16). The importance of ChoP adherence can be recapitulated *in vivo* where ChoP$^+$ variants show increased persistence in mouse lungs compared to isogenic mutants lacking ChoP (31). It is, therefore, believed that the

presence of ChoP on these organisms is an important mechanism allowing them to adhere to and colonize the respiratory epithelium.

Studies have also shown that ChoP expression on the bacterial surface can confer resistance to some host derived antimicrobials, the best known of which are the β-defensins. The β-defensins as well as hCAP18, a member of the cathelicidin family, have been isolated from the upper and lower respiratory tracts of humans. These positively charged peptides are thought to preferentially target bacterial cells because of their negatively charged membranes. Studies using *H. influenzae* have demonstrated that ChoP content increases in a dose dependent manner in response to treatment with the cationic linear antimicrobial peptide LL-37; indicating that ChoP provides a selective advantage for survival (32) likely by altering the overall surface charge of the bacterial membrane to be less negative.

As important as ChoP may be for colonization of the respiratory tract, the presence of ChoP on the bacterial surface is a double edged sword. Numerous studies have shown that while ChoP confers some survival advantages to the microbe such as increased persistence (33) and resistance to host derived antimicrobial compounds (32), it also has some disadvantages such as increased sensitivity to serum (33) which can ultimately lead to clearance of the bacteria. It has been shown that ChoP is the principal ligand for C-reactive protein (CRP), one constituent of normal human serum (NHS) which increases in concentration up to 1000-fold in response to tissue injury or inflammation. No deficiencies in CRP exist in humans, suggesting it is absolutely critical for human

survival (21, 34). CRP has the ability to protect the host via multiple pathways. It can opsonize bacteria by binding with the complement factor C1q, thereby allowing it to bind phagocytic cells via the C1q receptor or binding to the IgG Fc receptors. It also activates the classical pathway of complement via interaction with C1q (35). Binding of CRP to $ChoP^+$ bacteria *in vitro* has been shown to be an effective means of complement-mediated killing with both *H. influenzae* (Figure 1.2) and pathogenic piliated *Neisseria* (33, 34, 36). Thus, while providing the benefits of increased adhesion and colonization, the expression of ChoP by many pathogens leaves them vulnerable to serum-mediated killing by CRP.

Recently it has been shown that ChoP plays a very different role for intracellular bacteria. The intracellular pathogen *Legionella pneumophila* secretes a ChoP transferase, AnkX, via the Dot/Icm type IV transporter system, that then reversibly phosphorylcholinates the host GTPase Rab1 (37). Along with the dephosphorylcholinase Lem3, this system is proposed to mirror GTP/GDP exchange systems seen in human cells (38). When Rab1 is phosphorylcholinated, it prevents the formation of endosomes and provides a survival advantage for *L. pneumophila* (39).

ChoP can also be used by pathogens to modulate the global host immune response such as seen in filarial nematodes. The adaptive immune response has been shown to be affected by ChoP-containing molecules. Filarial nematodes as well as human placenta express surface and secreted proteins containing ChoP that attenuate the host adaptive immune response (20, 40). Individual nematodes within human hosts can survive for 5 or

more years, indicating they possess some means to evade or repress the host immune system. Patients infected with filaria have significant anti-ChoP antibody responses. *In vivo* models have shown that high concentrations, 25-50μg/mL, of ES-62, a secreted ChoP-containing filarial protein, results in significant activation of B cells (41). However, when physiologically relevant concentrations of ES-62 are used in mouse models, 10-100-fold less than the *in vivo* model described above, the result is the prevention of B cell proliferation (41)**.** When this experiment is repeated using ChoP conjugated to bovine serum albumin (BSA), the ability of recovered B cells to become activated via the B cell receptor (BCR) is reduced (42). ChoP also skews the T cells response towards a Th2 response, which results in dendritic cells and T cells producing more IL-4 and IL-10 while producing less IFN-γ. The end result is prevention of class switching to protective IgG2a antibodies, prevention of a protective Th1 response and induction of B and T cell anergy (20, 43). This may not only be beneficial to the parasite but may also protect the host from generating a damaging immune response.

H. influenzae also uses ChoP modification of its LOS to modulate the host innate immune response. The lipid A portion of LOS is recognized by Toll-like receptor 4 (TLR4) (44), which mediates a strong inflammatory response responsible for protection against *H. influenzae* in airway infections (45). It has been shown that purified LOS that is ChoP-modified ($ChoP^+$) is about 100-fold less bioactive than unmodified LOS. This means that $ChoP^+$ LOS generates a weaker inflammatory response compared to LOS without ChoP, including a decrease in the release of nitric oxide and TNF-α from

macrophages (46). This muted inflammatory response allows the ChoP$^+$ bacteria to persist longer than those not expressing ChoP.

Interestingly, in *H. influenzae*, phase-variation of ChoP on LOS favors an increase in ChoP$^+$ bacteria compared to ChoP$^-$ bacteria within biofilms from *in vivo* infections (46). However, there has been some contradictory evidence about how ChoP affects the ability of *H. influenzae* to form biofilms (46, 47). Currently, there is strong *in vitro* and *in vivo* evidence that strains with the ChoP phenotype "locked on" produce biofilms with significantly higher biomass and thickness than both the parent strain and an isogenic strain that is unable to incorporate ChoP into its LOS (48). In the *in vivo* chinchilla model of otitis media (middle ear) infection, while the ChoP$^+$ mutant was able to form more robust biofilms, it also had a significant survival defect in planktonic growth as seen by decreased colony counts from middle ear fluids. This difference is likely due to sensitivity to complement or other host factors in the planktonic form compared to the biofilm mode of growth (48). This difference underscores how ChoP can be beneficial in some circumstances while still creating significant costs to the organism in other conditions.

It is apparent that we have yet to fully understand the role and impact of ChoP in the context of pathogens. The presence of this molecule provides benefits in the context of certain host environments such as increased adhesion, protection from β-defensins, and the ability to attenuate an adaptive immune response. There are also distinct disadvantages including an increased sensitivity to serum which mediates killing through

CRP. This complicated dynamic relationship between ChoP, pathogens, and their eukaryotic hosts will remain an important area of research in the future.

Choline metabolism in *Pseudomonas aeruginosa*

P. aeruginosa can be grown in large varieties of nutrient poor/limiting conditions due to its high degree of metabolic versatility and diversity. This is partly due to the large number of regulatory genes encoded in its genome, nearly 10% of its genome, which have been shown to correlate with increased ability to survive in diverse environments (8). One molecule that can be used as a sole carbon, nitrogen or carbon and nitrogen source by *P. aeruginosa* is choline. Studies have shown that *P. aeruginosa* can metabolize choline and incorporate the *N*-methyl groups into fatty acids through the generation of acetyl-CoA and also utilize the carbon backbone to synthesize glycerol (49).

As useful as choline is to *P. aeruginosa*, it cannot synthesize choline *de novo*. To meet its nutritional requirements using choline as an energy source, *P. aeruginosa* contains a scavenging pathway to catabolize host phosphatidylcholine (PC) and sphingomyelin (SM) by using hemolytic phospholipase C (PlcH) (50). Once this enzyme acts, free phosphorylcholine (ChoP) is generated which can then be transported into the cell using multiple known and putative choline transporters, including two choline symporters, BetT1 and BetT3, and the ABC transporter CbcXWV (51). In the periplasm ChoP is dephosphorylated by phosphorylcholine phosphatase (PchP) to form choline (52), that is

then transported into the cytoplasm where it can then be further metabolized to glycine betaine (GB), dimethylglycine (DMG), sarcosine, and glycine (Figure 1.1) (49, 53, 54).

P. aeruginosa is one of a growing number of bacteria known to contain phosphatidylcholine (PC) as a component of its membrane. PC can be synthesized in *P. aeruginosa* by phosphatidylcholine synthase (Pcs) which acts by condensing cytidine 5'-diphospho(CDP)-diacylglycerol with choline (55). Also encoded in the genome is phospholipid *N*-methyltransferase (PmtA), which methylates phosphatidylethanolamine to form PC; however, it is believed that this gene is non-functional in *P. aeruginosa* (55).

ChoP-like modification in *P. aeruginosa*

Studies by Weiser *et al.* of the well-characterized *P. aeruginosa* laboratory strain PAO1 have shown that antibodies against ChoP reacted with a 43 kDa protein that was expressed at ambient temperatures (25^{o}C) but not at body temperature (37^{o}C) (Figure 1.3) (28). The temperature-dependent phase variation of the ChoP-like epitope is seen not only in laboratory strains but also in clinical isolates. Acute and chronic isolates however do not display similar degrees of this phase variation phenotype. Acute infection isolates display a normal temperature-dependent phase variation phenotype while chronic infection isolates display a higher ratio of ChoP-like expression at 37°C compared to 22°C (Figure 1.4) (18). The 43 kDa protein which displayed reactivity with the ChoP monoclonal antibody TEPC-15 was identified by mass spectrometry as the bacterial protein elongation factor Tu (EF-Tu) (18).

EF-Tu 'moonlighting' roles

EF-Tu is a surprising virulence factor as it is an essential protein whose traditional role is in transporting aminoacyl-tRNAs to the ribosome to facilitate protein chain elongation (56). However, it is becoming increasingly apparent that EF-Tu performs other functions in cells aside from its canonical role in protein chain elongation. These additional functions, termed 'moonlighting roles', for EF-Tu include chaperone-like properties involved in the bacterial stress response (57), initiation of Qβ phage replication, an as yet unknown function in the presence of high iron (58), and through its localization to the bacterial surface, involvement in adherence to numerous proteins and host factors (12, 18, 19, 59-63). The localization of EF-Tu to places other than the cytoplasm has been seen in a number of other bacteria, including in the cell wall of *Mycobacterium leprae*, the membrane of *Mycoplasma pneumoniae* and *Escherichia coli*, as well as the periplasm of *Neisseria gonorrhoeae* and *E. coli* (12, 64).

EF-Tu has two putative transmembrane domains, and in *M. pneumoniae* has been shown to be an integral membrane protein through membrane fractionation, the C-terminal of which is able to bind to the host factor Fn (12). Similarly, EF-Tu in *Lactobacillus johnsonii* and *Listeria monocytogenes* have been shown to bind mucin and fibrinogen, respectively (61, 62). In *P. aeruginosa*, EF-Tu has been shown to be associated with the outer membrane (Figure 1.5) and has the ability to bind Factor H and plasminogen as a means of evading the host immune system. Factor H is a fluid-phase regulator of the alternative complement pathway. A common strategy of complement evasion is the binding of Factor H, which works by promoting cleavage of C3b by the serine protease

Factor I, thus, accelerating decay of the alternative pathway C3 convertase C3bBb. In addition to Factor H, *P. aeruginosa* EF-Tu can simultaneously bind the zymogen plasminogen which is the precursor to plasmin, an enzyme that catalyzes fibrin degradation and aids in tissue invasion (63).

Modification of elongation factor Tu (EF-Tu)

Elongation factor Tu (EF-Tu) is a GTPase which is involved in the elongation of protein chains. When bound to GTP, EF-Tu forms a complex with aminoacyl-tRNA (aa-tRNA) and shuttles it to the A-site of the ribosome (65). Once the appropriate codon-anticodon match is found, the GTPase activity of EF-Tu is activated and rapid hydrolysis of GTP to GDP occurs. This hydrolysis causes a conformational change in EF-Tu causing it to dissociate from the ribosome. Next, the nucleotide exchange factor EF-Ts replaces GDP with GTP allowing the interaction with another aa-tRNA to repeat the cycle (66).

EF-Tu is one of the most abundant cytoplasmic bacterial proteins, representing 5-10% of total cellular protein and 10-fold molar excess over ribosomes (65). This makes sense when the traditional function of EF-Tu is taken into account as EF-Tu must be able to bring free aa-tRNAs to all ribosomes that are actively translating mRNA. Many but not all bacteria have two copies of this very important gene, including *P. aeruginosa* whose genome encodes *tufA* and *tufB*. Early studies showed that EF-Tu has the ability to be modified in a number of ways including phosphorylation and methylation (65).

EF-Tu is known to be phosphorylated in *E. coli* at threonine 382 by the kinase P1 Doc, which is part of the P1 *phd-doc* toxin-antitoxin system (67, 68). Only about 5-10% of the cellular EF-Tu has been shown to be phosphorylated (69). As the threonine side chain is shielded when EF-Tu is bound to GTP and aa-tRNA, the phosphorylation occurs just after GTP hydrolysis. This modification then inactivates EF-Tu by preventing the binding of aa-tRNA. It was originally postulated that the enhanced affinity of phosphorylated EF-Tu to EF-Ts, the nucleotide exchange factor, promoted quick GDP dissociation and nucleotide exchange thus recycling EF-Tu and allowing it to bind another aa-tRNA (65). New evidence suggests that when the *phd-doc* system is induced, a greater fraction of EF-Tu is phosphorylated than the usual 5-10%. This would lead to a stalling of translation which would allow the bacterial cell to remain in a dormant state where it is resistant to antibiotics targeting the translational machinery (68).

The most well studied post-translational modification of EF-Tu is methylation on lysine 56 in *E. coli* (70). This amino acid position is extremely well conserved in both prokaryotes and eukaryotes and is present as either a lysine or arginine, both of which can be methylated. It has been shown that during logarithmic growth phase lysine 56 is mono-methylated. As the cells transition to stationary phase there is a gradual decrease in monomethyllysine and concurrent rise in the amount of dimethyllysine (71). While methylation of EF-Tu at lysine 56 does not significantly alter its interaction with GTP, GDP, EF-Ts, or aa-tRNA, there is a twofold decrease in GTP hydrolysis (71). It is hypothesized that *in vivo*, methylation of EF-Tu prolongs the interaction of EF-Tu-GTP-aa-tRNA complex with the ribosome leading to an increase in translational accuracy (65,

71). Up to this date, the enzyme responsible for the methylation of EF-Tu in *E. coli* is unknown.

A recent study has examined the kinetics of *P. aeruginosa* EF-Tu both in the presence and absence of the nucleotide exchange factor EF-Ts (72). This was studied using *in vitro* assays with recombinant proteins expressed in and purified from *E. coli*. It was shown that *P. aeruginosa* EF-Tu has about a 6-fold higher affinity for GDP than for GTP where in *E. coli* that difference is 100-fold (72). They also showed that in the presence of EF-Ts, the affinity of EF-Tu for GDP was shifted significantly such that EF-Tu could function in significantly lower concentrations of GDP. They also developed an aminoacylation/translation system to monitor the functionality of *P. aeruginosa* EF-Tu during protein synthesis. It would be interesting to see if the use of EF-Tu with the ChoP-like modification in these *in vitro* assays affects any of the kinetic measurements seen by Palmer *et al*. (72).

SAM dependent methyltransferases

The methylation of biologically active molecules, such as EF-Tu, changes their physical properties and has broad effects on many biological functions (73). Perhaps the best known role for methylation has been the growing field of epigenetics in which methylation of histones or DNA can lead to gene silencing or activation. In prokaryotes, the restriction-modification system (RM system) has been extensively studied and provided us with many molecular tools used today. The RM system involves the methylation of bacterial DNA, which protects DNA from restriction endonucleases that

cleave unmethylated DNA at specific sequences (74). This allows the bacterium to distinguish between self DNA and that of invaders such as bacteriophage. Methylation is not confined to DNA, many substrates can be methylated: including small molecules, lipids, and proteins. Another well studied system that involves methylation is the chemosensory pathways of which there are four present in *P. aeruginosa* (75, 76). In these pathways, a methyltransferase such as CheR methylates a chemoreceptor which then modulates the ability of the receptor to autophosphorylate and regulate chemotaxis in response to the stimulant (75). The atoms targeted for methylation are also diverse and include nitrogen, oxygen, carbon, sulfur, and halides (77). It has become increasingly evident that methylation is a common modification used by all types of cells to control many cellular processes.

The molecule most often used as a methyl donor for the modification of such a large variety of substrates is *S*-adenosylmethionine (SAM) due to the favorable energetics of the reaction (77). SAM is the second most commonly used enzyme substrate after ATP (78) and is found in relatively large concentrations in *E. coli*, 184 μM-1.1 mM (79). It is the superfamily of SAM-dependent methyltransferases that is responsible for the transfer of methyl groups from SAM to the large variety of targets discussed earlier.

With the ability to modify such a large variety of substrates, this superfamily of enzymes is an interesting case of convergent evolution. Most of the enzymes in this superfamily share very little amino acid sequence identity, with the exception of a few sequence motifs. Even residues important for binding of SAM are poorly conserved. However,

when the tertiary structure is examined, it becomes clear that the structures within this superfamily fall broadly into five structural classes (class I-V) (Figure 1.6). The architecture between the classes is highly divergent while the core folds within each class are highly conserved (73, 77).

Even with structural similarity, there is still great diversity within the different classes. For example, within the Class I methyltransferase (MTases) there is no single way in which SAM is activated to transfer its methyl group, though all these MTases catalyze the in-line transfer of the methyl group at the S-CH_3 of SAM to the target substrate (77). The substrate binding regions also vary greatly within the classes, with each protein containing unique embellishments outside of the core domain to facilitate binding of their specific substrates. If the target is a protein, the amino acids to be methylated will likely be arginine or lysine. Both arginine and lysine are able to be methylated multiple times, with both being able to be mono- or dimethylated, and lysine being able to be trimethylated at the terminal amines.

DNA mismatch repair system-deficient mutator (hypermutator) strains

DNA replication is necessary for cell division to occur and while mutations do occur, cells contain machinery to maintain the fidelity of the copied DNA. This system is referred to as the mismatch repair system and the process itself is conserved between eukaryotes and prokaryotes. In prokaryotes, the proteins involved in this process are termed mutator or “mut” genes because when they are inactivated the frequency of mutations is significantly increased.

In *P. aeruginosa*, it is known that strains isolated from chronically infected patients undergo phenotypic changes which are often caused by the mutation of virulence genes. The resulting phenotypic changes include gain of mucoidy, loss of LPS O-antigen, quorum sensing and motility, and increases in mutation rate. High proportions of chronic infection isolates have mutations in *mutS* (40%) and *mutL* (60%) which cause the strains to have about a 2-log higher mutation frequency (7). When other "mut" genes are interrupted in *P. aeruginosa* the phenotype can be greatly exaggerated with between 1.5 and 140-fold differences in mutation frequency compared to wild type PAO1 (80). These strains are termed hypermutator strains and have been linked to higher rates of multi-antibiotic resistance due to the increased rate of chromosomal mutations (81); however, it is likely that these strains have a generalized adaptive advantage that is not linked to any specific traits (7).

In the context of EF-Tu modification, chronic infection isolates tend to have relatively more modified EF-Tu at 37°C compared to acute infection isolates. Within these chronic infection isolates, strains with the highest ratio of modified EF-Tu at 37°C/25°C were hypermutator strains. However, the hypermutator phenotype was not itself associated with EF-Tu modification at 37°C indicating that it is not necessary for a strain to be a hypermutator to have a higher ratio of EF-Tu modification (18).

Concluding Remarks

To colonize the respiratory tract and evade the host immune system, *P. aeruginosa* utilizes many of the same techniques as other pathogens. The surface localization of EF-Tu to the bacterial membrane is not unique to *P. aeruginosa*, yet the mechanism by which it is transported to the membrane is still unidentified in any microbe. ChoP mediated adhesion to colonize and persist in the respiratory tract is a recurrent theme in respiratory pathogens. However, *P. aeruginosa* is unique in the temperature-dependent phase variation of a ChoP-like molecule; which is generated by unknown pathways not homologous to those found in *H. influenzae*. These recent studies allow us to propose a model of EF-Tu modification in *P. aeruginosa*. EF-Tu is modified when the bacteria is subjected to growth temperatures closer to what would be encountered in the environment (Figure 1.7). Once this pathogen encounters a host, modified EF-Tu assists the bacterium in adhering to and colonizing the respiratory tract. During acute infections when *P. aeruginosa* is exposed to warmer temperatures, EF-Tu is no longer modified. The control of this temperature dependent phenotype is still unknown. Similarly, the exact role of ChoP-like molecules in the virulence of *P. aeruginosa* during acute and chronic infection is also somewhat of a mystery that remains to be elucidated.

The purpose of the research contained within this thesis is to help answer some of these remaining questions. We have mapped the modification on EF-Tu and determined that it is not ChoP, but rather it is a structural mimic of that molecule that confers some of the same advantages of ChoP to *P. aeruginosa*. We have characterized some of the functions of this modification and how it affects the pathogenesis of *P. aeruginosa*. Not only have

we identified the gene involved in the addition of this ChoP-like modification but made significant progress as to how this enzyme works. I will propose a model of how temperature affects the modification status of EF-Tu and examine some of the enzymatic properties of closely related variants that give us more insight into to how temperature affects EF-Tu modification.

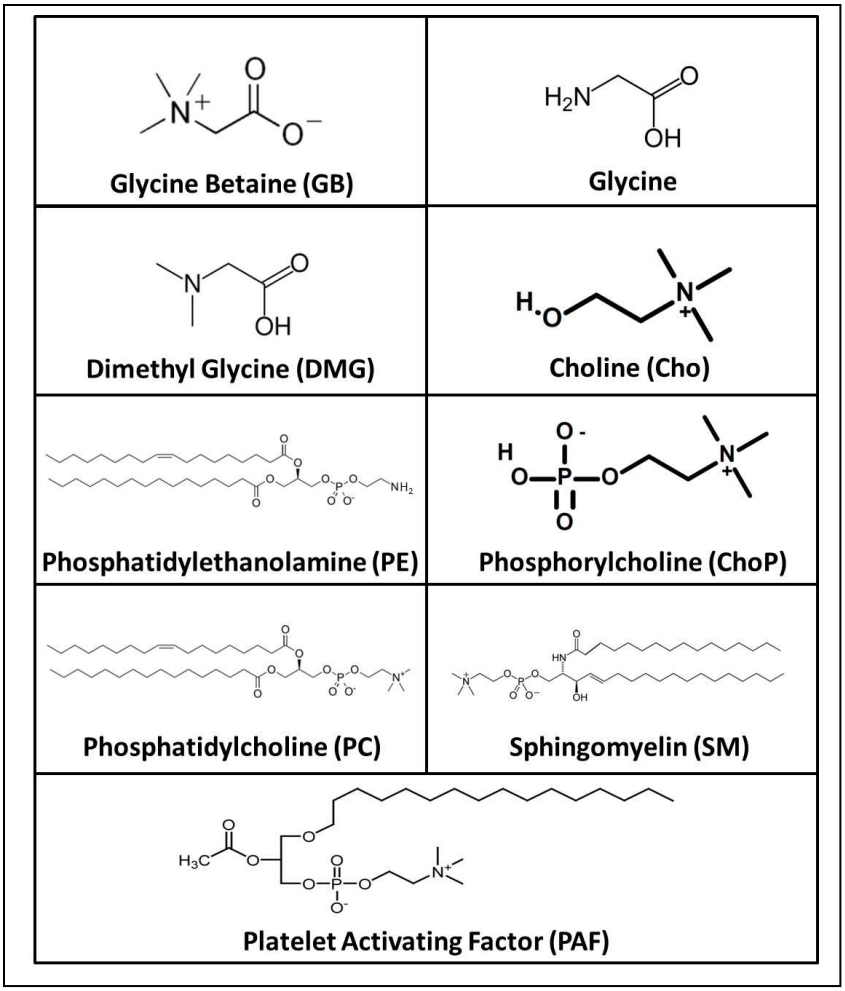

Figure 1.1. Compounds involved in choline metabolism and ChoP containing compounds.

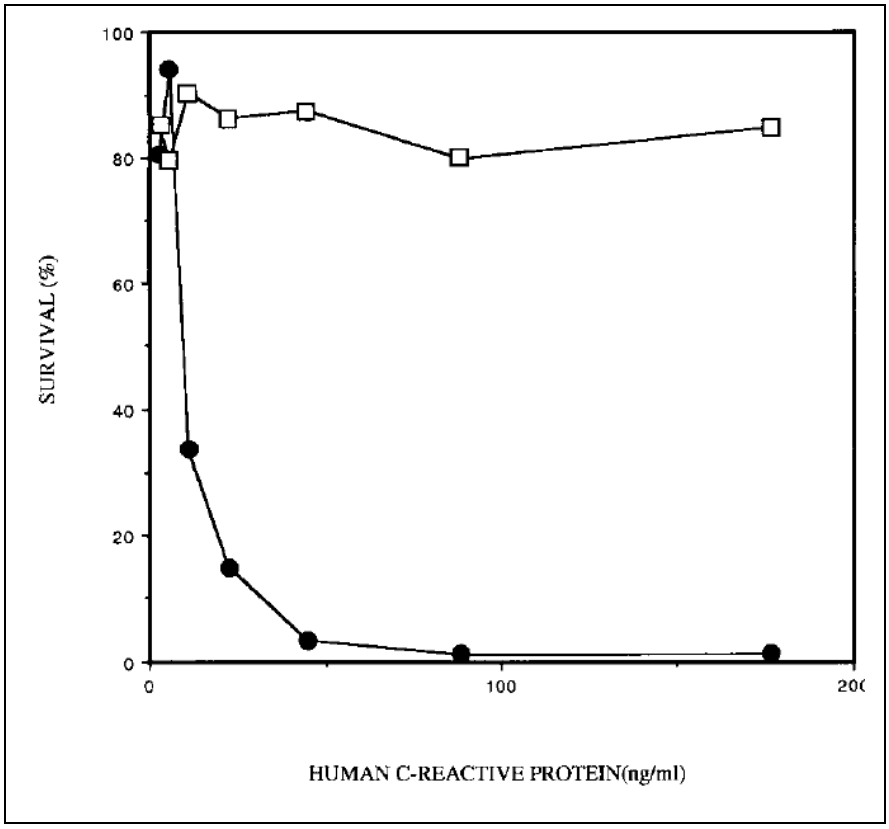

Figure 1.2. ChoP expression decreases *H. influenzae* survival in serum. The dose response to serum bactericidal assays of *H. influenzae* phase variants either expressing (solid circles) or not expressing (open squares) ChoP. Survival in 10% normal human serum (NHS) depleted of CRP with human CRP added back at indicated concentrations. Percent survival is compared to controls where complement was inactivated. Adapted from (33) and used with permission of Rockefeller University Press.

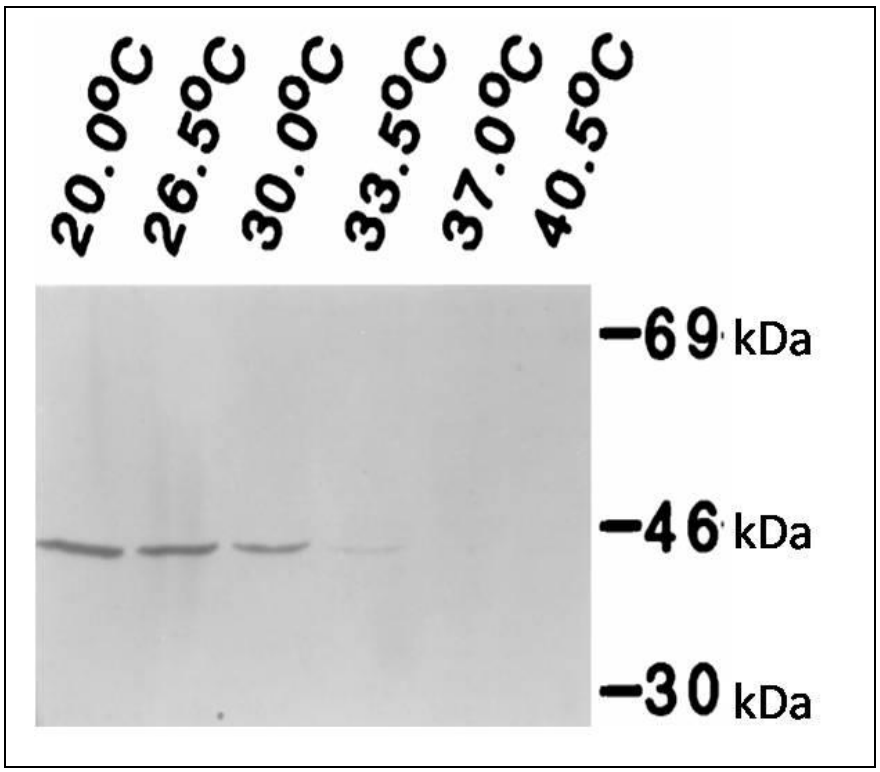

Figure 1.3. *P. aeruginosa* expresses ChoP-like molecule in a temperature dependent manner. Western blot using whole cell lysates from *P. aeruginosa* PAO1 grown to stationary phase at varying temperatures shows expression of ChoP on ~43 kDa protein. Adapted from (28) and used with permission of The American Society for Microbiology.

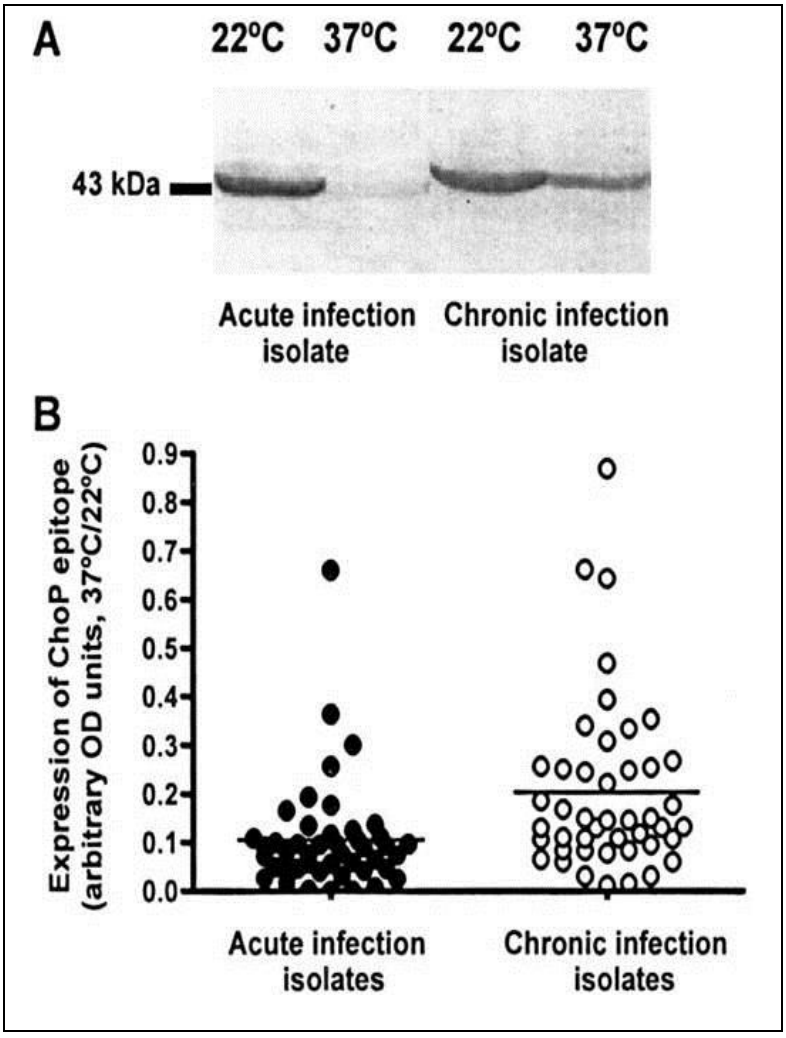

Figure 1.4. Expression of ChoP-like molecule among *P. aeruginosa* acute and chronic clinical isolates. (A) Representative Western blot of whole cell lysates from an acute and chronic isolate grown at 37°C and 22°C. (B) Densitometric analysis of expression of ChoP at 37°C and 22°C from acute and chronic clinical isolates. Adapted from (18) and used with permission of Oxford University Press.

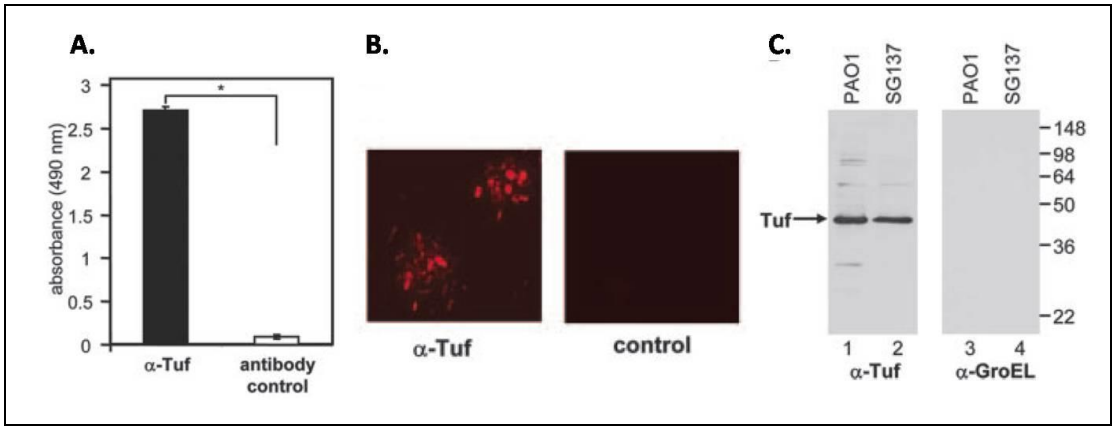

Figure 1.5. EF-Tu is on the surface of *P. aeruginosa*. (A) EF-Tu is detected at the surface of immobilized *P. aeruginosa* PAO1 using whole cell ELISA. Cells were immobilized on Maxisorp plates and detection of EF-Tu was done using polyclonal antiserum raised against recombinant EF-Tu. (B) Surface expression of EF-Tu on PAO1 as identified by immunofluorescence microscopy. Cells were incubated with a monoclonal anti-TufB antibody (left) and stained with AlexaFluor647-labeled secondary antibodies. The control (right) shows no reactivity of the secondary antibody in the absence of anti-TufB antibodies. (C) Surface proteins were biotinylated and purified by affinity chromatography in two different *Pseudomonas* strains, PAO1 and SG137. Purified proteins were separated by SDS-PAGE and Western blotted for the presence of EF-Tu using a monoclonal anti-EF-Tu antibody or the cytoplasmic chaperone protein GroEL using a polyclonal anti-GroEL antibody. EF-Tu was identified in the surface protein fraction in both *P. aeruginosa* strains while there was no observed cytoplasmic contamination of the purified proteins, as determined by the absence of GroEL. Adapted from (63) and used with permission. (Copyright 2007. The American Association of Immunologists, Inc.)

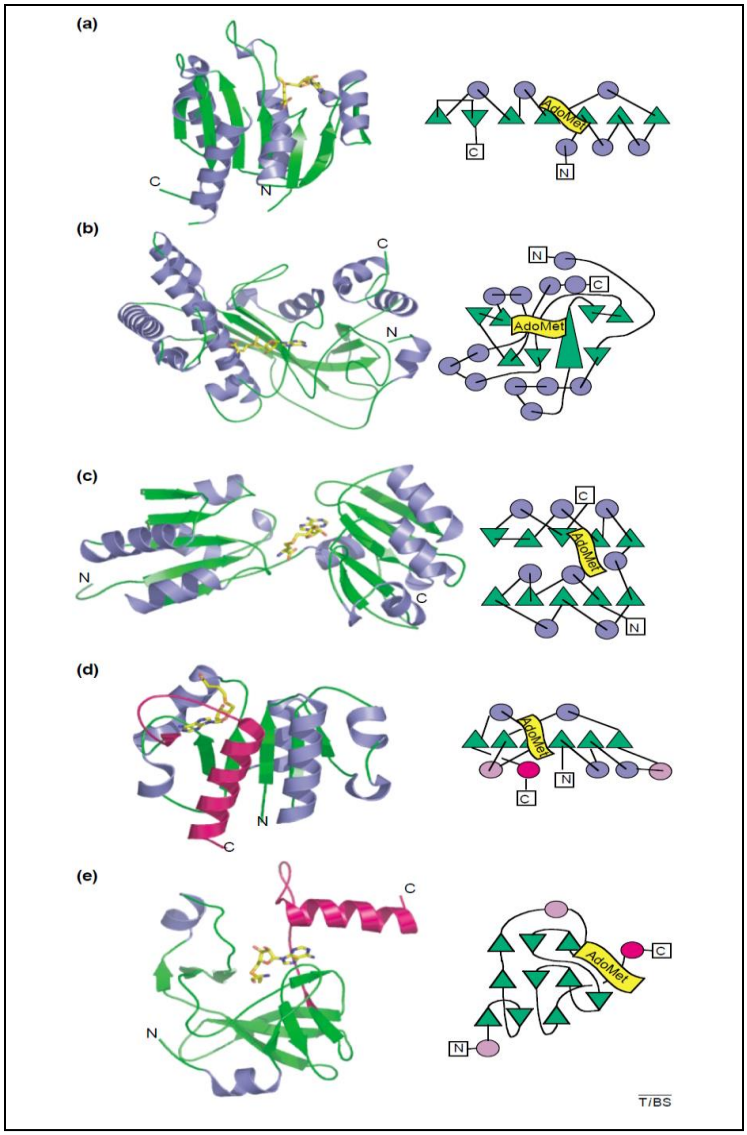

Figure 1.6. Classes of SAM-dependent methyltransferases. The tertiary structures of the five classes of SAM-dependent methyltransferases (MTases). In each case a representative tertiary structure (left) and topology diagram (right) is shown. (a) Class I: tertiary structures have been determined for >33 family members, most containing a seven-stranded β sheet flanked by α helices (enzyme: PDB code, M.HhaI:6MHT). (b) Class II: the reactivation domain of methionine synthase contains a series of long β strands and binds to AdoMet in a shallow groove on the surface of the domain

(MetH:1MSK). (c) Class III: the bilobal structure of CbiF contains an AdoMet-binding site between the two αβα domains, and a groove in the N-terminal domain is proposed to be the active-site cleft (CbiF:1CBF). (d) Class IV: the SPOUT family of RNA MTases contains a novel knot structure (magenta) at the C terminus that contributes to the AdoHcy-binding site (YibK:1MXI). (Helices that are not conserved between family members are shown in pale pink in the topology diagram.) (e) Class V: the SET-domain containing histone-lysine N-MTase family is formed by the combination of three small β sheets. The AdoMet-binding site is formed on a shallow groove of the protein and the substrate active site is proximal to the C-terminal tail, which is also involved in a knot-like structure (Set7/9:1O9S). Figures were generated using PYMOL (http://www.pymol.org). Adapted from (77) and used with permission of Elsevier LTD.

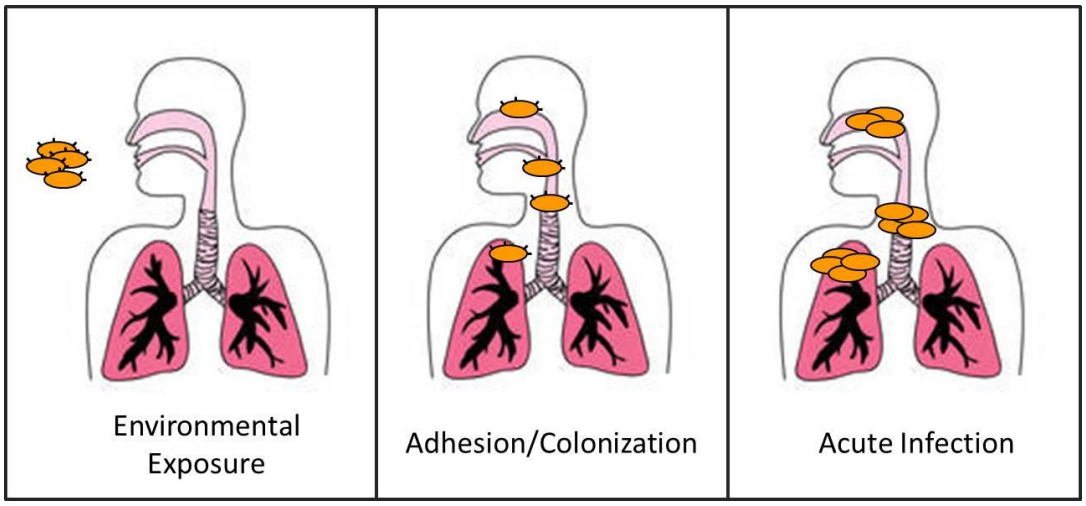

Figure 1.7. Model of EF-Tu methylation *in vivo*. Modification status of EF-Tu varies throughout the course of infection. *P. aeruginosa* in the environment modifies EF-Tu (Left). Once it enters the host, it uses this modification on EF-Tu to mediate adhesion to the respiratory epithelium (Middle). After initial adherence, the bacteria divide and colonize causing an acute infection of the respiratory tract during which expression of modified EF-Tu is lost.

Chapter 2

Identification of *eftM*, a gene which is responsible for the methylation of EF-Tu in *Pseudomonas aeruginosa*

Preceding, contributing to, and adapted from "Lysine Trimethylation of EF-Tu Mimics Platelet-Activating Factor To Initiate *Pseudomonas aeruginosa* Pneumonia" with permission from the American Society for Microbiology

Mariette Barbier, Joshua P. Owings, Inmaculada Martinez-Ramos, F. Heath Damron, Rosa Gomila, Jesus Blazquez, Joanna B. Goldberg, Sebastian Alberti.

mBio. 2013 June; 4(3)

*Screening of the PA14 transposon mutant library, mass spectrometry studies, and construction of the *eftM* deletion mutant PAO1Δ*eftM* were performed by our colleagues in the laboratory of Dr. Sebastian Alberti at Universidad de Las Islas Baleares, Palma de Mallorca, Spain.

Abstract

Pseudomonas aeruginosa is a Gram-negative opportunistic pathogen that is often associated with nosocomial pneumonia. A phosphorylcholine (ChoP)-like molecule has been previously identified by immunoreactivity on bacterial surface molecules in other respiratory pathogens. In *P. aeruginosa* this ChoP-like modification is found on elongation factor-Tu (EF-Tu). The pathway involved in the addition of this molecule to EF-Tu in *P. aeruginosa* is currently unknown, as this bacterium lacks previously described genes for the addition of ChoP in other pathogens. Here we identify a gene, *eftM*, which when interrupted prevents the ChoP-like modification of EF-Tu. We identify this modification at lysine 5 and find the nature of the modification was not phosphorylcholine but rather trimethylation of lysine 5. This trimethyllysine is a structural mimic of ChoP and confers similar but not identical phenotypes to *P. aeruginosa* as ChoP does to other respiratory pathogens.

Introduction

Pseudomonas aeruginosa is a Gram-negative opportunistic pathogen that infects patients with compromised immune systems. Incidences of disease caused by this pathogen are primarily nosocomial and associated with respiratory infection. *P. aeruginosa* is the second most common cause of ventilator-associated pneumonia in the United States and treatment is increasingly difficult to as multi-drug resistant strains continue to emerge.

Recently, the charged molecule phosphorylcholine (ChoP) has been recognized as a common epitope on the surface of respiratory pathogens. ChoP was first discovered to be

associated with the teichoic and lipoteichoic acids of the *Streptococcus pneumoniae* cell wall (24). This discovery led to further study of this epitope on other microbes and subsequent detection of ChoP on a range of both Gram-positive and Gram-negative bacteria, as well as numerous eukaryotic pathogens such including protozoa, fungi, and filarial nematodes. In most of these organisms, the ChoP moiety is associated with structural glycans or glycolipids (25, 26). The first exception to this was found in pathogenic *Neisseria*, *N. meningitidis* and *N. gonorrhoeae*, which express ChoP on their pili (fimbriae) (26, 27). Their commensal counterparts also express ChoP but it is linked to their lipopolysaccharide (LPS), providing evidence that ChoP can have distinct properties based upon the structure that is modified (27, 28). The mechanism for this difference in function has yet to be elucidated. More recently, ChoP has been found on yet another protein, outer membrane porin D, in the pathogen *Acinetobacter baumannii* where the modification facilitates similar functions to those seen in other respiratory pathogens (29).

The pathway involved in the addition of ChoP epitopes has been most extensively studied in *Haemophilus influenzae*. Choline is not necessary for growth of this pathogen and it cannot synthesize choline *de novo* so it must be obtained from the environment for incorporation into *H. influenzae* lipopolysaccharides (LPS) (2). The genes involved in choline transport and ChoP addition to LPS in *H. influenzae* are found at the *lic1* operon. This operon consists of four genes, *licA-licD*, which are also found in other pathogens that modify surface structures with ChoP, including *S. pneumoniae*. A list of the functions of the genes in this operon can be found in Table 2.1.

P. aeruginosa contains no homologues to any of the genes present in the *lic1* operon. However, a study by Weiser *et al.* of the well-characterized *P. aeruginosa* laboratory strain PAO1 has shown that antibodies against ChoP, TEPC-15, reacted with a 43 kDa protein when the cells were grown at ambient temperatures (25^{o}C) but not at temperatures more closely resembling body temperature (37^{o}C) (Figure 1.3) (28). The 43 kDa protein which displayed reactivity with the ChoP monoclonal antibody TEPC-15 was identified by mass spectrometry as the bacterial protein elongation factor Tu (EF-Tu) (18).

The purpose of this study was to identify the genes responsible for the ChoP-like modification of EF-Tu. Unlike *H. influenzae*, *P. aeruginosa* has extensive metabolic capabilities for the utilization of both choline and choline containing molecules such as phosphatidylcholine (PC) and sphingomyelin (SM) (Figure 2.1). As such, the use of radiolabelled choline as an energy source to identify downstream metabolic compounds proved impossible. To identify the genes involved in this ChoP-like modification, a comprehensive global approach would be necessary.

Methods and Materials

Strains, plasmids, and primers

A list of all strains, plasmids, and primers used in this study can be found in Table 2.2. *Pseudomonas* isolates were grown on *Pseudomonas* Isolation Agar (PIA) and

supplemented with antibiotics when appropriate: gentamycin (25 μg/ml), tetracycline (100 μg/ml), and carbenicillin (300 μg/ml). *E. coli* strains were grown on lysogeny broth agar (LA) supplemented with antibiotics when appropriate: kanamycin (50 μg/ml) or carbenicillin (100 μg/ml).

Preparation of whole-cell extracts

Cells were grown shaking in LB overnight at either 25°C or 37°C. Whole cell extracts were prepared by taking 0.5 ml equivalents of OD_{600} = 1.0 cultures, pelleting the cells, and resuspending in 30 μl water and 30 μl 2x Laemmli buffer (BioRad). Samples were then used for Western immunoblotting, as described below.

Standard Western immunoblot protocol

After generation of whole-cell extracts, samples were boiled for 10 minutes before running 10 μl aliquots on 10% Mini-PROTEAN TGX gels (BioRad). Proteins were transferred to polyvinylidene fluoride (PVDF) membranes (Bio-Rad), blocked for 1 hour at room temperature (RT) in 5% non-fat dry milk (NFDM), and incubated overnight at 4°C in primary antibody specific for phosphorylcholine (HAS [Statens Serum Institut, #87214] and TEPC-15 [Sigma-Aldrich, #M1421]), di/trimethyl lysine (Upstate, #07-756), FLAG M2 (Sigma-Aldrich, #F1804), or poly-histidine (THE His antibody, Genscript, #A00186) diluted in phosphate buffered saline + 0.05% Tween-20 (PBS-T). After incubation overnight at 4°C in primary antibody, blots were washed 3 times for 10 minutes each in PBS-T and incubated for 1 hour at RT in the appropriate horseradish peroxidase (HRP) conjugated secondary antibody (anti-mouse IgM, anti-mouse IgA, anti-

rabbit IgG, anti-mouse IgG, and anti-mouse IgG, respectively) diluted in PBS-T. Detection of binding was done using Clarity Western ECL Substrate (BioRad) and visualized using either Amersham Hyperfilm ECL (GE Healthcare) or the BioRad ChemiDoc MP imager and analyzed using Image Lab version 5.1 (BioRad). All Western immunoblots were performed in this manner unless otherwise noted.

Random *P. aeruginosa* transposon mutant library generation

A random, transposon mutant library was generated in the laboratory strain PAO1 using the EZ-Tn5 <Tet-1> kit (Epicentre) using a modified protocol in consultation with Epicentre Biotechnologies. Briefly, a stable transposome complex was generated by the mixture of 2 µl EZ-Tn5 <TET-1> transposon DNA (100 mg/ml in TE buffer [10 mM Tris-HCl (pH 7.5), 1 mM EDTA]), 4 µl EZ-Tn5 transposase, and 2 µl 100% glycerol. The solution was mixed by vortexing and incubated at RT for 30 minutes. After incubation at RT, the transposome complex was incubated a further 24 hours at 4°C. For electroporation of electrocompetent *P. aeruginosa* PAO1, 1 µl of the stable transposome complex was used. After electroporation, cells were allowed to recover for 30 minutes at 37°C before plating on LB + tetracycline (100 µg/ml) + 5 mM magnesium chloride.

Electrocompetent *P. aeruginosa*

Electrocompetent cells were generated using a protocol modified from Choi *et al.* (82). Briefly, cells were grown shaking overnight at 37°C in 10 mL of LB. At least 6 mL of overnight culture was pelleted and the supernatant removed, including any visible exopolysaccharides. Pellets were washed three times using sterile RT 300 mM sucrose.

The pellets were combined in 100 µl of sterile 300 mM sucrose. For electroporation, 100 µl of washed cells were added to an electroporation cuvette along with 1-2 µl of plasmid DNA. A pulse of 2500 volts was applied to the cuvette before the addition of 900 µl of LB. The cells were allowed to recover for 30 minutes shaking at 37°C before plating on *Pseudomonas* isolation agar (PIA) or LB with appropriate antibiotic selection.

Genomic DNA preparation

Genomic DNA was prepared using a modified protocol from Pospiech and Neumann (83). Briefly, cells were grown overnight and 1 mL of culture was removed for DNA isolation. Cells were pelleted by centrifugation and resuspended in 500 µl of STE buffer (20 mM Tris-Cl [pH 7.5], 75 mM NaCl, 25 mM EDTA). Lysozyme was added to a final concentration of 1 mg/ml and cells were incubated at 37°C for 30 minutes. After incubation, 50 µl of 10% SDS and Proteinase K to a final concentration of 0.5 mg/ml were added and the preparation was incubated at 55°C for 30 minutes. For removal of contaminating proteins, 190 µl of 5M NaCl and 760 µl of chloroform were added and the solution was shaken vigorously. Preparations were then centrifuged at 7K RPM for 10 minutes and the upper layer was removed and saved. To precipitate DNA, 500 µl of isopropanol was added to the removed fraction and mixed by inversion. Repeated pelleting and washing with 70% and 100% ethanol removes any further contaminants before briefly air drying the DNA pellets. Pellets were resuspended in 250 µl of sterile water and stored at 4°C.

Southern blotting

Genomic DNA was isolated as previously described and digested with SalI. After digestion, DNA was run on a 0.8% agarose gel prestained with ethidium bromide. The gel was imaged while illuminated with ultra violet light before depurination in 0.25 M HCl for 30 minutes at RT. The gel was then rinsed with water and washed twice for twenty minutes in denaturation solution (1.5 M NaCl and 0.5 M NaOH). Gel was then rinsed with water before washing twice for twenty minutes each with neutralization solution (1.5 M NaCl, 0.5 M Tris-HCl, pH 7.5). The DNA was transferred to a Hybond-N^+ nylon membrane (GE Healthcare) using overnight downward capillary transfer in 20x SSC buffer (3 M NaCl, 0.3 M sodium citrate, pH 7.0) after which the membrane was auto-crosslinked with a UV Stratalinker (Stratagene). Blot was then placed in a hybridization tube and blocked at 42°C for 15 minutes in pre-hybridization buffer (20 mL Amersham ECL gold hybridization buffer [GE Healthcare], 500 mM NaCl, 1g blocking agent). After pre-hybridization, the probe which was generated to the EZ-Tn5 <TET-1> transposon following the manufacturer's instructions for the Amersham ECL Direct Nucleic Acid Labelling and Detection Kit (GE Healthcare) was added to the solution and incubated overnight at 42°C overnight. The blot was then washed three times for ten minutes in primary wash buffer (6 M Urea, 0.4% SDS [wt/vol], 0.5x SSC) at 42°C and developed using ECL reagents in the detection kit.

Cloning of EF-Tu and EftM (PA4178)

To purify *P. aeruginosa* EF-Tu, we constructed the shuttle expression vector pUCP18ApGw(*tufB*), which encodes his-tagged EF-Tu, using the directions provided in the Invitrogen Gateway system (Life Technologies) and primers described in Table 2.2.

Essentially, *tufB* was amplified by PCR from the genome of PAO1 with the addition of an N-terminal 6x-histidne tag using primers *tufB*F and *tufB*R and cloned into the Entry vector, pENTR/SD/D-TOPO (Life Technologies). His-tagged EF-Tu was transferred to the Gateway compatible expression vector pUCP18ApGw, which was derived from pUCP18 (84) by cloning reading frame A from the Gateway Vector Conversion System (Life Technologies) into the SmaI site, using LR Clonase (Life Technologies). The resulting plasmid was named pUCP18ApGw(*tufB*).

To generate the mutant protein EF-Tu K5A, we used the protocol described above using primers *tufB*FK5A and *tufB*R, where the lysine 5-encoding codon of *tufB* is replaced by an alanine-encoding codon. The resulting plasmid was named pUCP18ApGw(*tufB* K5A). Three other EF-Tu constructs were also generated in this way, pUCP18ApGw (*tufB* K5C) using oJPO93/*tufB*R, pUCP18ApGw (*tufB* K5R) using oJPO94/*tufB*R, and pUCP18ApGw (*tufB* ΔK5) using oJPO95/*tufB*R.

eftM was also cloned into the shuttle expression vector pUCP18ApGw using the protocol described above with PAO1 genomic DNA as a template and primers PA4178F and PA4178R to add a C-terminal FLAG tag. The resulting plasmid was named pUCP18ApGw(*eftM*) (19).

Generation of *eftM* deletion mutant

We partially deleted *eftM* in the strain PAO1 using the procedure described by Quénée *et al.* (85) for gene deletion and antibiotic resistance marker recycling in *P. aeruginosa*

using the *cre-lox* system. Briefly, upstream and downstream PCR products (Table 2.2) of *eftM* were digested with either BamHI or EcoRI and HindIII and then cloned by three-way ligation into pEX100Tlink deleted for the HindIII site and digested with EcoRI and BamHI to produce plasmid pEX*eftM*, which was transformed into *E. coli* strain XL1-Blue. Transformants were selected on LB agar plates with 30 μg/ml ampicillin. The *lox*-flanked gentamicin resistance cassette (*aac1*), obtained from the HindIII-digested plasmid pUCGm*lox*, was cloned into the plasmid pEX*eftM* digested with the same enzyme, producing plasmid pEX*eftM*Gm, which was transformed into *E. coli* XL1-Blue. Transformants were selected on LB agar plates with 30 μg/ml ampicillin and 5 μg/ml gentamicin. These plasmids were then transformed into the *E. coli* helper strain S17-1. Plasmid pEX*eftM*Gm was transferred from *E. coli* S17-1 to PAO1, and selection for double recombinants using LB agar plates with 5% sucrose and 30 μg/ml gentamicin was performed to produce the PAO1Δ*eftM*Gm strain. Double crossovers were first screened for susceptibility to carbenicillin (200 μg/ml) and by PCR amplification using primers eftM-F-ErI and eftM-R-BhI (Table 2.2). For the removal of the gentamicin resistance cassette (to yield the PAO1Δ*eftM* mutant), plasmid pCM157 was electroporated into the mutant. Transformants were selected on LB agar plates with 250 μg/ml tetracycline. One transformant was grown overnight in LB broth with 250 μg/ml tetracycline in order to allow the expression of the *cre* recombinase. Plasmid pCM157 was then cured from the strains by three successive passages in LB broth. Selected colonies were then screened for susceptibility to tetracycline (250 μg/ml) and gentamicin (30 μg/ml) and were checked by PCR amplification and DNA sequencing (19).

Purification of recombinant EF-Tu

Plasmids containing the various EF-Tu constructs (Table 2.2) were transformed into PAO1 following the protocol previously described for electrocompetent *P. aeruginosa*. Each construct was used to start 50 ml overnight cultures shaking at 25°C in LB + carbenicillin (300 µg/ml) + 1 mM IPTG. Cells were pelleted with centrifugation and resuspended in 10 ml xTractor cell lysis buffer (Clontech) supplemented with lysozyme 0.2 mg/ml and 100U DNaseI. Suspensions were incubated on ice for 30 minutes before lysis using a French Pressure Cell (American Instrument Company) at 16-18k PSI. Cellular debris was removed by centrifugation at 12,857 x g for 10 minutes at 4°C. Supernatants were applied to columns containing equilibrated Ni-NTA agarose beads (Thermo Scientific). Columns were washed three times with 10 ml of wash buffer (50 mM NaH_2PO_4, 1M NaCl, 40 mM imidazole, 1% Triton X-100 [wt/vol], pH 8.0). Samples were eluted in 500 µl aliquots of elution buffer (50 mM NaH_2PO_4, 1M NaCl, 250 mM imidazole, pH 8.0) and stored at -20°C.

Mass spectrometry analysis of purified recombinant EF-Tu

Purified proteins (~30 µg) were digested with trypsin (0.2 mg) (Sigma-Aldrich) at 37°C overnight. Digested proteins were placed on a polished steel target (Bruker Daltonics), mixed with 1 µl of matrix (2,5-dihydroxybenzoic acid in 70/30 acetonitrile/water with 0.1% trifluoroacetic acid), allowed to air dry, and analyzed with an Autoflex III matrix-assisted laser desorption ionization–tandem time of flight (MALDI-TOF/TOF) mass spectrometer (Bruker Daltonics) equipped with a 200 Hz Smartbeam laser. Spectra were recorded in the reflector, positive mode, at a laser frequency of 200 Hz within a mass

range from 500 to 4,300 Da. The IS1 voltage was 19 kV, the IS2 voltage was maintained at 16.65 kV, the lens voltage was 8.30 kV, the reflector voltage was 21 kV, and the reflector 2 voltage was 9.7 kV. The spectra were calibrated using a peptide calibration standard (Bruker Daltonics) or autolysis trypsin peaks.

Results

Screening of choline pathway mutants

Previous work had identified a ChoP-like molecule present in *P. aeruginosa* when the cells were grown at 25°C and showed reduced expression as the cells were grown at increasing temperatures (Figure 1.3). Other respiratory pathogens also decorate surface molecules with ChoP, including *H. influenzae* which modifies its LPS with ChoP. In *H. influenzae*, choline is not necessary for growth but is necessary for incorporation of ChoP into LPS. When *H. influenzae* is grown on defined medium containing radiolabelled choline, the band that reacts with ChoP antibodies comigrates with the radiolabelled LPS (1). Unfortunately, *P. aeruginosa* has a much more extensive choline metabolic pathway and is able to metabolize choline into numerous metabolites (49). In order to determine if and how the choline metabolic pathway of *P. aeruginosa* contributed to the addition of the observed ChoP-like molecule to EF-Tu, *P. aeruginosa* mutants in this pathway were tested for their ability to modify EF-Tu. We hypothesized that disruption of the choline metabolic pathway would help us elucidate the pathway for EF-Tu modification.

All of the mutants used in this study (Table 2.2) were generated in the laboratory of Dr. Deb Hogan (Dartmouth Medical School) and many had been previously used to examine

the choline metabolic pathway (Figure 2.1) in *P. aeruginosa* (51, 86). These mutants included hemolytic phospholipase C (PlcH), phosphatidylcholine phosphatase (PchP), phosphatidylcholine synthase (Pcs), the transcriptional regulator of betaine catabolism (GbdR), along with the choline transporters CbcV, BetT3 and BetT1. Cells were grown in defined medium lacking or supplemented with choline at both the permissive temperature for modification, 25°C, or the non-permissive temperature, 37°C, and were screened using our standard Western immunoblot protocol. None of the mutants examined exhibited EF-Tu modification phenotypes that were different from the wild-type strain (Figures 2.2).

Screening of longitudinal clinical isolates

As many phenotypes differ between acute and chronic isolates, Barbier *et al.* tested the ability of these different types of isolates to modify EF-Tu (18). They found that chronic isolates generally have higher levels of the ChoP-like modification on EF-Tu at 37°C, the non-permissive temperature for PAO1, compared to acute isolates (Figure 1.4), as defined by the intensity of bands seen in Western blotting with ChoP-specific antibodies. In CF patients, acute infections eventually progress to clonally derived chronic infections. This allows for the direct comparison of strains from a single patient early and late during infection. We hypothesized that if we compared chronic isolates that had an altered EF-Tu modification phenotype to their earlier clonal isolates that did not exhibit this phenotype, we would be able to identify genes involved in the modification pathway. To do this, we would need to have a comprehensive understanding of the genomic changes which took place during the course of infection.

The laboratory of Dr. Jane Burns (Seattle Children's Research Institute) had previously characterized and sequenced longitudinal isolates from chronically infected cystic fibrosis patients (87). Not only did they reaffirm the clonality of these chronic infections, they mapped the genes which were mutated throughout the course of infection and identified 68 mutations between early and late isolates. We obtained this library which contained 35 sequential longitudinal isolates from a single patient (Figure 2.3) as well as smaller numbers of longitudinal isolates from 16 other patients (Table 2.2). We screened the earliest and latest isolate from each of these patients for variations in EF-Tu modification using our standard Western immunoblot assay and found that there was no difference in the temperature-dependent modification phenotype (Figure 2.4). This suggested that these strains did not contain any mutations in the pathways involved in the modification of EF-Tu.

Non-directed transposon mutagenesis

The use of transposable DNA elements has become a routine way to generate a library of mutants (88). These mutants hopefully represent insertions of the transposon and subsequent loss-of-function mutations in most if not all non-essential genes. I was able to generate a transposon mutant library in the laboratory strain PAO1. The randomness of the transposon insertion was validated using a Southern blot with the transposon DNA as a probe (Figure 2.5).

The next step was to find a suitable screen to identify mutants of interest. Initially I attempted to enrich for mutants where EF-Tu was not modified at 25°C through adsorption of those expressing the normal phenotype to magnetic beads which were conjugated to the anti-ChoP antibody HAS. The flow through was then tested in some high-throughput screening methods. Numerous high-throughput methods were tested including flow cytometry, colony immunoblot, dot blot, and ELISA. All of these methods relied upon the affinity and specificity of the anti-ChoP antibody, HAS, for modified EF-Tu. Using these methods, we had hoped to identify mutants that either expressed modified EF-Tu at both 25°C and 37°C, or mutants which did not modify EF-Tu at either temperature. Unfortunately, these methods proved inconsistent even when using control strains for true positive and negative results (Data not shown).

The most reliable test for the presence or absence of modified EF-Tu remained our standard Western immunoblot assay using whole cell lysates generated with strains grown overnight at either 25°C or 37°C. Fifty individual mutants from my random transposon mutant library were selected and tested using this method. Of those tested, clone #1 showed altered EF-Tu modification, while the other 49 strains exhibited the normal temperature dependent EF-Tu modification phenotype (Figure 2.6). The location of the transposon in clone #1 was identified by arbitrary PCR as interrupting the gene PA4832. However, upon retesting of this clone by Western immunoblot, it was revealed that the initial phenotype was a false positive and the phenotype was actually that of normal temperature dependent modification of EF-Tu (Data not shown).

Screening of PA14 ordered transposon mutant library

While screening of randomly generated transposons libraries is an effective tool for high throughput screening, many more mutants must be screened than genes in the genome to be certain saturation of the genome is reached. In *P. aeruginosa*, there exist two ordered transposon libraries, one is in the well-studied laboratory strain PAO1 (89) and the other is in the primary clinical isolate PA14 (90). We used a systematic analysis of the ordered, nonredundant PA14 transposon library to identify mutants lacking in modified EF-Tu. This was done by Western immunoblot with the anti-ChoP antibody TEPC-15 was performed using whole cell lysates of 5,514 individual mutants grown at 25°C (19). Screening of this library resulted in the identification of a single mutant, PA14-_09870::MAR2xT7, which was deficient in its ability to modify EF-Tu at 25°C (Figure 2.7) (19).

To confirm that this gene was responsible for the modification of EF-Tu in both PA14 and PAO1, the corresponding mutant from the comprehensive PAO1 transposon mutant library (89), PW8081 (PA4178-C06::ISlacZ/hah), was obtained and tested and confirmed the lack of EF-Tu modification (Figure 2.7). The transposon was located in a gene annotated as a hypothetical methyltransferase by the *Pseudomonas aeruginosa* Community Annotation Project (PseudoCAP) because there was no similarity to previously reported sequences (91). The open reading frame was identified in the laboratory strain PAO1 as PA4178 which we refer to as *eftM* (EF-Tu-modifying enzyme) (19).

To confirm that the gene identified by the transposon screen, *eftM*, was in fact responsible for the observed phenotype, it was necessary to clone *eftM* and perform a complementation study. *eftM* was cloned from PAO1 with the addition of an engineered C-terminal FLAG tag into the *Pseudomonas* expression vector pUCP18ApGw. This plasmid was then used to transform the *eftM* deletion mutant strain PAO1Δ*eftM*. When *eftM* was constitutively expressed from this plasmid, not only was the modification restored at 25°C but there was a loss of temperature dependence such that EF-Tu was also modified at 37°C (Figure 2.8). While there was always an increase in expression at 37°C when PAO1Δ*eftM* contained the pUCP18ApGw(*eftM*) plasmid, there was not consistently more than observed at 25°C. Interestingly, when whole cell lysates from the *E. coli* strain used to propagate this plasmid were examined, it was observed that *eftM* was able to modify *E. coli* EF-Tu at both temperatures (Figure 2.8).

As EF-Tu is an extremely well conserved protein (Figure 2.9) (92, 93) the ability of *eftM* to modify *E. coli* EF-Tu suggested that *eftM* from *P. aeruginosa* might be able to function in a variety of heterologous systems. To test this, the broad host range pUCP18ApGw(*eftM*) plasmid was used to transform *Klebsiella pneumoniae* and *Burkholderia sp.* which typically exhibit no modification of EF-Tu (Figure 2.10). Surprisingly when *eftM* was expressed in *K. pneumoniae*, there was observed modification of EF-Tu (Figure 2.11). However, expression in all tested *Burkholderia* strains resulted in no observed EF-Tu modification (Data not shown).

Further bioinformatic analysis of the EftM protein showed that it is conserved in all completed genomes of *P. aeruginosa* strains present at http://www.pseudomonas.com (91), with one exception, the CF patient isolate *P. aeruginosa* DK2 which is known to have genomic deletions (94, 95). Of these *P. aeruginosa* strains, PA7 has the lowest sequence identity (87%), while all other strains have >99% sequence identity, to PAO1 EftM. Homologs of EftM are also present in many other *Pseudomonas* species, including *P. mendocina*, *P. stutzeri*, *P. fulva*, and *P. syringae*. All of the species of *Pseudomonas* which contain a homologue of *eftM* and have been tested are capable of modifying EF-Tu (Figure 2.12) except for *P. fulva*, which has mutations in the predicted SAM binding domains. BLAST analysis using the EftM protein sequence indicates the broad distribution of homologs within other gammaproteobacteria (including *Shewanella* sp. and *Vibrio* sp.), as well as within the *Firmicutes* (19).

EftM trimethylates EF-Tu at lysine 5

In an effort to identify the residue(s) in EF-Tu that are modified by *eftM* we undertook a tandem mass spectrometry approach. We purified recombinant EF-Tu from *P. aeruginosa* PAO1 as well as the *eftM* deletion mutant, PAO1Δ*eftM*, grown at the temperature that is permissive for modification, 25°C, and digested them with trypsin for use in mass spectrometry analysis. Initially, the mass spectrum was searched for any peptide with an increase in mass of 184 Da, which corresponds to the molecular weight of ChoP. This analysis did not reveal any peptides containing a ChoP modification. The mass spectrum was then searched for shifts that corresponded to trimethylated lysine as the structure is similar to that of ChoP. After further analysis, we identified a peak in the

sample from the deletion mutant with a mass of 708.365 Da which corresponded to the peptide EKFER (Figure 2.13A, top). Similar analysis of the protein purified from wild-type PAO1 identified a peak for the same peptide with a mass of 750.412 Da (Figure 2.13A, middle). This increase of 42.047 Da corresponded to the addition of three methyl groups (42 Da) to lysine residue 5. Similar analysis of recombinant EF-Tu expressed in PAO1 with a point mutation where lysine 5 was mutated to an alanine (K5A) revealed that the peptide EAFER was unable to methylated and had a corresponding molecular mass of 651.319 Da (Figure 2.13A, bottom). Western blot analysis of these purified recombinant EF-Tu's confirmed that only the wild type EF-Tu purified from wild type PAO1 was recognized by the anti-ChoP antibody, TEPC-15 or HAS, and by the anti-di/trimethyl lysine antibody (See Standard Western immunoblot methods for complete antibody descriptions). Neither EF-Tu K5A purified from with type PAO1 nor the wild-type EF-Tu purified from PAO1Δ*eftM* was recognized by either the anti-ChoP or the anti-di/trimethyl lysine antibodies (Figure 2.13C) (19). Interestingly, when lysine 5 of EF-Tu was deleted or mutated to an arginine and was expressed in wild-type *P. aeruginosa*, it was still able to be modified (Figure 2.14). However, when lysine 5 was mutated to a cysteine, the resulting recombinant protein was unable to be modified *in vivo* (Figure 2.14). The exact sites of these modifications have not yet been determined by mass spectrometry.

Discussion

Previous studies done in collaboration with our laboratory had shown that there was modification of EF-Tu in *P. aeruginosa* (18). Furthermore, this modification was

believed to be ChoP based upon reactivity of whole cells lysates on Western immunoblots with anti-ChoP antibodies (28). It was perhaps not surprising to identify this type of modification on *P. aeruginosa* as it has been well documented that ChoP is present in numerous other respiratory pathogens (9). In the host, ChoP is the portion of platelet activating factor (PAF) which mediates binding its cognate receptor platelet activating factor receptor (PAFR). This receptor is broadly distributed throughout the host including in the heart, brain, liver, vascular system, circulating immune cells, endothelial cells, and the lungs (96, 97).

In these pathogens, ChoP acts to mimic the host molecule PAF and exploits this ability to bind PAFR. In doing so, these respiratory pathogens are able to better colonize the respiratory epithelium which results in increased persistence in the host (9). Because the presence of this molecule can lead to such pathology in other respiratory pathogens it was of great interest that it had been observed in the very important nosocomial pathogen *P. aeruginosa*. We undertook the task of identifying both where on EF-Tu this modification was located as well as what genes might be involved in the addition of this molecule.

Initially we believed that a targeted approach might identify mutants that were unable to add this ChoP-like molecule to EF-Tu. It had previously been seen in *H. influenzae* that the addition of radiolabelled choline led to the addition of radiolabelled ChoP to its LPS. The pathway involved in this process was identified as the *lic1* operon of which *P. aeruginosa* does not contain a homologue. However, *P. aeruginosa* does metabolize choline as it can be utilized as both a carbon and nitrogen source for general metabolism

instead of the singular use seen in *H. influenzae*. Given this general metabolic use of choline, there exist multiple choline transporters and salvage mechanisms in *P. aeruginosa* (Figure 2.1). This provided the logical place to start our search: genes involved in the synthesis, uptake, and scavenging of choline and choline metabolites.

We examined numerous mutants provided by our colleagues at Dartmouth Medical School which were deficient in various aspects of choline metabolism. These included mutants in phosphatidylcholine synthase (Pcs), phosphorylcholine phosphatase (PchP), the glycine betaine pathway transcriptional regulator GbdR, the choline transporters BetT1, BetT3, and CbcXWV, and phospholipase C (PlcH; which acts to degrade phosphatidylcholine (PC) and sphingomyelin (SM) to ChoP and provides the scavenging mechanism for *P. aeruginosa* to salvage choline from the host where both PC and SM are abundant). It also has been previously reported that *P. aeruginosa* contains a homologue to pilin phosphorylcholine transferase A (*pptA*) from *N. meningitidis* (98). However, the similarity of the homologue was low, 26%, and we were unable to locate any information with regards to this putative gene (98) so we were unable to test this mutant directly. Theoretically, this mutant would have been tested by our comprehensive screening of the PA14 transposon mutant library.

None of the tested mutants in any of these pathways exhibited abnormal modification of EF-Tu phenotypes (Figure 2.2). We believed that two scenarios could be responsible for the lack of abnormal modification phenotypes. First, it is possible that there is an unidentified *de novo* choline synthesis pathway in *P. aeruginosa* which would not have

been tested by our directed mutants. The second possibility is that choline is not necessary for the addition of the ChoP-like modification to EF-Tu. This could be the result of an alternative synthesis scenario for ChoP that would not require choline as an intermediate or, as would later be determined, the molecule modifying EF-Tu is not ChoP.

Another strategy tested was trying to take advantage of the observation that chronic isolates generally have higher levels of the ChoP-like modification at 37°C compared to acute isolates (Figure 1.4) as defined by the intensity of bands seen in Western blotting with ChoP specific antibodies. This strategy is limited in that not all chronic isolates display a higher level of ChoP-like modification at 37°C. Additionally, measuring the intensity of the bands could be misleading if the measured intensity at 25°C is rather low. This could artificially increase the ratio even if the observed intensity at 37°C is itself low in comparison to other isolates. Even with these caveats we believed it was important to utilize the numerous sequenced longitudinal chronic isolates available at Seattle Children's Hospital. Our hope was that an early isolate would display normal EF-Tu modification while the latest obtained clonal isolate would display an abnormal EF-Tu modification phenotype, allowing us to simply check which genes had been mutated between the isolates. Unfortunately, all of the tested isolates displayed normal EF-Tu modification phenotypes which left us with the unenviable task of screening the entire PA14 ordered transposon mutant library by Western immunoblot.

Given the size of the library, 5800 mutants representing about 4600 of the 5584 open reading frames in PA14, and ineffectiveness of all tested high-throughput screens, we decided to only screen for loss-of-function mutations at 25°C. We were aware that this would bias our results such that we would miss any potential repressors or inhibitors that would be present at 37°C. Incredibly, the screening of the PA14 library yielded only a single mutant, of the 5,514 tested, which did not modify EF-Tu at 25°C (Figure 2.7). This gene was identified, the phenotype confirmed using both the PA14 and PAO1 transposon mutant libraries, and named *eftM*. To determine if modification at both temperatures could be due to duplication of *eftM* numerous acute, chronic, and type strains of *P. aeruginosa* were tested via Southern blotting to determine copy number. Southern blotting revealed that each strain tested had only a single copy of *eftM* (Figure 2.15).

The function of the gene was predicted to be that of a SAM-dependent methyltransferase and showed little similarity to the ChoP transferases identified in other bacteria. This coupled with our previous data showing disruption of the choline pathway did not prevent modification of EF-Tu suggested a few alternative hypotheses. First, it is possible that we had identified a glycine *N*-methyltransferase which is rare in most bacteria (99) as part of a previously unidentified *de novo* choline synthesis pathway in *P. aeruginosa*. Second, it is possible that the modification of EF-Tu is not dependent on choline at all and instead, we are detecting a different molecule that mimics ChoP.

Analysis of the *eftM* gene showed a broad distribution within the gammaproteobacteria indicating that its function may be of importance throughout this class of organisms.

Interestingly, when this gene was exogenously expressed in other gammaproteobacteria such as *E. coli* and *Klebsiella* sp., but not betaproteobacteria such as *Burkholderia* sp., the encoded protein was able to modify EF-Tu in those organisms. This is likely not due to differences in EF-Tu as it is an extremely well conserved protein (93), especially the N-terminus (Figure 2.9).

Mass spectrometry analysis of modified EF-Tu revealed the latter hypothesis to be correct. The modification was identified as trimethylation of lysine residue 5 of EF-Tu and was confirmed by site directed mutagenesis of this residue (Figure 2.13). While the inactivation and complementation studies provided good evidence that EftM was indeed involved somehow in the methylation of EF-Tu, it did not provide conclusive evidence of direct methylation of EF-Tu by EftM. Direct evidence of EF-Tu methylation will be addressed in Chapter 3.

Though we have shown that EF-Tu in *P. aeruginosa* is not modified with ChoP, trimethylation does seem to confer many of the same properties. For instance, we have shown that trimethylated EF-Tu does mediate interaction with PAFR similar to that seen by other pathogens which decorate their surface with ChoP. In mice, clinical isolates that were methylation positive were less able to colonize mice when the mice were treated with increasing levels of a PAFR antagonist (18). This was recapitulated *in vitro* by showing that methylation positive bacteria had decreased adherence and invasion of airway epithelial cells when they treated with the same PAFR antagonist (18). This suggested an interaction between the bacteria and PAFR. In our most recent manuscript,

we further studied if this binding was due to modified EF-Tu or another adhesin. To do this, we fluorescently labelled purified modified and unmodified EF-Tu and examined their ability to bind airway epithelial cells. We found that modified EF-Tu bound to these cells significantly better than unmodified EF-Tu (19). When we examined differences in virulence of PAO1 with the isogenic PAO1Δ*eftM* mutant which does not methylate EF-Tu, we found that it took significantly more PAO1Δ*eftM* bacteria to reach the lethal dose that would kill 50% of the mice (LD_{50}) compared to PAO1 (19). However, unlike modification with ChoP, methylation of EF-Tu does not increase the susceptibility of *P. aeruginosa* to serum mediated complement activity in the same way that ChoP decoration does in other pathogens (9, 19, 29). This suggests that the host interacts slightly differently when surface structures are methylated instead of modified with ChoP.

Our observation that EF-Tu is methylated in *P. aeruginosa* is not the first time modification of this essential translation factor has been identified though it is the first time trimethylation of EF-Tu has been identified in bacteria. Other modifications of EF-Tu alter the kinetic properties of the enzyme for its normal function in protein chain elongation. We observed no major effects on the growth of *P. aeruginosa* when *eftM* was disrupted (Figure 2.16) but that does not rule out altered kinetic properties of trimethylated EF-Tu compared to unmodified EF-Tu. To date, we have been unable to determine the ratio of modified to unmodified EF-Tu *in vivo* which could give us insight into if we should even expect to see an effect on growth when EF-Tu is methylated. We will continue these efforts using mass spectrometry with known EF-Tu concentrations as

well as by the generation of antibodies specific for un-, mono-, di- and trimethylated EF-Tu.

We have definitively shown that the gene *eftM* is involved in the modification of EF-Tu. Further, we have shown that what was previously believed to be ChoP modification is actually trimethylation of lysine. It will be interesting to see if what are believed to be ChoP modifications on other bacteria are actually trimethylation. This is important because methylation seems to confer similar but slightly different properties to pathogens. In addition, methylation of an essential translation factor could alter its traditional function in ways which we do not yet understand. If modification of EF-Tu leads to a survival advantage for these bacteria, *eftM* could represent a novel therapeutic target for the development of antimicrobial compounds.

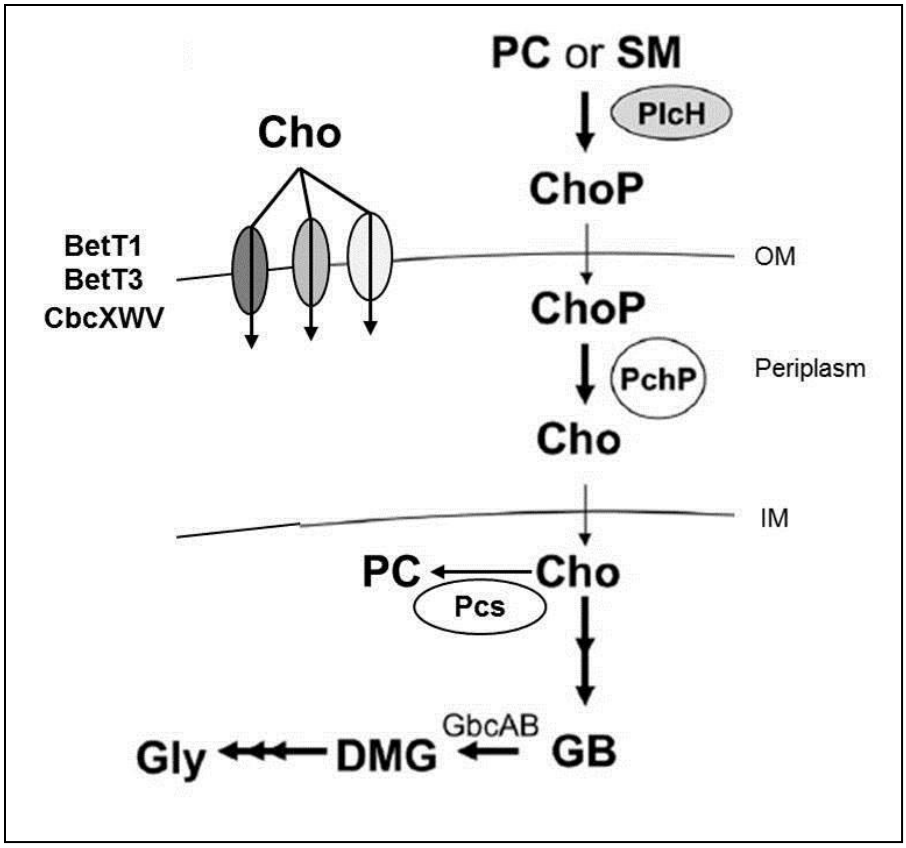

Figure 2.1. Choline metabolic pathways in *P. aeruginosa*. Phosphatidylcholine (PC) and sphingomyelin (SM) can be degraded by phospholipase C (PlcH) outside of the cell. This phosphorylcholine (ChoP) can then be transported across the cell membrane by any of three outer membrane transporters that are specific for ChoP and choline, BetT1, BetT3, and CbcXWV. In the periplasm, ChoP can be dephosphorylated by phosphorylcholine phosphatase (PchP) to form choline. This choline is then transported into the cytoplasm where it can either be further metabolized or used to make PC by phosphatidylcholine synthase (Pcs). Adapted from (86) and used with permission of The American Society for Microbiology.

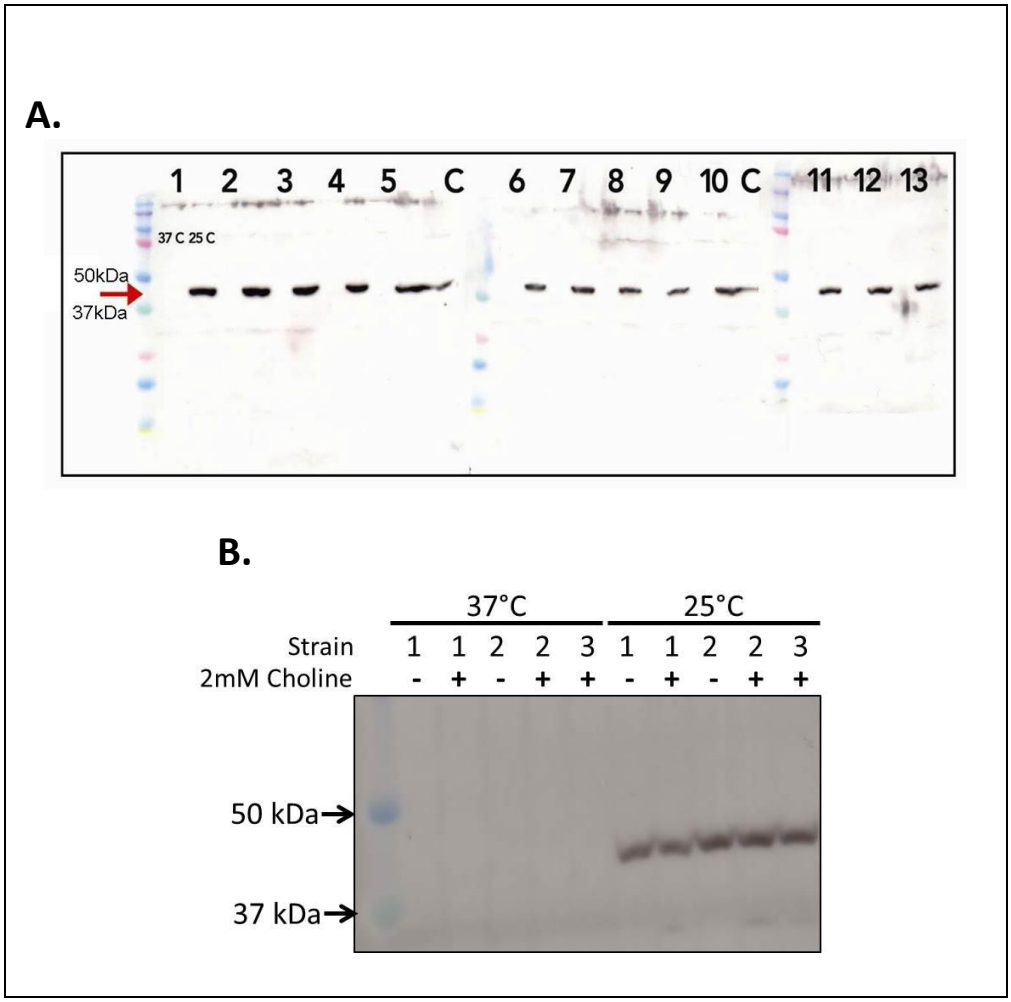

Figure 2.2. Screening of *P. aeruginosa* choline metabolic pathway mutants. *P. aeruginosa* strains deficient in the choline metabolic pathway exhibit normal EF-Tu modification. (A) Western blot using the anti-ChoP antibody HAS of whole cell lysates from strains with various mutations in the choline pathway grown in LB + 20 mM choline at both 37°C and 25°C. Strains from 1-13 are as follows: (1) PAO1 (DH395) Δ*pcs*, (2) PAO1 (DH395) Δ*pcs* + *pcs*, (3) PAO1 (DH395), (4) PAO1 (DH395) *pchP::tn*, (5) PA14 (DH122) Δ*pcs*, (6) PA14 (DH122), (7) PA14 (DH122) Δ*gbdR*, (8) PAO1 (DH1006) Δ*pcs*, (9) PAO1 (DH1006) Δ*pcs* + *pcs*, (10) PAO1 (DH1006), (11) PAO1 (DH1006) Δ*plcH*, (12) PAO1 (DH1006) Δ*gbdR*, and (13) PAO1 (DH1006) Δ*gbdR* +

gbdR. (B) Western blot using the anti-ChoP antibody HAS of whole cell lysates from strains with various mutations in the choline pathway grown in MOPS + pyruvate with and without 20 mM choline at both 37°C and 25°C. Strains from 1-3 are as follows: (1) PA14 (DH122), (2) PA14 (DH122) Δ*cbcV* Δ*betT3 betT1::pMQ*, and (3) PA14 (DH122) Δ*pcs*.

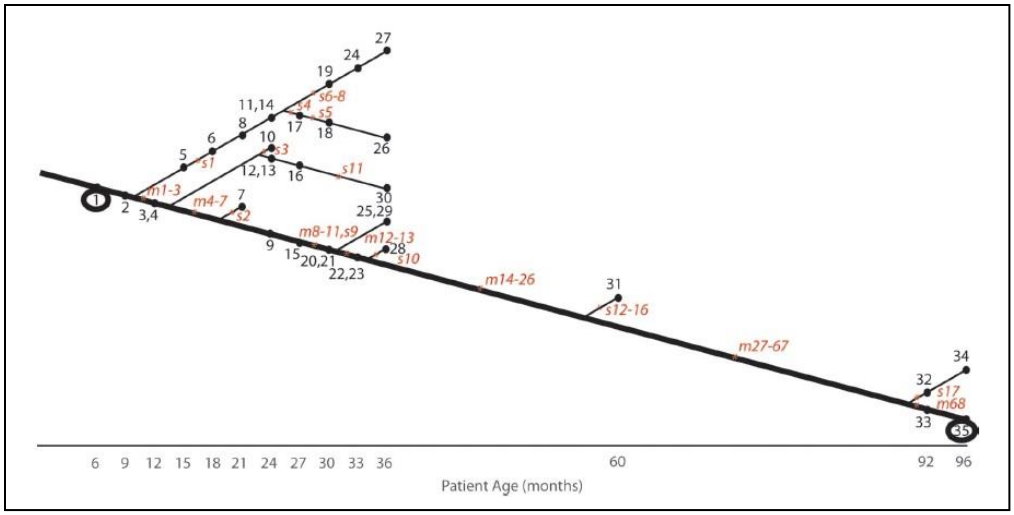

Figure 2.3. Tree showing mutations that occurred in longitudinal *P. aeruginosa* isolates from a single chronically infected CF patient. Isolates are numbered 1–35 in black type. Isolates 1 and 35, both circled, are the respective 6- and 96-month isolates whose genomes were sequenced and examined in this study. Mutations are shown in red italic type; mutations present in the 96-month isolate are numbered m1–m68, and mutations present only in intermediate isolates are numbered s1–s17. Mutations s9 and m52 are both in the same highly mutable repeat and appear to have occurred consecutively during the infection. Adapted from (87) and used with permission (Copyright 2006. National Academy of Sciences, USA.)

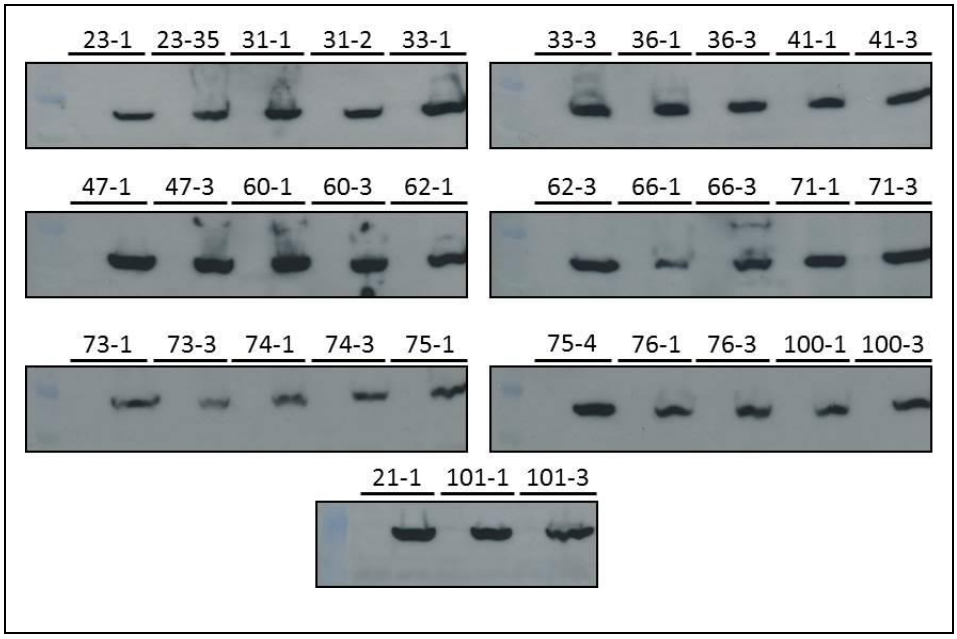

Figure 2.4. Screening of longitudinal patient isolates. Longitudinal *P. aeruginosa* clinical isolates from 17 chronically infected CF patients were tested for ability to modify EF-Tu. The first and last isolates from each patient were tested by growth at both 25°C and 37°C and Western blotting whole cell lysates for expression of modified EF-Tu using anti-ChoP antibodies.

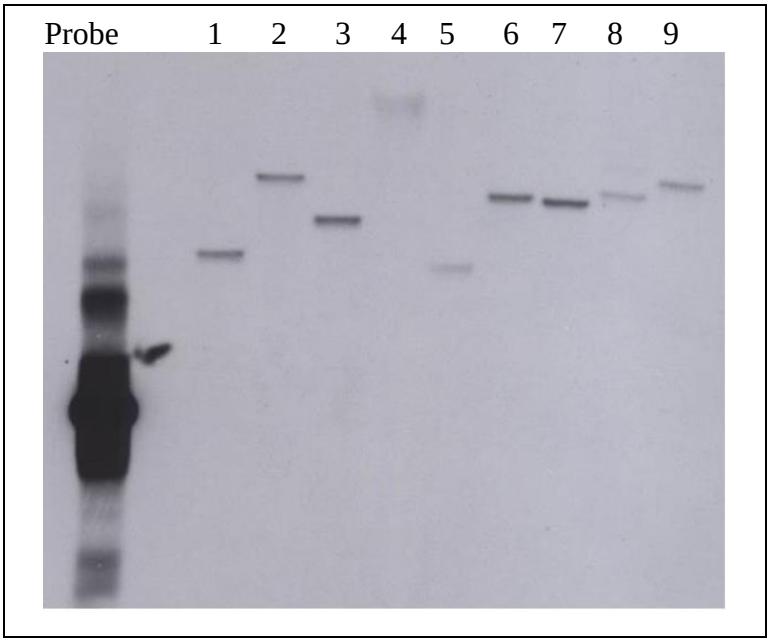

Figure 2.5. Validation of *P. aeruginosa* random transposon mutagenesis library. A Southern blot using SalI digested DNA from 9 randomly selected transposon mutants from the generated *P. aeruginosa* PAO1 EZ-Tn5 <TET-1> library. Genomic DNA was digested and probed with biotinylated EZ-Tn5 <TET-1> transposon DNA. Each clone showed hybridization with the probe at a different size suggesting the transposon inserted randomly into the genome.

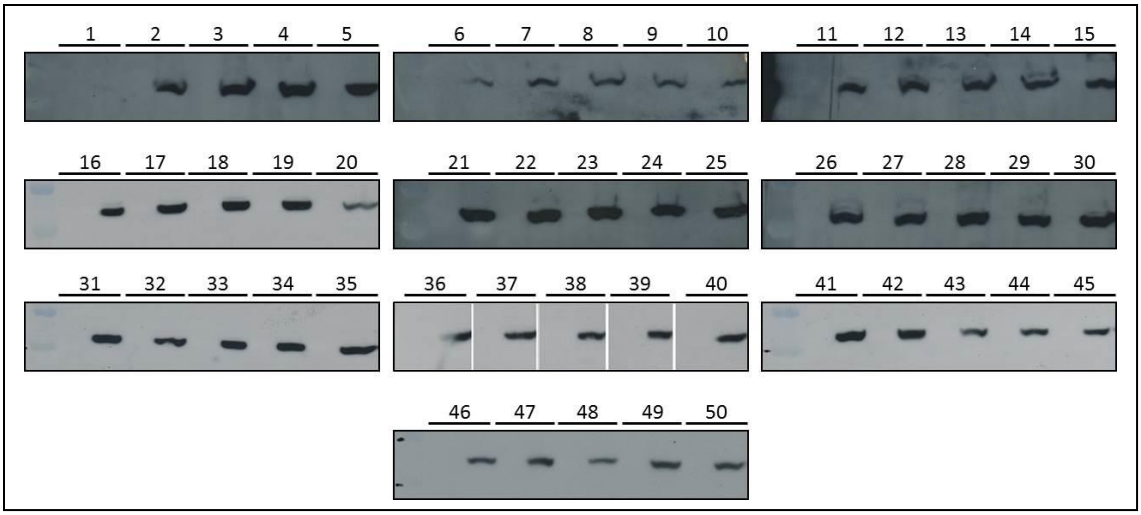

Figure 2.6. Screening of random *P. aeruginosa* transposon mutants. Western blot screening of 50 randomly selected transposon mutants from the generated EZ-Tn5 <TET-1> PAO1 library. Clones were grown at both 25°C and 37°C and Western blotting of whole cell lysates for expression of modified EF-Tu was performed using anti-ChoP antibodies. Clone 1 seemed to exhibit an altered modification phenotype but upon further testing was shown to have a normal EF-Tu modification profile (Data not shown).

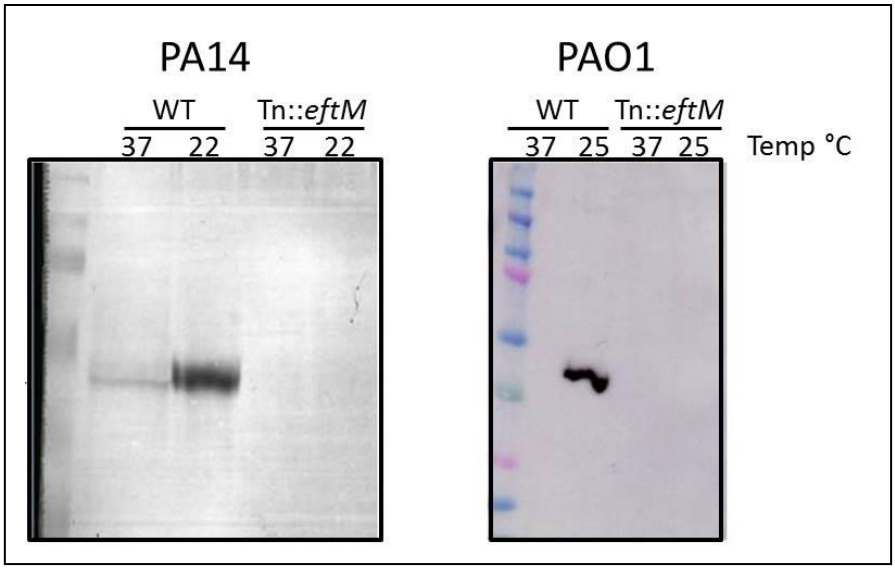

Figure 2.7. Modification of EF-Tu is linked to PA4178. (A) A single transposon mutant from the PA14 ordered transposon library, PA14_09870::MAR2xT7, has an altered EF-Tu modification phenotype when grown at 37°C and 25°C (lanes 3 and 4, respectively). Wild-type PA14 shows the normal temperature dependent modification phenotype at 37°C and 25°C (lanes 1 and 2, respectively) (Mariette Barbier). (B) The location of the transposon in PA14 corresponded to the gene PA4178 in strain PAO1. A transposon mutant in the gene PA4178 on the background strain PAO1 was obtained from the University of Washington Genome Sciences, PW8081. This mutant also showed no modification of EF-Tu at 37°C or 25°C (lanes 3 and 4, respectively). The wild-type showed normal temperature dependent modification phenotype at 37°C and 25°C (lanes 1 and 2, respectively).

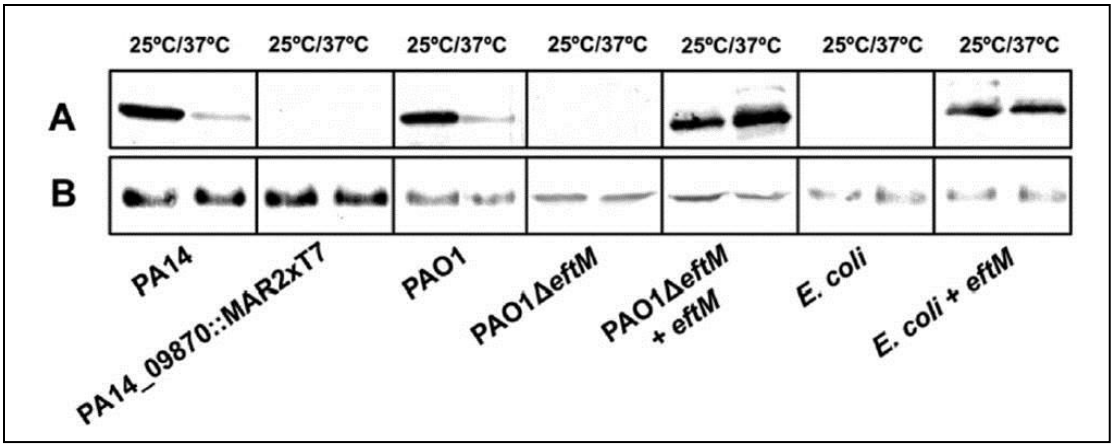

Figure 2.8. Western blot analysis of EF-Tu modification in different strains. Proteins of whole-cell extracts from different strains grown at 25°C or 37°C were subjected to electrophoresis and immunoblot analysis using antibodies specific for ChoP (monoclonal antibody TEPC-15) (A) or specific for EF-Tu as a loading control (B). The +*eftM* strains contained the plasmid pUCP18ApGw(*eftM*), a high copy number plasmid that constitutively expresses *eftM*. Adapted from (19) and used with permission of The American Society for Microbiology.

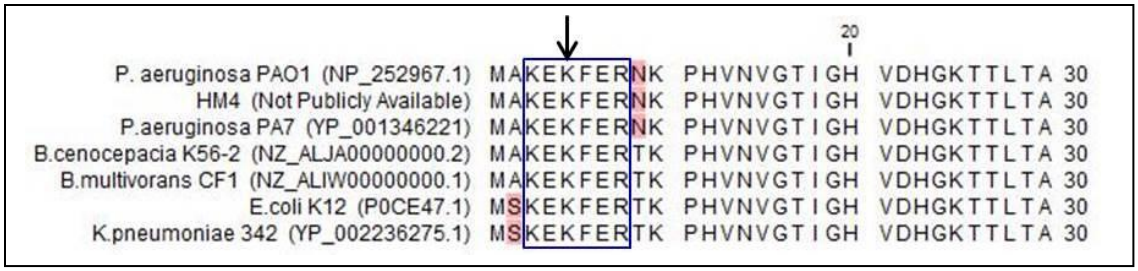

Figure 2.9. Amino acid sequence alignment of EF-Tu from various bacteria.

Alignment of amino acid sequences from various bacteria shows that the N-terminus of EF-Tu is extremely well conserved. Lysine 5 is uniformly conserved in all strains examined. Blue box indicates conserved KE**K**FER motif in all strains that may act as a possible recognition site for EftM. Solid red boxes indicate differences from the majority consensus sequence.

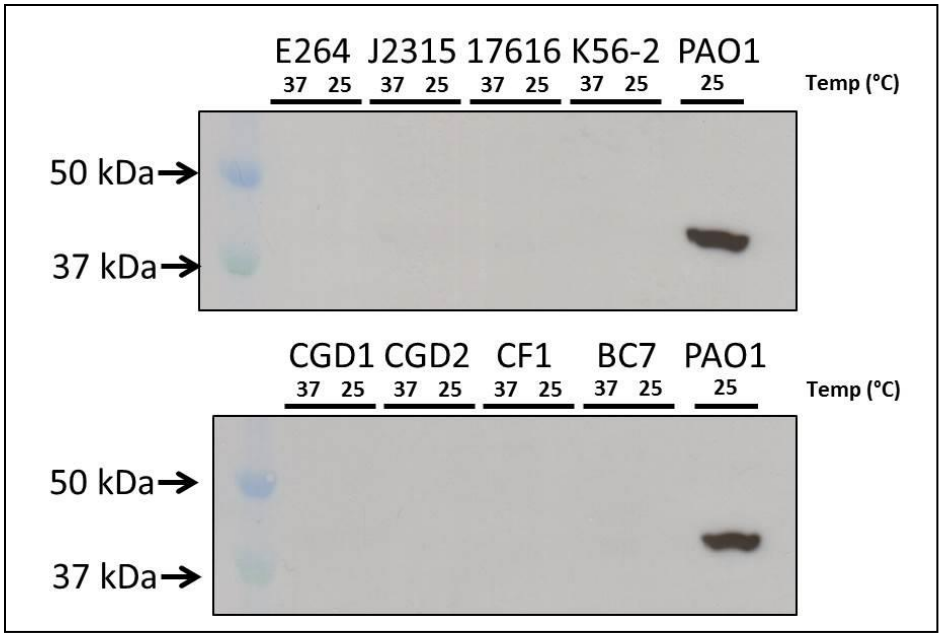

Figure 2.10. *Burkholderia* sp. are unable to modify EF-Tu. *Burkholderia sp.* are Gram-negative opportunistic pathogens of the class betaproteobacteria that are also known respiratory pathogens. Various species were tested by Western blotting of whole cell lysates from cells grown at both 37°C and 25°C using the anti-ChoP antibody. Strains 17616, CGD-1, CGD-2, and CF1 are all *B. multivorans*. Strains J2315, K56-2, and BC7 are all *B. cenocepacia*. Strain E264 is *B. thailandensis*. None of these strains contain a homologue to *eftM*. PAO1 grown at 25°C was used as a positive control.

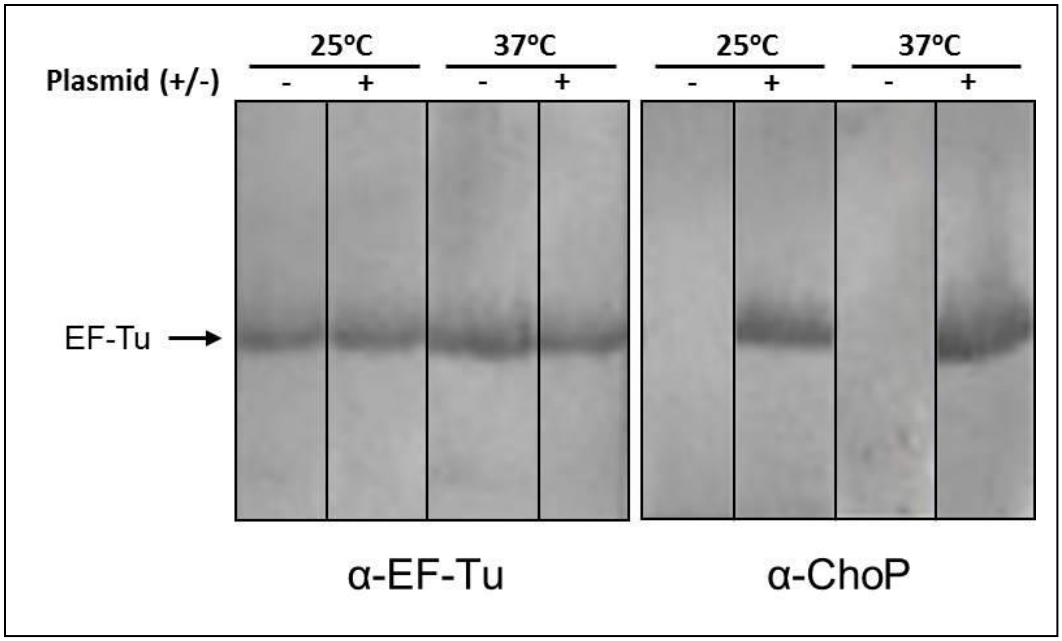

Figure 2.11. Exogenous expression of *eftM* in *K. pneumoniae* allows for expression of methylated EF-Tu. Western blots done using whole cell lysates from *K. pneumoniae* 52KO grown at low (25^{o}C) or high (37^{o}C) temperatures with (+) or without (-) the plasmid pUCP18ApGw *eftM*. Detection of protein on blots was done using either anti-EF-Tu antibody or anti-ChoP antibody (monoclonal antibody TEPC-15). (Mariette Barbier)

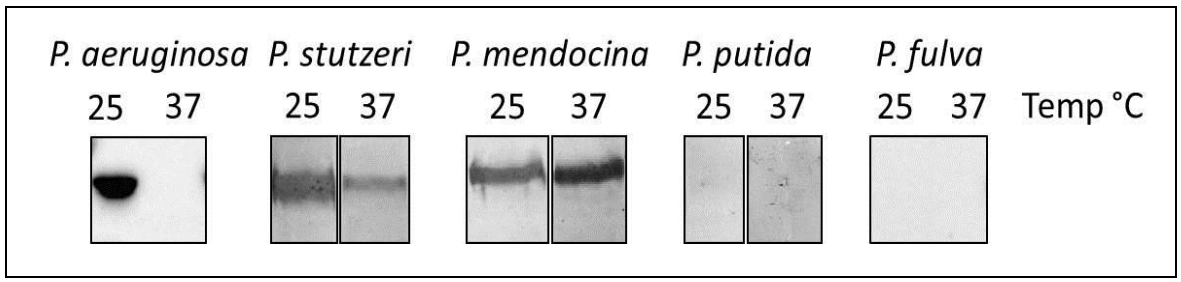

Figure 2.12. Ability of other *Pseudomonas* to naturally modify EF-Tu. Strains were grown at indicated temperature and whole cell lysates were tested by Western blotting using the anti-ChoP antibody TEPC-15 for modified EF-Tu. Both *P. stutzeri* and *P. mendocina* contain homologues of *eftM* and modify EF-Tu. *P. putida* is the only strain that does not contain a homologue of *eftM* and as expected, it does not modify EF-Tu. *P. fulva* contains a homologue of *eftM* but there is no observable methylation of EF-Tu likely due to an amino acid mutation in one of the predicted SAM binding domains. (Testing of all strains except *P. fulva* was done by Mariette Barbier and Inmaculada Martiez-Ramos).

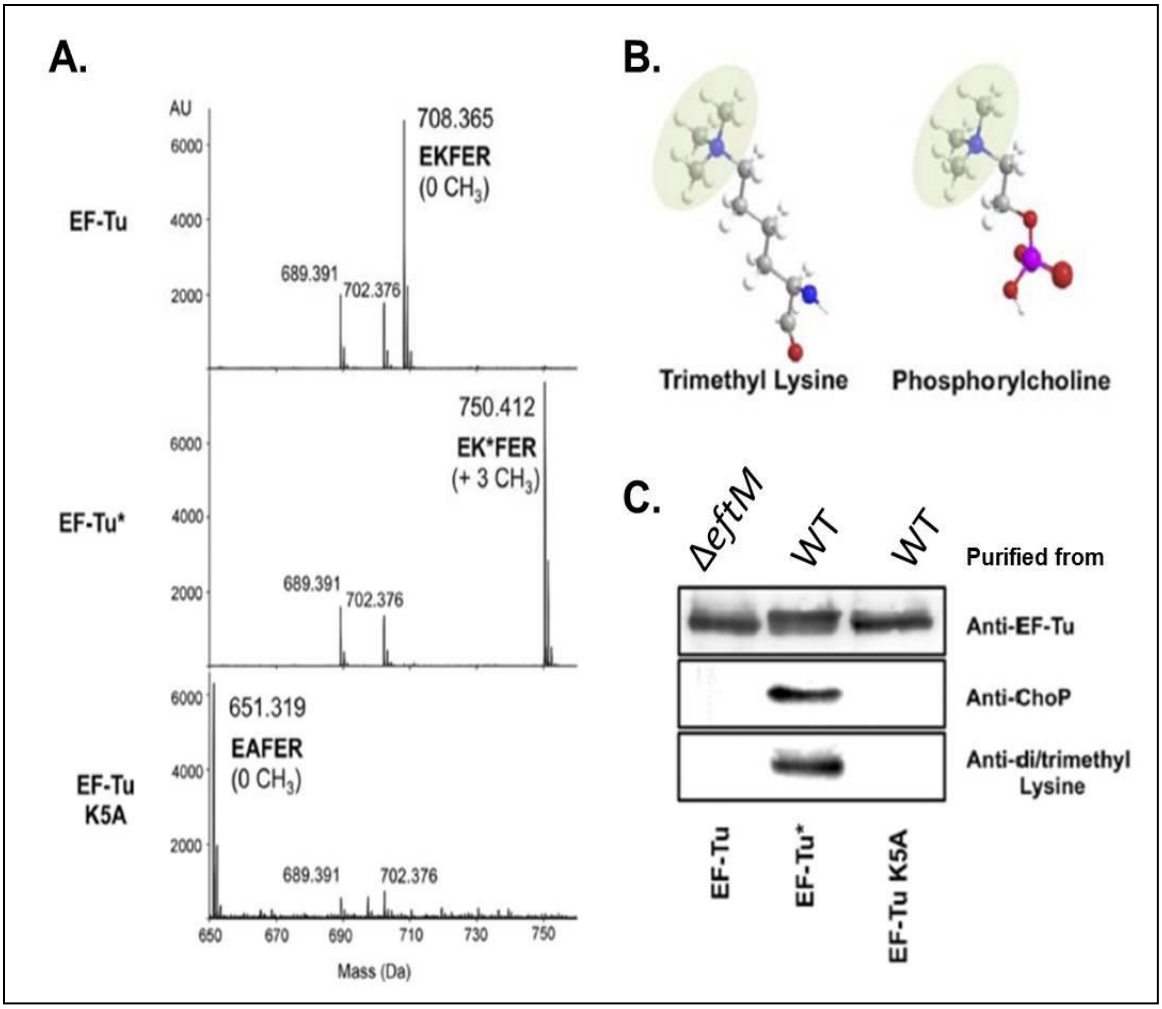

Figure 2.13. Trimethylation of EF-Tu by the elongation factor Tu-modifying enzyme (EftM). (A) Tandem mass spectrometry analysis of purified EF-Tu from the EftM-deficient mutant PAO1Δ*eftM* (EF-Tu, top), from the WT strain PAO1 (EF-Tu*, middle), and from PAO1 harboring the plasmid containing a K5A mutation in the *tufB* gene (EF-Tu K5A, bottom) digested with trypsin. All spectra contain peaks for two unmodified peptides at 689 Da (GTVVTGR, amino acids 228-234) and 702 Da (LLDEGR, amino acids 268-273). Mass spectrometry analysis had EF-Tu sequence coverage of approximately 38%. (B) Molecular structure of trimethyl lysine and phosphorylcholine with the methyl groups shadowed on both molecules. Atoms of

hydrogen, carbon, nitrogen, oxygen, and phosphorus are colored in white, gray, blue, red, and pink, respectively. (C) A Western blot of recombinant wild-type EF-Tu isolated from the EftM-deficient mutant (EF-Tu) and from the WT strain PAO1 (EF-Tu*) and recombinant EF-Tu harboring a K5A mutation in the *tufB* gene isolated from PAO1 (EF-Tu K5A) was probed with anti-EF-Tu, anti-ChoP (monoclonal antibody TEPC-15), and anti-di/trimethyl lysine antibodies. Adapted from (19) and used with permission of The American Society for Microbiology.

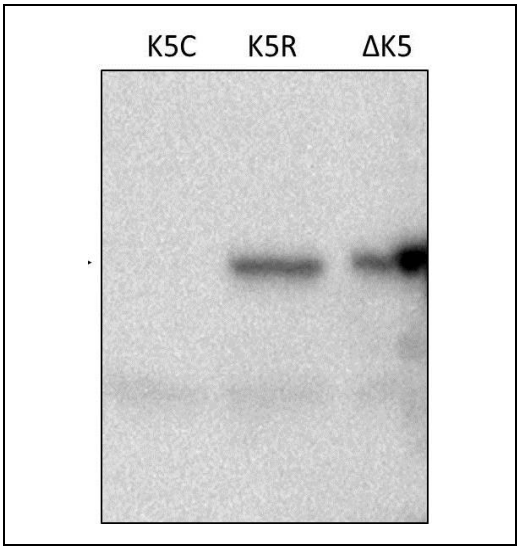

Figure 2.14. Western blot of recombinant EF-Tu isolated from PAO1. Recombinant EF-Tu variants were expressed in *P. aeruginosa* PAO1 grown at 25°C. Recombinant proteins were then affinity purified and used for Western blotting with the anti-di/trimethyl lysine antibody to examine methylation status. When lysine 5 is deleted or mutated to an arginine, methylation of EF-Tu is still detected. However, when lysine 5 is mutated to cysteine no EF-Tu methylation is observed.

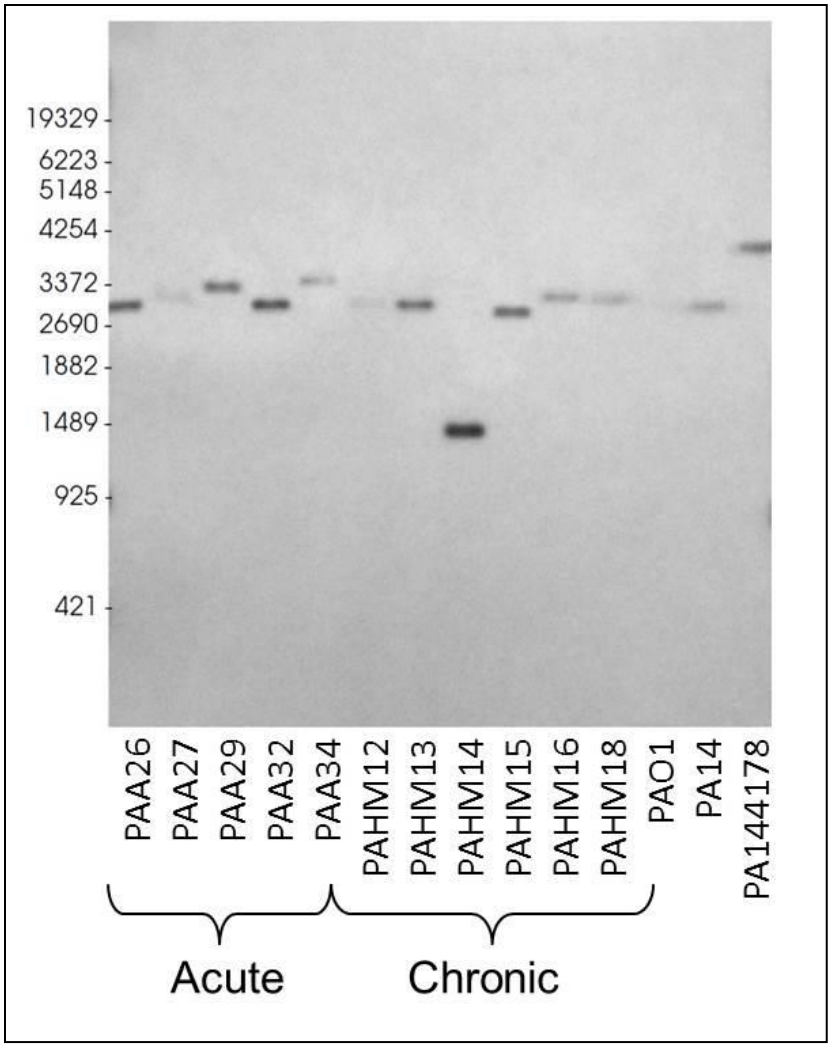

Figure 2.15. Type strains and clinical isolates of *P. aeruginosa* contain a single copy of *eftM*. Southern blot analysis was done using gDNA from 5 acute infection isolates, 6 chronic infection isolates, and 3 type strains. The blot was probed with a biotinylated PCR product of the entire *eftM* locus. Variations in size of the fragment are likely due to local variation in the sequence. Provided by Mariette Barbier.

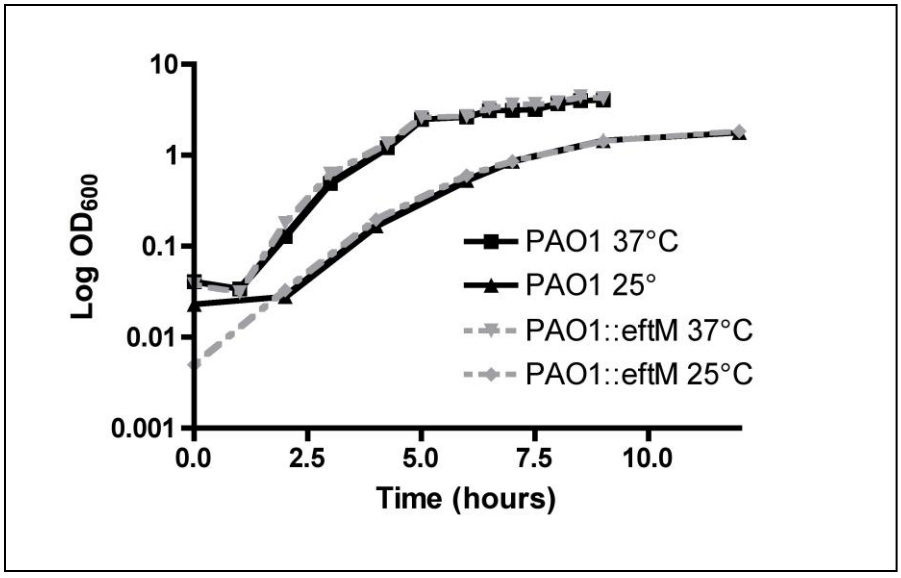

Figure 2.16. *eftM* does not affect growth of *P. aeruginosa.* Wild-type PAO1 and an isogenic mutant with a transposon insertion in *eftM* were grown at both 25°C and 37°C in LB. Optical density was monitored over time and plotted on a log scale. No difference in growth was observed between the wild-type and mutant at either temperature.

Table 2.1. Genes in the *lic1* operon in *H. influenzae*

Gene	Function	Description	Reference
lic1A	Choline kinase	Phosphorylates choline	(1)
lic1B	Choline transporter	Transports choline into cells	(2)
lic1C	Pyrophosphorylase	Activates choline using nucleoside diphosphate (CDP-Choline)	(1)
lic1D	Phosphorylcholine transferase	Transfers ChoP from activated NDP-choline to LOS	(1)

Table 2.2. List of strains, plasmids, and primers used in Chapter 2

Strain	Description	Source	Reference
DH909	PAO1 (DH395) Δ*pcs*	Deb Hogan	
DH920	PAO1 (DH395) Δ*pcs* + *pcs*	Deb Hogan	
DH395	PAO1 (DH395)	Deb Hogan	
DH503	PAO1 (DH395) *pchP::tn*	Deb Hogan	(86)
DH606	PA14 (DH122) Δ*pcs*	Deb Hogan	
DH122	PA14 (DH122)	Deb Hogan	(86)
DH466	PA14 (DH122) Δ*gbdR*	Deb Hogan	(86)
DH1142	PAO1 (DH1006) Δ*pcs*	Deb Hogan	
DH1143	PAO1 (DH1006) Δ*pcs* + *pcs*	Deb Hogan	
DH1006	PAO1 (DH1006)	Deb Hogan	
DH1079	PAO1 (DH1006) Δ*plcH*	Deb Hogan	
DH1007	PAO1 (DH1006) Δ*gbdR*	Deb Hogan	
DH1008	PAO1 (DH1006) Δ*gbdR* + *gbdR*	Deb Hogan	(86)
DH1596	PA14 (DH122) Δ*cbcV* Δ*betT3 betT1::pMQ*	Deb Hogan	(51)
AMT0021-1	Cystic fibrosis longitudinal isolate	Jane Burns	(87)
AMT0023-1	Cystic fibrosis longitudinal isolate	Jane Burns	(87)
AMT0023-35	Cystic fibrosis longitudinal isolate	Jane Burns	(87)
AMT0031-1	Cystic fibrosis longitudinal isolate	Jane Burns	(87)
AMT0031-2	Cystic fibrosis longitudinal isolate	Jane Burns	(87)
AMT0033-1	Cystic fibrosis longitudinal isolate	Jane Burns	(87)
AMT0033-3	Cystic fibrosis longitudinal isolate	Jane Burns	(87)
AMT0036-1	Cystic fibrosis longitudinal isolate	Jane Burns	(87)
AMT0036-3	Cystic fibrosis longitudinal isolate	Jane Burns	(87)
AMT0041-1	Cystic fibrosis longitudinal isolate	Jane Burns	(87)
AMT0041-3	Cystic fibrosis longitudinal isolate	Jane Burns	(87)

Table 2.2 continued List of strains, plasmids, and primers used in Chapter 2

Strain	Description	Source	Reference
AMT0047-1	Cystic fibrosis longitudinal isolate	Jane Burns	(87)
AMT0047-3	Cystic fibrosis longitudinal isolate	Jane Burns	(87)
AMT0060-1	Cystic fibrosis longitudinal isolate	Jane Burns	(87)
AMT0060-3	Cystic fibrosis longitudinal isolate	Jane Burns	(87)
AMT0062-1	Cystic fibrosis longitudinal isolate	Jane Burns	(87)
AMT0062-3	Cystic fibrosis longitudinal isolate	Jane Burns	(87)
AMT0066-1	Cystic fibrosis longitudinal isolate	Jane Burns	(87)
AMT0066-3	Cystic fibrosis longitudinal isolate	Jane Burns	(87)
AMT0071-1	Cystic fibrosis longitudinal isolate	Jane Burns	(87)
AMT0071-3	Cystic fibrosis longitudinal isolate	Jane Burns	(87)
AMT0073-1	Cystic fibrosis longitudinal isolate	Jane Burns	(87)
AMT0073-3	Cystic fibrosis longitudinal isolate	Jane Burns	(87)
AMT0074-1	Cystic fibrosis longitudinal isolate	Jane Burns	(87)
AMT0074-3	Cystic fibrosis longitudinal isolate	Jane Burns	(87)
AMT0075-1	Cystic fibrosis longitudinal isolate	Jane Burns	(87)
AMT0075-4	Cystic fibrosis longitudinal isolate	Jane Burns	(87)
AMT0076-1	Cystic fibrosis longitudinal isolate	Jane Burns	(87)
AMT0076-3	Cystic fibrosis longitudinal isolate	Jane Burns	(87)
NC-AMT0100-1	Cystic fibrosis longitudinal isolate	Jane Burns	(87)
NC-AMT0100-3	Cystic fibrosis longitudinal isolate	Jane Burns	(87)
NC-AMT0101-1	Cystic fibrosis longitudinal isolate	Jane Burns	(87)
NC-AMT0101-3	Cystic fibrosis longitudinal isolate	Jane Burns	(87)
PAO1	Wild type		
PAO1Φ*eftM*	PAO1 transduced with phage F116L disrupting *eftM*, Tet^r		
PW8081	PA4178-C06::ISlacZ/hah, Tet^r		(89)

Table 2.2 continued. List of strains, plasmids, and primers used in Chapter 2

Strain	Description	Source	Reference
PAO1Δ*eftM*	Partial deletion of *eftM* derived from PAO1		(19)
PA14			(90)
PA14_09870::MAR2xT7	PA14 with a transposon insertion in *eftM*, Gent^r		(90)
Plasmids			
pUCP18ApGw(*tufB*)	pUP18ApGw + *tufB* N-terminal 6x-His fusion, Carb^r		(19)
pUCP18ApGw(*tufB* K5A)	pUP18ApGw + *tufB* K5A N-terminal 6x-His fusion, Carb^r		(19)
pUCP18ApGw(*eftM*)	pUP18ApGw + *eftM* C-terminal FLAG fusion, Carb^r		(19)
pUCP18Ap	Escherichia-Pseudomonas shuttle vector, Carb^r		(84)
pUCP18ApGw	Gateway® compatible version of pUCP18Ap, Carb^r		
pENTR/SD/D-TOPO	Gateway® compatible directional cloning entry vector with Shine-Dalgarno sequence; Kan^r	Life Technologies	
Primers	**Sequence**		
tufBF	CACCATGCATCATCATCATCATATGGCTAAAGAAAAATTTGA		(19)
tufBR	TTATTCGATGATCTTGGCAACC		(19)
tufBFK5A	CACCATGCATCATCATCATCATATGGCTAAAGAAGCATTTGA		(19)
oJPO93	CACCATGGCTAAAGAATGCTTTGA		
oJPO94	CACCATGGCTAAAGAACGATTTGA		
oJPO95	CACCATGGCTAAAGAATTTGA		
PA4178 For	CACCATGGACTACAAGGATGACGATGACAAGATGTCCGCCACCGCG		(19)
PA4178 Rev	CTAGCGCTTCACGCAGACGAACAG		(19)
eftM-F-BhI	CCTTTGGGGATCCGGGAAC		(19)
eftM-R-HdII	GCTGAAGTAAGCTTCGGGGC		(19)
eftM-F-HdII	GGCAGAAGCTTCACCTTCGG		(19)
eftM-R-ErI	CGTCGCGGAATTCGCGGTTG		(19)

Chapter 3

Pseudomonas aeruginosa EftM is a SAM-dependent methyltransferase that methylates lysine 5 of elongation factor-Tu

Joshua P. Owings, Samantha M. Prezioso, Jeffrey Meisner, John J. Varga, Emily Kuiper, Natalia Zelinskaya, Graeme L. Conn, Eric B. Dammer, Duc M. Duong, Nicholas T. Seyfried, Sebastián Albertí, and Joanna B. Goldberg.

*Mass spectrometry analysis was done in the lab of Dr. Nicholas Seyfried, genomic replacement of *eftM* was done by Samantha Prezioso, and structural modeling of EftM was done by Dr. Jeffrey Meisner at Emory University, Atlanta, GA.

Abstract

Pseudomonas aeruginosa is a Gram-negative opportunistic pathogen that modifies elongation factor-Tu (EF-Tu) such that it can functionally mimic an important modification used by other respiratory pathogens to enhance adhesion and invasion of the respiratory epithelium. The nature of the modification of EF-Tu in *P. aeruginosa* was determined to be trimethylation of lysine 5 which occurs in a temperature-dependent manner where the modification is generally only seen when the bacterium is grown at temperatures close to ambient, but not at higher temperatures (37°C). The gene responsible for this modification was identified and named EF-Tu modifying enzyme (EftM). Differential modification of EF-Tu at different temperatures is not due to differences in transcription of *eftM*. Bioinformatic analysis of EftM showed little amino acid sequence similarity to known proteins but was predicted to be a SAM-dependent methyltransferase. Analysis of the amino acid sequence of EftM performed using HHpred suggested homology to Class I *S*-adenosyl-L-methionine (SAM)-dependent methyltransferases. We confirmed biochemically that EftM is a SAM-dependent methyltransferase that directly methylates lysine 5 of EF-Tu both *in vivo* and *in vitro*. Mass spectrometry analysis of products from these reactions confirmed that EF-Tu is trimethylated at lysine five. The methyltransferase activity of PAO1 EftM is slightly higher at 25°C compared to 37°C, while the rate of degradation of EftM expressed in *P. aeruginosa* is significantly decreased at 25°C compared to 37°C allowing for a longer half-life of the protein. The difference in the rate of degradation suggested an increase in protein stability at 25°C and was confirmed by heat pre-treatment of EftM. Pre-incubation at 37°C abolished methyltransferase activity while methyltransferase activity

was retained when pre-incubated at 25°C. These results suggest that the *in vivo* temperature-dependent phenotype is not transcriptionally regulated but is instead due to differences in the steady state levels of the EftM protein at different temperatures.

Introduction

The establishment of an infection initially requires that a pathogen attach to host cells to avoid clearance by physical means and to facilitate tissue tropism. Once a pathogen adheres, it must multiply and survive challenges from the host. To survive in this environment, pathogens have numerous virulence factors that vary from species to species. In *P. aeruginosa*, these virulence factors include phospholipases, exoproteases, type III secreted effectors, and siderophores (100). Some virulence factors also function as adhesins and include such surface exposed factors as lipopolysaccharide (LPS), flagella, and pili. These features allow bacteria to adhere to and invade epithelial cells but frequently make the bacterium susceptible to recognition by the host immune system. In respiratory pathogens, one strategy to evade the host immune response and increase the adhesive capacity of these molecules is the covalent modification of these surface exposed molecules with phosphorylcholine (ChoP). This modification can be found on the teichoic and lipoteichoic acids of *Streptococcus pneumoniae* (24) as well as the lipooligosaccharide of *Haemophilus influenzae* (26). This modification aids these pathogens in evasion or modulation of the host immune response as well as increase adhesion and invasion of the respiratory epithelium (9).

P. aeruginosa is an opportunistic Gram-negative pathogen which is the cause of significant morbidity and mortality in cystic fibrosis (CF) patients. When we looked for ChoP in this pathogen, we found that antibodies specific for ChoP reacted with a 43 kDa protein at ambient temperatures (25^{o}C), but not at temperatures more closely resembling body temperature (37^{o}C). Peptide analysis determined that the modification was on elongation factor-Tu (EF-Tu) (28). The traditional role of EF-Tu is in transporting aminoacyl-tRNAs to the ribosome to facilitate protein chain elongation (56). Numerous recent studies have shown that EF-Tu plays other roles in addition to its canonical function, these are termed 'moonlighting roles.' These roles include chaperone-like properties involved in the bacterial stress response (57), an as yet undetermined function in the presence of high iron (58), localization to the bacterial surface, and involvement in adherence to numerous proteins and host factors (12, 18, 19, 59-63).

Further analysis revealed that in *P. aeruginosa* that EF-Tu was not modified with ChoP but trimethylation of lysine 5 which structurally and functionally mimics ChoP (19). The trimethylation of lysine in *P. aeruginosa* provides functions similar to ChoP in other respiratory pathogens, including an increased ability to adhere to and invade the respiratory epithelium of the host (9). To identify the gene(s) responsible for this modification, we undertook a systematic screening of the ordered transposon mutant library from *P. aeruginosa* PA14 (90) and identified a single transposon mutant that was deficient in EF-Tu methylation. The transposon had disrupted a 'hypothetical' gene we termed EF-Tu modifying enzyme, *eftM* (PA4178). Deletion of *eftM* confirmed a loss of EF-Tu modification and complementation of the deletion mutant with plasmid-mediated

expression restored methylation of EF-Tu. Taken together, these data suggested that *eftM* played an important role in the modification of EF-Tu, but did not determine the direct function of EftM.

In this study, we confirm the annotated function of *eftM* as a *S*-adenosyl-L-methionine (SAM)-dependent methyltransferase. We purified both EftM and EF-Tu and developed *in vitro* methylation assays to determine the function and substrate of EftM. Previous work had identified the temperature-dependent methylation of EF-Tu *in vivo* as well as the loss of regulation when *eftM* was overexpressed, but did not address how this regulation occurred. We determined that the temperature-dependent phenotype is not a result of transcriptional regulation of *eftM*. This phenotype is instead largely a product of the temperature dependent stability of the EftM enzyme and its steady state levels. EftM exhibits a lower activity at high temperatures indicative of heat sensitivity and *in vitro* exposure to 37°C for any length of time abolishes the methyltransferase activity of the enzyme. In addition to decreased activity, at higher temperatures there is a significant decrease in the half-life EftM. Taken together, this data supports the idea that the temperature-dependent methylation of EF-Tu occurs because differences in steady state levels of EftM and rapid degradation of the protein at high temperatures.

Methods and Materials

Bacterial strains, plasmids and primers

The strains and plasmids used in this study are listed on Table 3.1. All primers used for cloning, sequence analysis, and RT-qPCR are also listed on Table 3.1.

RT-qPCR

An overnight culture of relevant strains was used to inoculate LB to OD_{600}=0.01. Cultures were incubated at 37°C or 25°C until a density of OD_{600}=0.5 was reached. 1mL aliquots were removed, pelleted, and resuspended in 1mL of TRIzol reagent (Life Technologies) before RNA purification according to manufactures instructions (Life Technologies). cDNA was generated using MultiScribe Reverse Transcriptase (Applied Biosystems) and gene-specific primers (Table 3.1). qPCR was run with FastStart SYBR green master mix (Roche) and gene-specific primers (Table 3.1): 95°C 10 min; 40 cycles of 95°C, 15 seconds, 60°C, 60 seconds; melt curve. Data was normalized to *omlA* and analyzed using GraphPad Prism version 4.0c for Mac (GraphPad Software, San Diego, California USA).

Preparation of whole-cell extracts

Cells were grown shaking in lysogeny broth (LB) (101) overnight at either 25°C or 37°C. Whole cell extracts were prepared by taking 0.5 ml equivalents of OD_{600} = 1.0 cultures, pelleting the cells, and resuspending in 30 µl water and 30 µl 2x Laemmli buffer (BioRad). Samples were boiled for 10 minutes before running 10 µl aliquots on 10% Mini-PROTEAN TGX gels (BioRad) and performing Western immunoblot analysis.

Plasmid construction

The *eftM* gene was cloned from PAHM23 into the *Pseudomonas* expression vector pUCP18ApGw, as previously described (19). Briefly, amplification of the coding

sequence was done using genomic DNA from PAHM23 as template with primers oJPO18 and oJPO19 (Table 3.1). The amplicon was cloned into the Gateway entry vector pENTR/SD/D-TOPO (Life Technologies) following manufacturer's instructions. The entry vector was propagated in TOP10 *E. coli* (Life Technologies) grown in LB supplemented with kanamycin (50 µg/ml) to purify the entry plasmids. Coding sequences were verified by sequencing with M13 Forward (-20) and M13 Reverse primers. Gateway LR Clonase II enzyme mix (Life Technologies) was used to clone from the entry vector into the destination vector pUCP18ApGw (19). The resulting plasmid was named pJPO7 and transformed into chemically competent DH5α cells with selection on LA + carbenicllin (100 µg/ml). Purified plasmid was used to transform PAO1Δ*eftM*.

The coding sequence of PAO1 *tufB* (PA4277) and PAO1 *tufB* K5A were amplified with an engineered N-terminal hexahistidine affinity tag using primer pairs tufBF/tufBR or tufBFK5A/tufBR, respectively (19). Amplicons were cloned into the Gateway entry vector pENTR/SD/D-TOPO (Life Technologies) following manufacturer's instructions. Entry vectors were propagated in TOP10 *E. coli* (Life Technologies) grown in Lysogeny Broth (LB) supplemented with kanamycin (50 µg/ml) to purify the entry plasmids. Coding sequences were verified by sequencing with M13 Forward (-20) and M13 Reverse primers. Gateway LR Clonase II enzyme mix (Life Technologies) was used to clone from the entry vector into the destination vector pDEST14 (Life Technologies) and the resulting plasmid was transformed into chemically competent DH5α cells with selection on LA + carbenicllin (100 µg/ml). pDEST14 vectors containing N-6xHis *tufB* or *tufB* K5A were named pJPO4 and pJPO5, respectively and were transformed into the

expression strain BL21-AI (Life Technologies) with selection on LA + carbenicllin (100 µg/ml).

The coding sequences of PAO1 *eftM* (PA4178), PAHM23 *eftM* and PAHM4 *eftM* were amplified from genomic DNA from PAO1, PAHM23, and PAHM4 respectively, using primers oJPO20/oJPO21 and oJPO90/oJPO119 listed on Table 3.1. PCR products were digested with NdeI and HindIII (NEB) for cloning into pCOLD II (Takara Bio) in-frame with an N-terminal hexahistidine affinity tag. Ligated plasmids were transformed into chemically competent DH5α cells and grown on LB + carbenicillin (100 µg/ml) for plasmid maintenance and sequencing. Resulting plasmids, named pJPO1, pJPO2, and pJPO10 respectively, were then transformed into rubidium chloride chemically competent BL21 cells (NEB) containing the pG-Tf2 helper plasmid coding for groES-groEL-tig (Takara Bio).

PAO1 *eftM* and PAHM4 *eftM* were cloned into pHERD20T where expression is controlled with the arabinose-inducible/glucose-repressible P_{BAD} promoter (102). PAO1 *eftM* was cloned using primers oJPO120/oJPO121 to amplify the coding sequence from PAO1 genomic DNA with the addition of engineered 5' and 3' restriction sites as well as a C-terminal FLAG tag. PAHM4 *eftM* was done in a similar fashion using primers oJPO122/oJPO123 with PAHM4 gDNA as the template. The amplicons and plasmid were digested with NcoI and HindIII before ligation using Fast-Link DNA ligation (Epicentre). Plasmids were transformed into chemically competent DH5α cells with selection on LA + carbenicllin (100 µg/ml). The insert was sequenced using pHERD

sequencing primers pHERD-SF and pHERD-SR (Table 3.1). The resulting plasmids were named pJPO6 and pJPO9, respectively, which were transformed into *P. aeruginosa* PAO1*ΔeftM* and selected on PIA + carbenicillin (300 µg/ml).

Purification of EF-Tu

Purification of his-tagged EF-Tu was done by propagating BL21-AI cells containing pJPO4 or pJPO5 in 1L cultures of ZYM-5052 supplemented with 0.2% arabinose [wt/vol] and carbenicillin (100 µg/ml) (103). Cultures were incubated overnight shaking at 25°C for 14 hours. Cells were pelleted at 12,000 x g for 10 minutes at 4°C and resuspended in 25 ml of Lysis buffer (GoldBio Bacterial Cell Lysis Buffer and 10 mM imidazole), 100 µl of DNase I (10 mg/ml, GoldBio), 300 µl ProBlock Gold Protease Inhibitor (GoldBio), and 0.2 mg/mL lysozyme (Roche). Cell suspensions were lysed using a French Pressure Cell (American Instrument Company) at 16-18k PSI. Lysates were then subjected to centrifugation at 12,000 x g for 10 minutes at 4°C to remove cellular debris before applying the supernatants to a column containing HisPur Ni-NTA resin (Thermo Scientific). Columns were washed three times with 1 ml wash buffer (50 mM sodium phosphate, 150 mM sodium chloride, 20% glycerol [vol/vol], 6 mM β-mercaptoethanol, 50 mM imidazole, pH 7.4) and eluted in four sequential 1 ml fractions of elution buffer (wash buffer + 250 mM imidazole, pH 7.4). Aliquots were removed from each elution to use for protein concentration determination by Bradford assay using the Bio-Rad Protein Assay (Catalog #500-0006) according to manufacturer's instructions. Aliquots were also added to an equal volume of 2x Laemmli buffer (BioRad) and run on

10% Mini-PROTEAN TGX gels (BioRad) before staining with GelCode Blue (Thermo Scientific) according to manufacturer's instructions.

Purification of EftM

Purification of his-tagged EftM was done by propagating BL21 cells containing pJPO1, pJPO2 and pJPO10 along with the helper plasmid pG-Tf2 overnight at 37°C in LB containing chloramphenicol (20 µg/ml) and carbenicillin (100 µg/ml). For protein expression, a 1L LB + carbenicillin (100 µg/ml) + chlorampheincol (20 µg/ml) + tetracycline (5 ng/ml) culture was started by the addition of 14 ml of the previously grown starter culture and incubated at 37°C until the OD_{600} reached 0.8-1.0. Cultures were then cooled in a 15°C water bath for 30 minutes before the addition of 0.5 mM IPTG for induction. Induced cultures were incubated shaking at 15°C for 20 hours.

Cells were pelleted at 12,000 x g for 10 minutes at 4°C. Cell pellets were resuspended in 25 ml of M Lysis buffer (50 mM Tris-HCl, 10 mM magnesium acetate, 250 mM ammonium chloride, 20% glycerol [vol/vol], 6 mM β-mercaptoethanol, 10 mM imidazole, pH 7.5), 100 µl DNase I (10 mg/ml, GoldBio), 300 µl ProBlock Gold Protease Inhibitor (GoldBio), and 0.2 mg/mL lysozyme (Roche). Cell suspensions were lysed using a French Pressure Cell (American Instrument Company) at 16-18k PSI. Lysates were then subjected to centrifugation at 12,000 x g for 10 minutes at 4°C to remove cellular debris before applying the supernatants to a column containing HisPur Ni-NTA resin (Thermo Scientific). Columns were washed three times with 1 ml wash buffer (50 mM Tris-HCl, 150 mM NaCl, 50 mM imidazole, 5 mM $MgCl_2$, 20% glycerol

[vol/vol], 6 mM β-mercaptoethanol, pH 7.5) and eluted in four sequential 500 µl fractions of elution buffer (wash buffer + 250 mM imidazole). Aliquots were removed from each elution to use for protein concentration determination by Bradford assay using the Bio-Rad Protein Assay (Catalog #500-0006) according to manufacturer's instructions. Aliquots were also added to an equal volume of 2x Laemmli buffer (BioRad) and run on 10% Mini-PROTEAN TGX gels (BioRad) before staining with GelCode Blue (Thermo Scientific) according to manufacturer's instructions.

SAM-binding assay

SAM binding was determined by differential radial capillary action of ligand assay (DRaCALA) modified from Roelofs *et al.* (104). In brief, 49µM of EftM or EftM G50R were briefly incubated (45 sec) with 5 µM [^{3}H]SAM (Perkin-Elmer, #NET155050UC) at room temperature before 3 µl aliquots were spotted onto a nitrocellulose membrane in triplicate. A "no protein" negative control was also performed using only buffer and [^{3}H]SAM. After allowing the membranes to dry, they were imaged by exposure to a tritium phosphor screen (GE Healthcare) for at least 18 hours before detection using a Typhoon FLA7000 phosphorimager (GE Healthcare). The fraction of SAM bound (F_B) was determined using the technique described by Roelofs *et al*. (104). Briefly, the intensity and radius of both the inner and outer spots were determined using ImageJ (105). Intensities and radii for each spot were then used to determine the fraction bound using the equation provided in Roelofs *et al*. (104). Results were plotted and analyzed by one-way ANOVA with Tukey's multiple comparison test using GraphPad Prism version 4.0c for Mac (GraphPad Software, San Diego, California USA).

Methyltransferase assay

A methyltransferase assay was developed and the detection of products was done by Western blotting for methylation. Reactions contained 1x HMT Buffer (NEB, 50 mM Tris-HCl, 5 mM $MgCl_2$, 4 mM DTT, pH 9 @ 25°C), 10 μM EF-Tu, and varying SAM and EftM concentrations. Reactions were allowed to incubate at 25°C or 37°C for varying amounts of time and heat inactivated by boiling in 2x Laemmli sample buffer (BioRad) for 5 minutes. The standard methyltransferase assay was done by combining 1 mM SAM, 10 μM EF-Tu, 10 μM EftM, and 1x HMT Buffer before incubation at 25°C for 20 minutes.

Heat pre-treatment was done by pre-incubating the protein at either 25°C or 37°C. The enzymes were incubated for varying times ranging from 5 to 60 minutes. At each time point, an aliquot of enzyme was removed and used in a methyltransferase assay at 25°C, as described above. Methyltransferase assays were allowed to proceed for 20 minutes before heat inactivation by boiling in 2x Laemmli sample buffer (BioRad) for 5 minutes. All samples were run on 10% Mini-PROTEAN TGX gels which were transferred to PVDF membranes and analyzed by Western blot using antibodies to detect di/trimethyl lysine (Millipore, 07-756).

***In vivo* stability assay**

A pulse-chase assay using an arabinose-inducible/glucose repressible expression plasmid, pHERD20T, was used (106). *P. aeruginosa* PAO1*ΔeftM* was transformed with pJPO6 or

pJPO9 and selected on PIA + carbenicillin (300 µg/ml). Strains were grown overnight at 37°C in LB + carbenicillin (300 µg/ml) and back-diluted 1:20 in LB + carbenicillin (300 µg/ml). After growth for 2 hours at 37°C, 2% arabinose [wt/vol] was added to induce expression of the proteins of interest. Cells were induced at 25°C for 2 hours before centrifugation at 12,857 x g for 2 minutes at 25°C. Pellets were washed in LB and resuspended in LB containing carbenicillin (300 µg/ml) and 1% glucose [wt/vol] to inhibit further transcription of *eftM* from pHERD20T. Resuspended cells were split equally and incubated at either 25°C or 37°C. Whole cell extracts were prepared by taking 0.5 ml equivalents of OD_{600} = 1.0 cultures at various intervals. Pellets were resuspended in 30 µl water and 30 µl 2x Laemmli buffer (BioRad) before boiling for 10 minutes.

Samples generated from PAO1*ΔeftM* transformed with pJPO6 were run on 10% Mini-PROTEAN TGX gels (BioRad) and transferred to low fluorescence PVDF membranes. Membranes were blocked in Odyssey blocking buffer (Li-Cor Biosciences) at room temperature for 2 hours before the addition of both primary antibodies anti-RpoA (1:2500) and anti-FLAG (1:2000) in Odyssey blocking buffer + Tween-20 [0.2% vol/vol]. Blots were incubated in primary antibodies for one hour at room temperature before washing and incubation with secondary antibody, IRDye 800CW goat anti-mouse IgG (Li-Cor) diluted 1:20000 in Odyssey blocking buffer + Tween-20 [0.2% vol/vol], at room temperature for 45 minutes. Imaging of blots was done using the Odyssey Classic imager (Li-Cor) and analyzed using Odyssey Imaging Software Version 2.1 (Li-Cor).

Samples generated from PAO1*ΔeftM* transformed with pJPO9 were subjected to the standard Western immunoblot analysis described below.

Genomic replacement of *eftM*

Genomic insertion into strain PAO1Δ*eftM* was done as previously described (107). Briefly, *eftM* and the 500 bp upstream region were cloned from PAO1 using primers SMP10 and SMP45. Amplicon and pUC18T-mini-Tn7T-Tp were digested with EcoRI-HF/BamHI-HF (NEB) and ligated using T4 ligase (NEB). Ligated plasmid (pSP05) was transformed into RbCl-competent *E. coli* DH5α for plasmid maintenance. Both pSP05 and pTNS3 (108) were electroporated into competent *P. aeruginosa* PAO1Δ*eftM* prepared as described (Chapter 2) and plated on PIA + trimethoprim (1500 μg/ml). Insertion into the chromosome was confirmed by PCR using primers P_{Tn7R} and $P_{glmS\text{-down}}$ as seen in Table 3.1.

Western immunoblot analysis

All Western blots were performed by running samples on 10% Mini-PROTEAN TGX gels (BioRad), transferring proteins to PVDF membranes (BioRad), and blocking for 1 hour in 5% non-fat dry milk [wt/vol]. After blocking, blots were incubated in primary antibody specific for di/trimethyl lysine (Upstate), FLAG M2 (Sigma-Aldrich), or RpoA (Neoclone) overnight at 4°C. Blots were incubated in appropriate secondary antibodies (anti-rabbit IgG, anti-mouse IgG, or anti-mouse IgG respectively) conjugated to horseradish peroxidase at room temperature for 1 hour. Antibody binding was detected using BioRad Clarity Western ECL reagent and the BioRad ChemiDoc MP imager. All

images were analyzed using Image Lab version 5.1 (BioRad) including densitometry analysis of specific bands.

MS-MS

Overnight in-gel chymotrypsin digestion was performed on *in vitro* reactions and peptides were extracted with a solution of 5% formic acid and 50% acetonitrile and speed vacuumed to dryness. An equal volume of each peptide sample resuspended in loading buffer (0.1% formic acid, 0.03% trifluoroacetic acid, 1% acetonitrile) and peptide eluents were separated on a 15 cm 1.9 μm C18 (Dr. Maisch, Germany) self-packed column (New Objective, Woburn, MA) by a NanoAcquity UHPLC (Waters, Milford, FA) and monitored on an Q-Exactive Plus mass spectrometer (ThermoFisher Scientific , San Jose, CA). Elution was performed over a 120 minute gradient at a rate of 325 nl/min with buffer B ranging from 3% to 80% (buffer A: 0.1% formic acid and 5% DMSO in water, buffer B: 0.1 % formic and 5% DMSO in acetonitrile). The mass spectrometer cycle was programmed to collect one full MS scan followed by 10 data dependent MS/MS scans. The MS scans were collected at a resolution of 35,000 (300-1800 m/z range, 1,000,000 AGC, 100 ms maximum ion time) and the MS/MS spectra were acquired at a resolution of 17,500 (2 m/z isolation width, 30% collision energy, 10,000 AGC target, 50 ms maximum ion time). Dynamic exclusion was set to exclude previous sequenced peaks for 30 seconds within a 10 ppm window. The SageN Sorcerer SEQUEST 4.3 algorithm was used to search and match MS/MS spectra to a complete semi-chymotryptic *E. coli* database harboring the recombinant EF-Tu sequence from *P. aeruginosa* PAO1 strain (total with 11,541 entries), including pseudo-reversed *E. coli* decoy sequences (109, 110).

Searching parameters included mass tolerance of precursor ions (±20 ppm) semi-chymotryptic restriction, dynamic modifications for oxidized Met (+15.9949 Da), tri-methyl lysine (+42.0470 Da), 4 maximal modification sites and a maximum of two missed cleavages. Only b and y ions were considered for scoring (Xcorr) and Xcorr along with ΔCn were dynamically increased for groups of peptides organized by a combination of chymotrypticity (fully or partial) and precursor ion charge state to remove false positive hits along with decoys until achieving a false discovery rate (FDR) of < 5% (< 0.25% for proteins identified by more than one peptide). The FDR was estimated by the number of decoy matches (nd) and total number of assigned matches (nt). FDR = 2*nd/nt, assuming mismatches in the original database were the same as in the decoy database (111). Following discovery based identification of the trimethylated EF-Tu lysine 5 peptide (m/z= 398.2) and corresponding unmodified peptide (m/z = 377.2), both were quantified on an Orbitrap XL hybrid mass spectrometer (ThermoFisher Scientific, San Jose, CA) using a targeted MS approach essentially as described (112). A user defined precursor mass tolerance of ±20 ppm was employed for extracted ion chromatogram (XIC) based quantification.

Results

EftM is a SAM-binding protein

Our previous work identified the *P. aeruginosa* gene, *eftM*, as necessary for the methylation of EF-Tu. We found that *P. aeruginosa* PAO1 methylates EF-Tu at 25°C but not 37°C (Figure 3.3), while a transposon mutant in *eftM* did not methylate EF-Tu at either temperature (19). During our survey of EF-Tu modification patterns among clinical

isolates (18), we identified PAHM23, which lacked modification of EF-Tu at both 25°C and 37°C, as detected by Western blot analysis of whole cell lysates (Figure 3.3). PCR of DNA from PAHM23 with primers designed to sequences upstream and downstream of the PAO1 *eftM* coding sequence was performed. Sequencing of the PCR product revealed a single nucleotide substitution (G148C) in the *eftM* coding sequence of PAHM23 compared to PAO1, which resulted in a non-synonymous amino acid mutation of glycine 50 to arginine (G50R) (Figure 3.2). The gene from PAHM23 was cloned into the expression plasmid pUCP18ApGw and transferred to the PAO1Δ*eftM*. As seen previously, expression of wild-type *eftM* under control of the constitutively expressed *lac* promoter restored modification of EF-Tu but there was a loss of temperature dependence such that EF-Tu was modified at both 25°C and 37°C (Figure 3.3) (19). Unlike PAO1 *eftM*, constitutive exogenous expression of PAHM23 *eftM* did not restore methylation of EF-Tu (Figure 3.3), indicating that EftM G50R is non-functional.

Pseudomonas.com classified EftM (PA4178) as a "hypothetical protein" that has a region with homology to class I *S*-adenosyl-L-methionine (SAM)-dependent methyltransferases (91). Amino acid 50 which is mutated in PAHM23 EftM is in the well-conserved E/DXGXG SAM-binding domain present in class I methyltransferases (77). To determine SAM-binding ability of EftM and EftM G50R, these genes were cloned into the cold-shock inducible vector pCOLD II (Takara). Recombinant proteins were overexpressed with the addition of a hexahistidine tag to allow for purification by Ni-NTA affinity chromatography. Equal molar (49 μM) concentrations of EftM and EftM G50R were used for DRaCALA to determine relative ability to bind SAM. EftM G50R

bound 46% less SAM, F_B=15%, compared to the wild-type EftM, F_B=28%, indicating the mutant has significantly decreased SAM binding ability (Figure 3.4).

EftM and SAM are necessary and sufficient to methylate EF-Tu

To determine if EftM is able to directly methylate EF-Tu, an *in vitro* methyltransferase assay was developed. Recombinant hexahistidine-tagged EftM proteins, wild-type and G50R, were overexpressed in *E. coli* and purified. Similarly, the substrate for this reaction, *P. aeruginosa* EF-Tu, was hexahistidine tagged, overexpressed, and purified from *E. coli*. A mutant form of EF-Tu was also purified: EF-Tu K5A is substituted in the previously identified methylation site (19). When purified EftM (~28 kDa) was incubated with both SAM and wild-type EF-Tu (~43 kDa) at 25°C for 20 minutes, we detected modification of EF-Tu by Western blot analysis of the reaction products using an anti-di/trimethyl lysine antibody (Figure 3.5). EftM is the enzyme responsible for modifying EF-Tu, and we observed no modification when EftM was not present (Figure 3.5, lane 2). Similarly, we observed that EF-Tu was not modified when SAM was not present in the reaction, indicating SAM is necessary for the reaction (Figure 3.5, lane 3). Based upon our *in vivo* overexpression where EftM G50R was unable to modify EF-Tu in cells (Figure 3.3), we predicted and observed a similar result in the *in vitro* assay (Figure 3.5, lane 4). Confirming our previous data (19), EF-Tu with an alanine mutation at lysine 5 was not modified (Figure 3.5, lane 5). Analysis of the reaction products by mass spectrometry confirmed that only in the presence of EftM is EF-Tu trimethylated at lysine 5 (Figure 3.6). Taken together, these results indicate that both EftM and the cofactor SAM are necessary to methylate EF-Tu on lysine 5.

Temperature-dependent methyltransferase activity is not due to transcriptional regulation of *eftM*

Previously, our laboratory reported that most *P. aeruginosa* strains methylate EF-Tu in a temperature-dependent manner in which EF-Tu is methylated at ambient temperature (<25°C) and remains unmethylated at body temperature (37°C) (Figure 3.3) (18). As EftM is the enzyme responsible for this modification, we hypothesized that transcriptional regulation of *eftM* at different temperatures contributed to the temperature dependent phenotype seen *in vivo*. To test this, we examined the transcript levels of EftM at both 25°C and 37°C. RT-qPCR was performed using primers specific for *eftM* and normalized to the control gene *omlA* (PA4765) (113). We saw that there was no difference in transcript levels of *eftM* when the cells were grown at 25°C compared to 37°C with a fold change of 0.7 ± 0.2 (Figure 3.7). This suggests that transcriptional regulation of *eftM* is not responsible for the observed temperature dependent modification phenotype. To validate our RT-qPCR assay, we used a nearby gene, *piv* (PA4175) that encodes protease IV, which is known to exhibit temperature responsiveness at the level of transcription, as a positive control (114-116). This analysis was consistent with previous studies showing *piv* exhibited about a 5-fold increase in transcription at 25°C compared to 37°C, 4.8 ± 1.0 (Figure 3.7).

EftM methyltransferase activity is lower at 37°C compared to 25°C

To test the activity of EftM at both the permissive (25°C) and the non-permissive temperatures (37°C), serial dilutions of EftM were made and methyltransferase assays

were initiated by the addition of SAM before incubation at the experimental temperature. Assays were allowed to proceed for 20 minutes before heat-inactivating the proteins and assaying by Western blotting for di/trimethyl lysine (Figure 3.8). Visual examination of the data suggested that 4-fold more EftM was necessary at the higher temperature to maintain equivalent activity.

To further test if incubation at 37°C is inactivating EftM, the enzyme was pre-incubated at either 25°C or 37°C for various amounts of time before subsequently removing aliquots to be used for the *in vitro* methyltransferase assay at 25°C. As seen in Figure 3.9, pre-incubation of EftM at 25°C for various times had no effect on the activity, while pre-treatment of EftM at 37°C for as little as 5 minutes results in no detectable *in vitro* methyltransferase activity, which recapitulates the phenotype seen *in vivo*. The lower panel of Figure 3.9 shows that there is no degradation of either EftM or EF-Tu confirming that neither protein is being degraded during this assay. If EftM is stabilized at 37°C by its ligand, SAM, pre-incubation at that temperature in the presence of SAM might prevent loss of activity. However, enzyme subjected to this pre-incubation at 37°C in the presence of 2 mM SAM still lost its methyltransferase activity (Data not shown).

As the activity of EftM appeared to be sensitive to temperature, seen in Figure 3.8, we examined if this temperature sensitive activity could be caused by a lower EftM stability. One of the hallmarks of *in vivo* protein instability is an increase in the rate of protein degradation. To detect differences in the protein stability, we employed a pulse-chase model where C-terminally FLAG-tagged EftM is expressed from the arabinose-

inducible/glucose repressible plasmid pHERD20T in the PAO1 mutant lacking *eftM*, PAO1Δ*eftM*. After a 2 hour incubation in the presence of 2% arabinose, the cells were washed and 1% glucose was added to inhibit further transcription of *eftM*. Protein levels were monitored by periodically removing samples and immunoblotting with antibodies to detect the presence of the FLAG-tagged protein and for RpoA as a protein loading control using the Odyssey scanner (Figure 3.10A). To determine the rate at which EftM is degraded, the integrated intensity of each band was determined using the Odyssey software and the intensity at Time 0 was set to 100% of produced protein. Relative protein concentrations were then used to plot the percent protein remaining over time (Figure 3.10B). Linear regression analysis of the data points indicates that the degradation of EftM is significantly higher at 37°C compared to 25°C ($P<0.0001$). The slopes of the lines can be used to calculate the half-life of the protein at either temperature with the half-life of EftM at 37°C being 45 minutes while at 25°C it is about 4 times longer, 172 minutes.

EF-Tu modification in clinical isolate PAHM4

The clinical isolate PAHM4 is a hypermutator strain that was isolated from a chronic bronchiectasis patient and exhibits numerous phenotypic differences from the laboratory strain PAO1. A comprehensive overview of the phenotype and genotype of PAHM4 is currently in preparation by our laboratory. One relevant phenotype is that PAHM4 modifies EF-Tu at both 25°C and 37°C (Figure 3.11). Similar to other isolates (Figure 2.15), duplication of the *eftM* genetic locus does not seem to be responsible for the observed EF-Tu methylation phenotype. Sequencing of *eftM* revealed that numerous

mutations resulted in 28 amino acid differences between PAHM4 and PAO1; however, unlike the differences between PAO1 and PAHM23, none of the mutations occur in any of the predicted SAM binding domains (Figure 3.2). When PAHM4 EftM was purified using the same techniques as PAO1 EftM, the yield was significantly higher, perhaps suggesting some of the mutations function to stabilize the protein (Figure 3.12).

Purified PAHM4 EftM was subjected to the same tests as PAO1 EftM. It has relatively the same affinity for SAM as determined by DRaCALA (Figure 3.4) suggesting that none of the mutations are involved in SAM binding, which is consistent with our protein alignment (Figure 3.2). Surprisingly, PAHM4 EftM has similar sensitivity to temperature when the enzyme was heat pre-treated and used for methyltransferase assays (Figure 3.13). Since EftM from both PAO1 and PAHM4 have similar sensitivity to temperature, we hypothesized that they would have similar stability resulting in similar protein half-lives *in vivo*. Interestingly, PAHM4 EftM has a longer observed half-life when compared to PAO1 (Figure 3.14). Our experiments suggest that the difference between PAHM4 and PAO1 may be in their kinetic properties. Time course methyltransferase assays performed using identical enzyme concentrations show that PAHM4 EftM methylates much more quickly than wild-type at 25°C (Figure 3.15).

Discussion

Our previous work showed that the presence of *eftM* was necessary for the methylation of EF-Tu *in vivo* (19). This was supported by bioinformatic analysis of the nucleotide sequence of EftM from strain PAO1 (PA4178) deposited on pseudomonas.com (91),

which predicted *eftM* to encode a 'hypothetical protein' with a functional classification of a SAM-dependent methyltransferase. We analyzed the amino acid sequence of EftM using a homology detection and search program, HHpred (117). This search revealed that EftM shares predicted structural features of a Class I SAM-dependent methyltransferases. The core domain of Class I methyltransferases consists of 7 β-strands with three α-helices on either side of the β-sheet (Figure 3.16, light blue). This fold loosely divides the protein into two halves (lobes) with one lobe binding SAM (Figure 3.16, pink) and the other specific for the substrate to be methylated (77).

Utilizing SAM, the large superfamily of methyltransferases can modify an astonishing array of substrates ranging from small molecules and proteins to DNA and RNA. With the ability to modify such a large variety of substrates, this superfamily of enzymes is an interesting case of convergent evolution where many different structures and sequences have evolved to perform the same biochemical reaction. Most of the enzymes in this superfamily share very little amino acid sequence identity with the exception of a few sequence motifs. However, when the tertiary structure is examined, it becomes clear that the structures within this superfamily fall broadly into five structural classes (class I-V). The architecture between the classes is highly divergent while the core folds within the each class are highly conserved. (77)

Of the proteins identified by HHpred as structurally homologous to EftM, DesVI has been the most rigorously studied with a published crystal structure (118). DesVI is involved in the biosynthesis of the macrolide antibiotic erythromycin in the bacteria

Streptomyces venezuelae. It uses SAM to add two methyl groups to dTDP-3-amino-3,4,6-trideoxy-α-D-glucopyranose to form dTDP-desosamine which is added to another molecule to form erythromycin (118). This crystal structure was used to generate a model of the predicted tertiary structure of EftM (Figure 3.16) bound to SAM using PyMOL, molecular visualization software (The PyMOL Molecular Graphics System, Version 1.5.0.4 Schrödinger, LLC). The rather large variable region of EftM (Figure 3.16, blue) is similar to that seen in DesVI and contains an α-helix and four anti-parallel β-strands. The variable domains of this class of proteins (Figure 3.16, blue) are responsible for substrate specificity and are often embellished to varying extents as seen in EftM. Another similarity to DesVI is the addition of a second embellishment, an N-terminal helix, which lies between the core domain and first embellishment (118).

Through the screening of clinical isolates, we identified a mutant deficient in methylation of EF-Tu. Cloning and sequencing of *eftM* from this isolate (PAHM23) surprisingly revealed a single nucleotide substitution resulting in a non-synonymous amino acid mutation, G50R. This mutation is located in a characterized SAM-binding motif seen in Class I methyltransferases often referred to as motif I, E/DX**G**XG (Figure 3.16B) (73), which is present from amino acids 46-52 of EftM. Purification of both wild-type and G50R EftM proteins continually yielded low protein concentrations that prevented substrate-ligand interaction analysis by traditional techniques such as isothermal titration calorimetry (ITC). A simple, quantitative assay had been developed by Roelofs *et al*. to examine protein-ligand interactions using small molecules such as cyclic-AMP and cyclic-di-GMP (104). This assay proved to be ideal because it had been shown to be

accurate using other small molecules and the total protein requirements were relatively low. We first validated this assay using a commercially available SAM-dependent methyltransferase, SET7 (BioRad). We determined the Kd of binding to SAM using DRaCALA was 9 ± 2 μM (Figure 3.17), which is similar to the value reported in the literature of 10.0 μM as determined by ITC (119). When this assay was used to determine binding of EftM to SAM, we were able to show that the G50R mutant was deficient in SAM binding (Figure 3.4), further validating the bioinformatics analysis (Figure 3.2). While binding of the G50R mutant to SAM was not zero, as predicted, we believe this is due to contamination of the protein preparation (Figure. 3.1b). As trans-complementation of PAO1Δ*eftM* with the EftM G50R protein did not allow for methylation of EF-Tu (Figure 3.3), this mutant protein served as our negative control in our *in vitro* assays. We also identified a mutant, PAHM4 EftM, which was able to methylate EF-Tu at both temperatures tested (Figure 3.11). Interestingly, this mutant had similar SAM binding capabilities as wild-type PAO1 EftM (Figure 3.4).

Our previous work had established that *eftM* was necessary *in vivo* for the methylation of EF-Tu (19). However, a direct cause and effect relationship between the protein and the modification was not revealed, it was only inferred that the enzyme was directly acting upon EF-Tu. The results of our *in vitro* methyltransferase assay reported here indicate that *eftM* is both necessary and, in the presence of the cofactor SAM, sufficient for the methylation of EF-Tu at lysine 5 in *P. aeruginosa*. SAM is a commonly used cofactor (78), second only to ATP. In the cytoplasm of *E. coli*, it is found in relative abundance, 184 μM-1.1 mM (79). Choline on the other hand is relatively scarce in bacteria. Most can

only obtain choline through scavenging of choline or choline containing compounds from their environment as they lack *de novo* choline synthesis pathways (9). The ability to use an abundant compound such as SAM to achieve similar survival advantages to ChoP may allow *P. aeruginosa* the metabolic flexibility to focus its energy elsewhere.

The data presented here suggest a mechanism for the regulation of the EF-Tu methylation phenotype that is seen *in vivo*. The traditional points of regulation for protein expression are transcriptional, translational, and post-translational regulation. There is no evidence that *eftM* is controlled at the transcriptional level by varying the copy number of coding mRNAs at different temperatures. This corroborated previous findings which had been measured independently by two different technologies, RNA-Seq and DNA microarray (114, 115). Additionally, all three technologies determine that the levels of *eftM* transcript are relatively low at both temperatures that appears to correlate with low levels of protein expression.

The idea that EftM has low steady state expression levels is supported by the genomic insertion of a single copy of the PAO1 *eftM* gene along with 500 bp upstream of the gene into the PAO1Δ*eftM* strain (Figure 3.18). The strain containing a single copy of this gene showed temperature-dependent methylation of EF-Tu. In contrast, the constitutive expression of *eftM* driven by the promoter on a multi-copy plasmid showed no temperature-dependent regulation of EF-Tu modification. The differences seen with gene dosage support the idea that small perturbations in steady state levels of EftM manifest itself as detectable or undetectable levels of EF-Tu modification.

To further examine how small changes in cellular levels of EftM affect modification of EF-Tu, we focused on differences in EftM activity and stability at 25°C and 37°C. Analyzing the amount of enzyme needed to reach similar levels of methylation, it would appear that EftM is about 4-fold more active at 25°C compared to 37°C (Figure 3.8). The apparent difference in activity can be explained by two contributing mechanisms. First, it could be that the enzyme is indeed less active at higher temperatures and has a decreased ability to add methyl groups at those temperatures; which is what we observed in (Figure 3.8) where it appears that more EftM is necessary at 37°C to achieve similar levels of methylation as seen at 25°C. Second, it could be that the enzyme is unstable at higher temperatures where structural integrity is lost, this could manifest itself as an apparent decrease in activity. However, the modification itself appears to be stable under these conditions. When the enzyme was pretreated at either 25°C or 37°C before being used in a standard methyltransferase assay at the permissive temperature of 25°C, it appears that the enzyme very rapidly loses activity when incubated at 37°C (Figure 3.9). This seemingly contradicts our activity data that shows EftM activity is present using high concentrations of the enzyme incubated at 37°C. A possible explanation for this is that heating of the 37°C sample was not immediate. As a result, as the reaction warmed to 37°, EftM continued to methylate EF-Tu before it was inactivated by the higher temperatures. PAHM4 EftM also exhibits this sensitivity to temperature *in vitro* (Figure 3.13) even though methylation of EF-Tu is seen at both temperatures *in vivo* (Figure 3.11) suggesting that there may be other factors present in PAHM4 to stabilize EftM. This loss of activity is presumably due to a loss of stability which *in vivo* could result in

the protein being rapidly degraded. This data appears to indicate that both mechanisms appear to be contributing to the observed phenotype.

To determine the half-life of EftM *in vivo*, we used a pulse-chase method with an arabinose-inducible/glucose-repressible system. Only recently are we beginning to understanding how bacteria use regulated proteolysis to affect tight control over protein levels within the cell (120, 121). Protein levels are quite dynamic and are typically measured as the half-life of a particular protein. The half-life of proteins *in vivo* varies greatly from protein-to-protein. Generally, as temperatures increase, proteins become unstable and expose degradation signals known as degrons normally hidden within the protein, leading to an increased rate of degradation (120). However, it is generally accepted that the optimal growth temperature for *P. aeruginosa* is closer to the temperature of the human body, 39°C (122). Additionally, as *P. aeruginosa* has the ability to infect humans, all essential cellular proteins must have the ability to function at 37°C. We determined that the half-life of PAO1 EftM at 37°C, 45 minutes, is significantly shorter than at 25°C, 172 minutes, which would indicate a loss of stability at higher temperatures (Figure 3.10). However, we have yet to monitor the half-life of the RNA message during this pulse chase, so it remains a possibility that the transcript itself is more stable at 25°C compared to 37°C. Interestingly, PAHM4 EftM also seems to be more quickly degraded at 37°C compared to 25°C; however, it seems to be degraded significantly slower than PAO1 EftM (Figure 3.14). This is supported by our data that shows pre-treatment of EftM at 37°C abolishes activity of the enzyme (Figure 3.9).

The differences in properties of EftM at different temperatures are similar to the phase variation that is seen in organisms that express ChoP. Those organisms have evolved various ways to alter their ChoP phenotype including differential gene expression via traditional regulation or slipped-strand mispairing during chromosome replication (9). Temperature sensitivity of the modifying enzyme adds a new epigenetic mechanism to the repertoire of phase variation.

From the perspective of the bacterium, the selective advantage to having modified EF-Tu would be during the initial interaction with human epithelial cells which would allow for increased adherence. Once the bacterium enters the body, the EftM protein would be quickly degraded and the only modified EF-Tu present would be that which was previously modified at environmental temperatures. This is supported by our data (Figure 3.10A, lower panel) and previous data which shows that after switching to growth in higher temperatures, modified EF-Tu persists for at least 4 hours and is presumably dependent on the rate of EF-Tu and not EftM turnover (28). This allows the bacterium to benefit from the increased adherence without the metabolic cost of using available SAM.

Our data suggests a model where the steady state levels of EftM are extremely important in its ability to modify EF-Tu. At lower temperatures, such as 25°C, EftM is stable and able to accumulate above the threshold for modification of EF-Tu. However, when the temperature is raised to 37°C, EftM is less stable which increases the likelihood that it is degraded and thus keeps the steady state pool of EftM relatively low. This low steady state level at high temperatures is below the threshold of which we would be able to

detect the product of the enzyme, modified EF-Tu. This is supported by the data from the PAHM4 EftM variant. The protein has a slightly longer half-life *in vivo* suggesting that it may be able to accumulate to a slightly higher concentration in the cells which would allow for methylated EF-Tu to accumulate above our limit of detection. Another possibility is that a demethylase specific for EF-Tu exists in PAO1 which is missing in PAHM4 or not regulated in the same fashion as in PAO1 such that it is not expressed at 37°C. Considering PAHM4 EftM has similar affinities for SAM and similar temperature sensitivity as PAO1 EftM, it is possible that it has a higher affinity for its substrate EF-Tu. A higher affinity for EF-Tu would allow it to methylate the substrate more quickly, which is what is seen in Figure 3.15.

It has not escaped our attention that the methylation of proteins interacting with the translational machinery of the cell could impact their performance in terms of efficiency and/or fidelity. Being that EF-Tu is an essential protein involved in the elongation of nascent protein chains, it is possible that methylation could result in changes to its function. Indeed, it has been previously shown that in *E. coli*, methylation of EF-Tu lysine 56 results in a decreased rate of tRNA-dependent GTPase activity (70). While no difference was observed in growth rate between the wild-type and PAO1Δ*eftM* mutant in nutrient rich media (19), it remains to be seen whether methylation of EF-Tu at lysine 5 impacts other aspects of its canonical or ‘moonlighting’ functions.

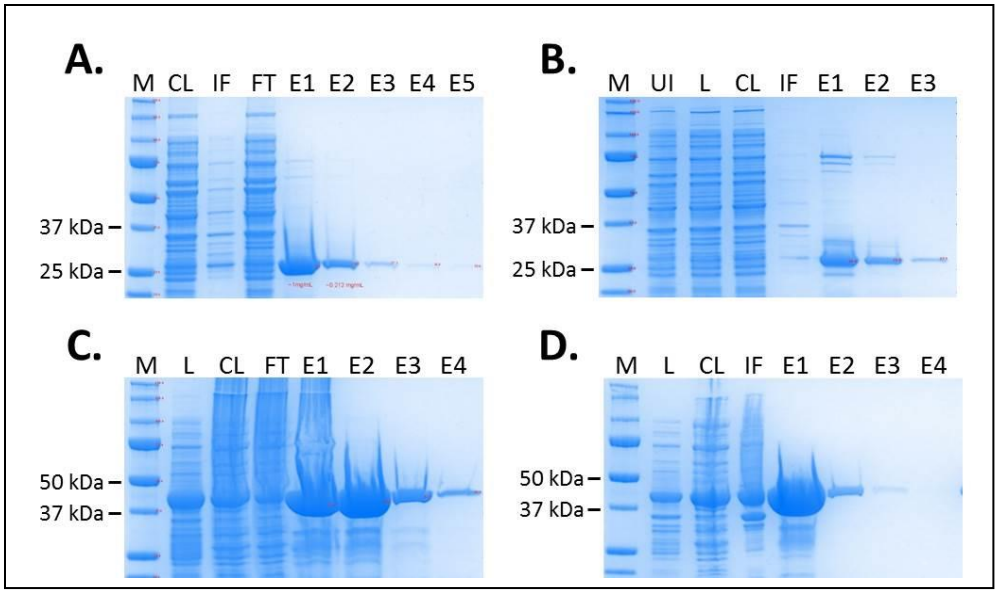

Figure 3.1. Representative purifications of EftM and EF-Tu. (A) His-tagged EftM, (B) His-tagged EftM G50R, (C) His-tagged EF-Tu, and (D) His-tagged EF-Tu K5A were purified according to protocols in Chapter 3. After purification, collected fractions were run on SDS-PAGE gels and stained with GelCodes Blue. Fractions are as follows: M – Marker, UI – Uninduced cells, L – Lysates of induced cells, CL – Cleared lysate with cellular debris removed, IF – Insoluble fraction, FT – Column flow through, E – Elutions.

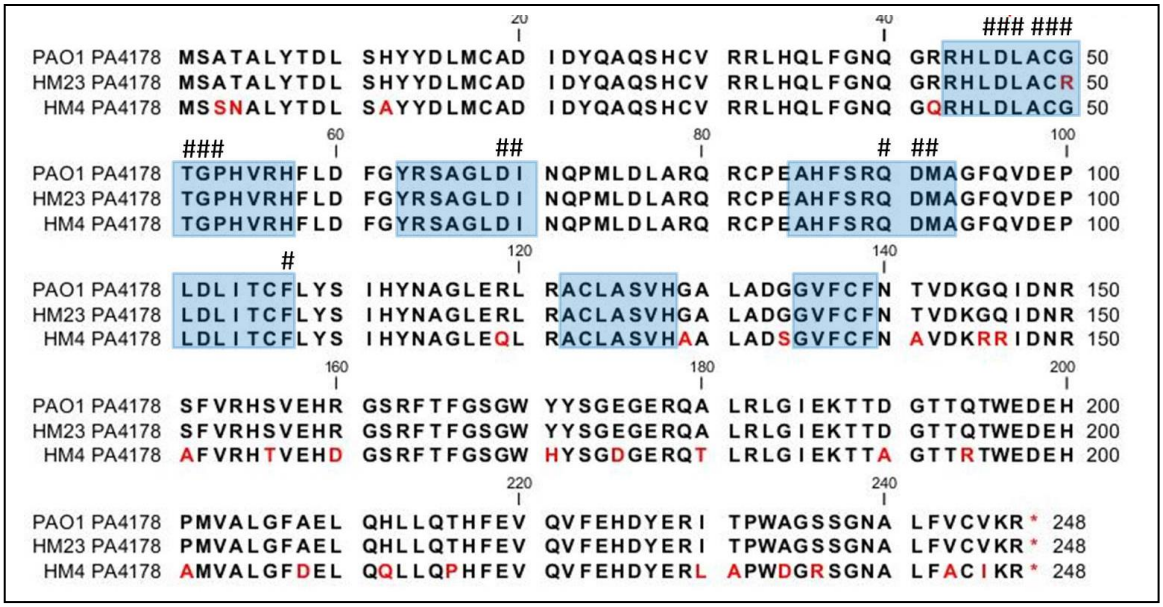

Figure 3.2. Amino acid sequence alignment of EftM in various *P. aeruginosa* strains. Amino acid sequences of EftM from PAO1 (typical EF-Tu modification), PAHM23 (no modified EF-Tu), and PAHM4 (modified EF-Tu at both 25°C and 37°C) were aligned with PAO1 EftM as the reference sequence. Blue boxes indicate amino acids within predicted methyltransferase domain and # indicate amino acids within the predicted SAM binding domain. VLE/DXGXGXG is the conserved motif I that is important for SAM binding, although only the GXG portion is present in EftM (amino acids 50-52). Differences from the PAO1 reference sequence are shown in red within the sequence.

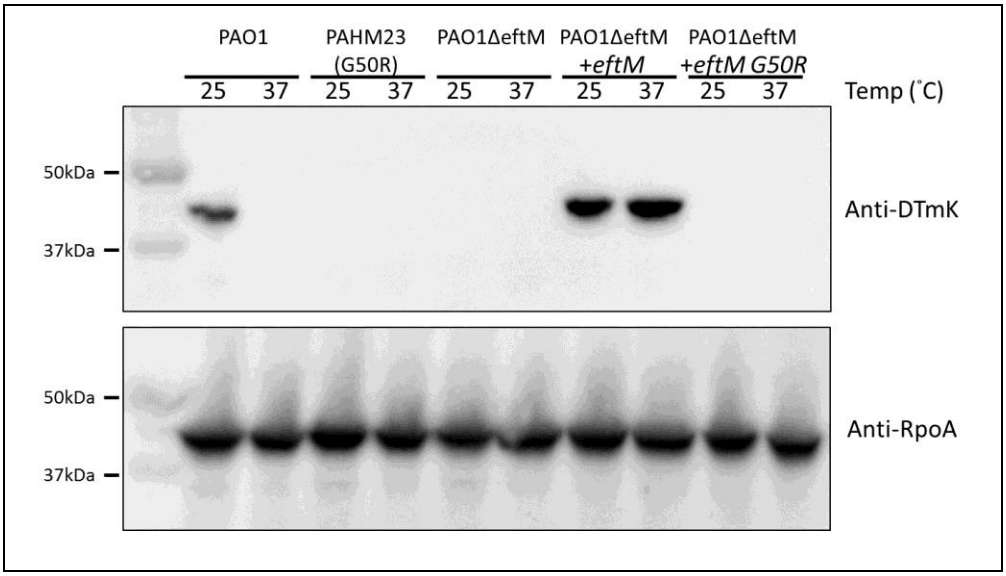

Figure 3.3. *P. aeruginosa* strains expressing wild-type *eftM* methylate EF-Tu *in vivo*. Western blot analysis of whole cell lysates from PAO1 wild-type and strains expressing various *eftM* mutants were grown at both 25°C or 37°C and blotted against both anti-di/trimethyl lysine (upper) and anti-RpoA (lower). PAHM23 is a clinical isolate containing a G50R amino acid mutation in *eftM*, PAO1Δ*eftM* is an isogenic PAO1 strain with a 100-bp deletion in *eftM* which was also complemented with high copy number constitutive expression plasmid pUCP18ApGw(eftM) (+*eftM)* or pJPO7 (+*eftM G50R*).

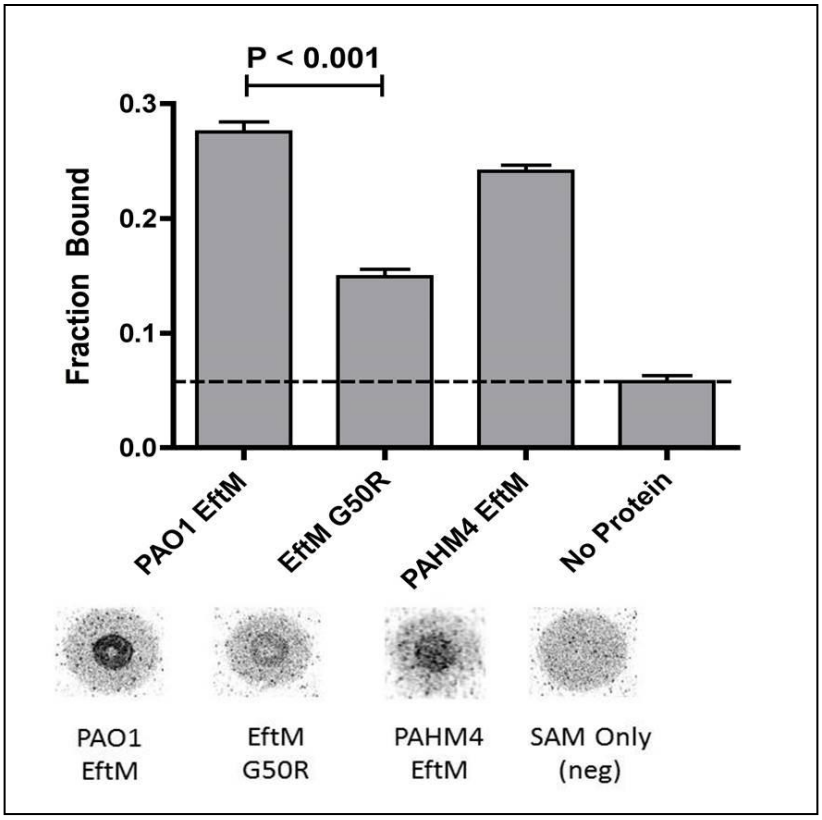

Figure 3.4. SAM binding capacity of EftM. Fraction bound of ^{3}[H]-SAM (5 μM) to EftM (49 μM), EftM G50R (49 μM), or PAHM4 EftM (47 μM) using DRaCALA (upper). EftM G50R has a 2-fold decrease in binding to SAM compared to both the wild-type ($P < 0.001$) and PAHM4 EftM (Not statistically tested due to different protein concentrations) at room temperature. Even using slightly less protein (likely within the margin of error for the protein assay), there is no difference in SAM binding between PAO1 and PAHM4 EftM. Dotted line indicates the level of background for the no protein negative control. Lower panel shows representative images from each protein used to calculate the fraction bound. Data represents the average values from three trials ($n = 3$).

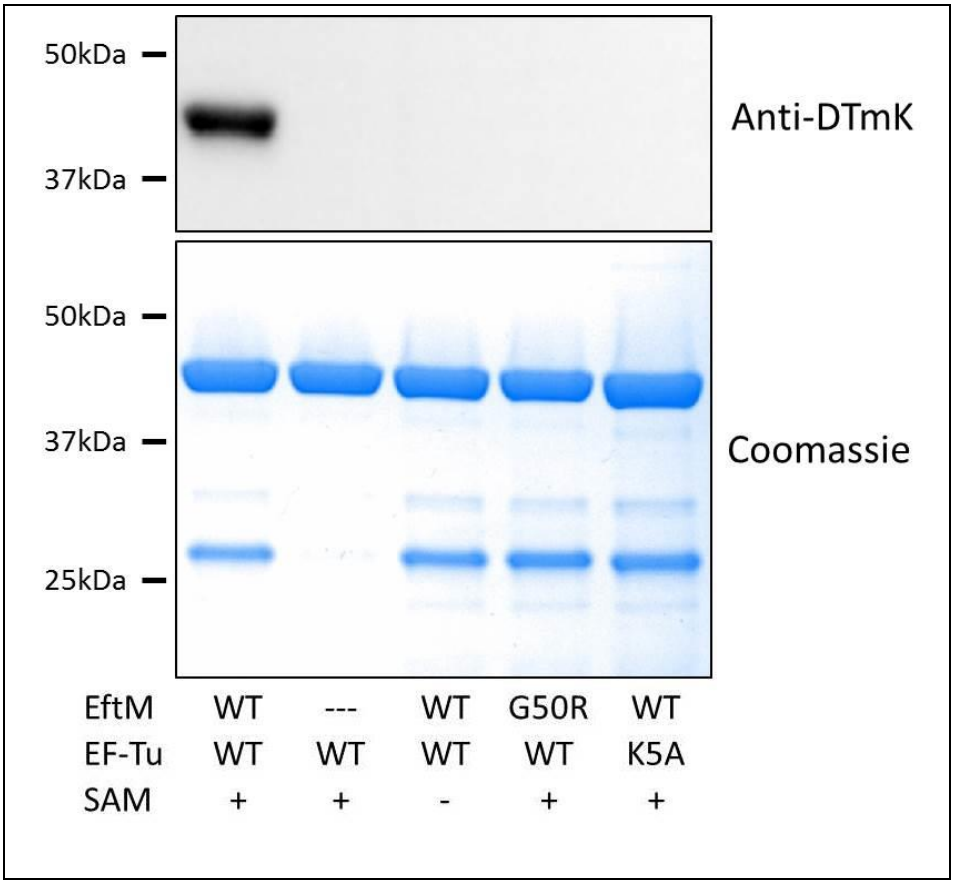

Figure 3.5. SAM and EftM are sufficient to methylate EF-Tu *in vitro.* A representative i*n vitro* methylation assay (n = 3) using purified wild-type (WT) EftM (~28 kDa, 6 µM) or a mutant in the E/DX**G**XG SAM binding domain (G50R) and purified wild-type EF-Tu (~43 kDa, 10 µM) or EF-Tu K5A shows that EftM requires SAM and is only able to methylate EF-Tu at K5. Upper panel is products of the methyltransferase assay Western blotted for di/trimethyl lysine and the lower panel is a Coomassie stained gel of the same reaction products.

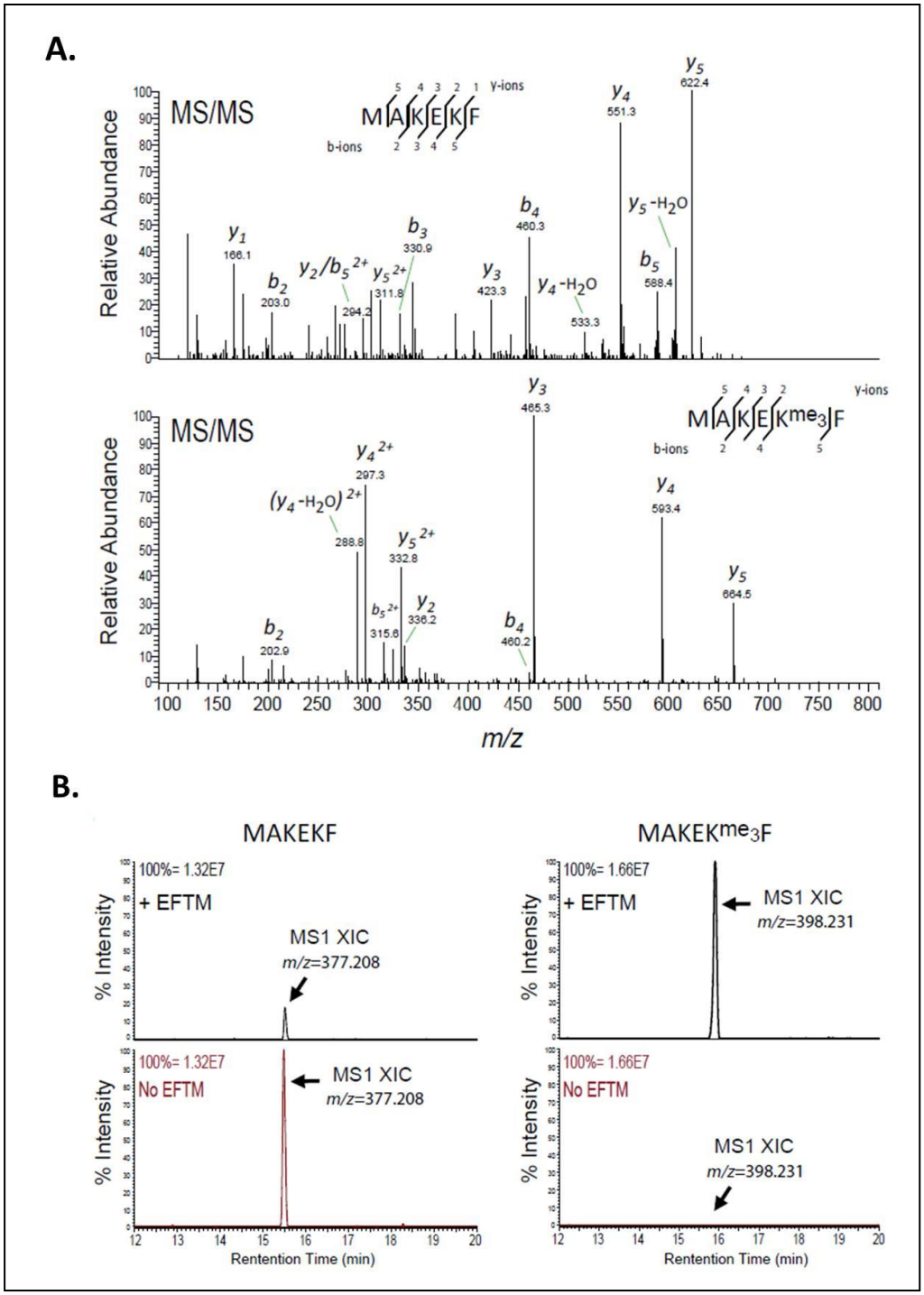

Figure 3.6. *In vitro* lysine 5 trimethylation and quantification on recombinant EF-Tu. Recombinant EF-Tu was incubated with or without recombinant EftM and SAM. Peptides were examined by LC-MS/MS following chymotrypsin digestion. (A**)** A

representative MS/MS spectrum of the EF-Tu doubly charged (M+2H) unmodified peptide sequence corresponding to amino acids 1-6 (top). A representative MS/MS spectrum of the doubly charged (M+2H) EF-Tu peptide (amino acids 1-6) corresponding to trimethylation of lysine 5 (bottom). A mass shift of 42 Da is observed on y_2 and y_3 ions on the modified MS/MS spectrum compared to the unmodified peptide spectrum, which unambiguously assigns the site of lysine trimethylation to residue 5. (B) Precursor (MS1 scans) extracted ion chromatograms (measured as the percentage intensity using ±20 ppm mass tolerance) for the trimethylated EF-Tu lysine 5 peptide (*m/z* = 398.231) in the EftM treated and untreated samples (left). Precursor extracted ion chromatograms for the unmodified EF-Tu peptide (*m/z* = 377.208) is also shown (right). *X*-axis indicates the retention time when the peptide eluted from the LC column. Peptide intensities were normalized to 100% for sample with the most intense signal in each panel.

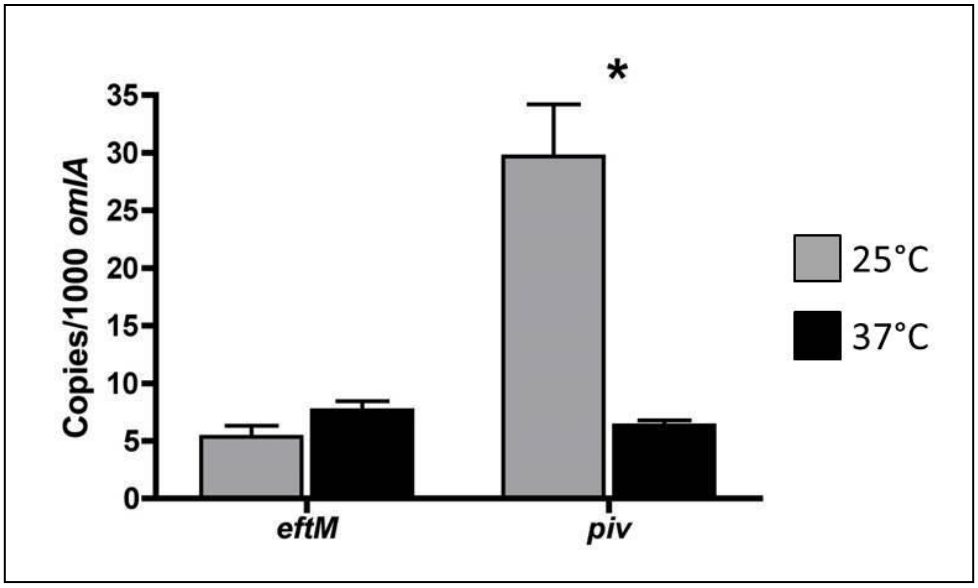

Figure 3.7. *eftM* transcript levels are not temperature sensitive. RT-qPCR shows that there is no statistical difference in transcript levels of *eftM* (n = 3) at 25°C compared to 37°C, 0.7 ± 0.2 fold decrease at 25°C compared to 37°C, relative to the control gene *omlA*. A gene that is known to be upregulated at 25°C, *piv* (n = 3), shows 4.8 ± 1.0 fold increase at 25°C compared to 37°C relative to the control gene *omlA*.

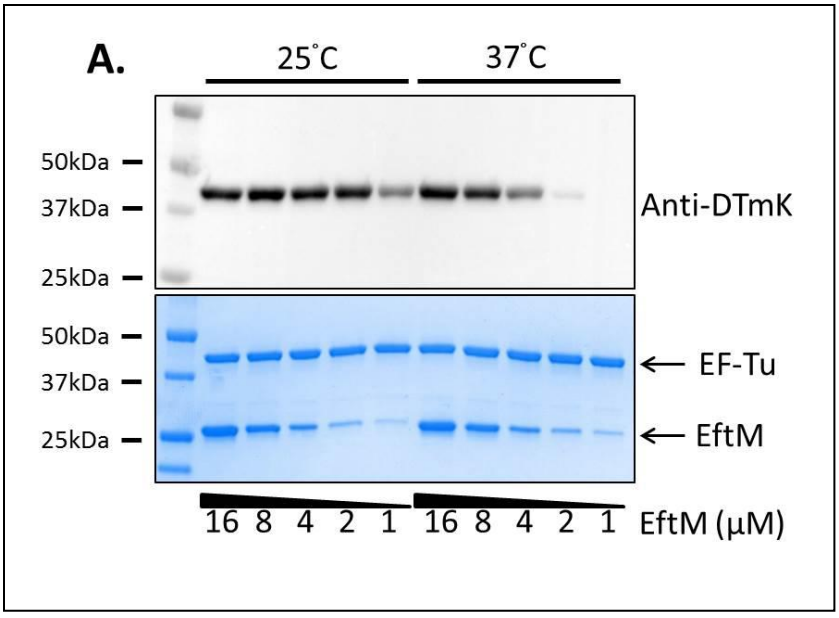

Figure 3.8. EftM methyltransferase activity varies by temperature.

(A) Representative (n = 3) Western blot (upper) from methyltransferase reaction products using varying concentrations of EftM (16 μM-1 μM) at both 25°C and 37°C blotted for di/trimethyl lysine. Same reaction products stained with GelCodes blue (lower).

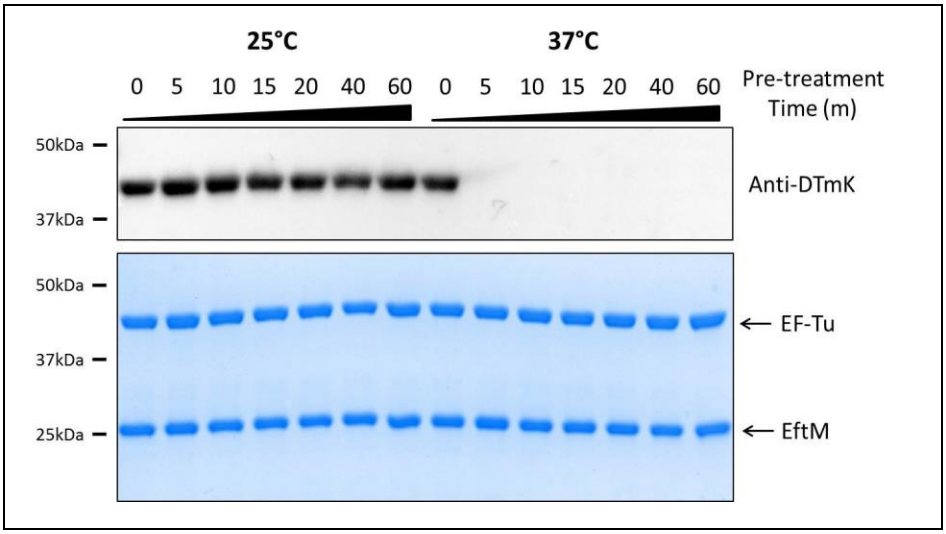

Figure 3.9. EftM methyltransferase activity is temperature sensitive. Representative Western blot (upper) of products from methyltransferase assays done at 25°C after a pre-incubation (0 min-60 min) at 25°C or 37°C and blotted with antibodies to di/trimethyl lysine. Loss in activity of EftM is not due to protein degradation as seen by Coomassie staining of reaction products (lower) (n = 5).

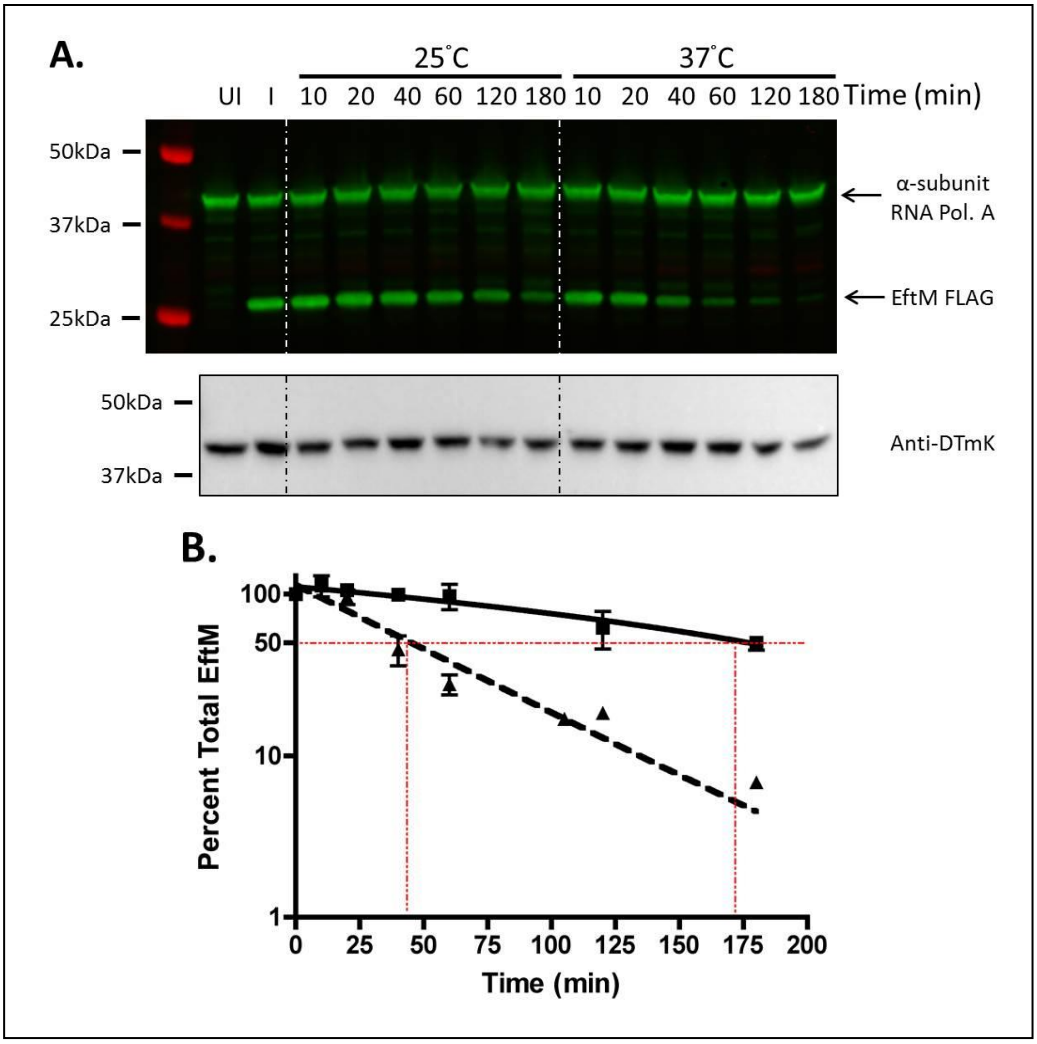

Figure 3.10. EftM has a shorter half-life *in vivo* at 37°C compared to 25°C. Strain PAO1Δ*eftM* was complemented with *eftM* on a plasmid, pHERD20T, under control of the arabinose-inducible/glucose-repressible P_{BAD} promoter. Production of EftM was induced for 2 hours at 25°C with 2% arabinose [wt/vol] before washing the cells and resuspending in LB + 1% glucose [wt/vol]. Cultures were then split and incubated at either 25°C or 37°C and the (A) *in vivo* degradation of EftM was monitored by Odyssey Western blotting for recombinant FLAG-tagged EftM (28 kDa) and the α-subunit of RNA polymerase (37kDa) as a loading control (upper panel). Methylation status of EF-

Tu was monitored by Western blot of these same samples using anti-di/trimethyl lysine antibodies (lower panel). (B) The rate of degradation was plotted by using integrated intensity analysis of the bands in the Odyssey blots generated (A) using time zero as 100% intensity (n = 3). Linear regression analysis of data points was done and slopes were determined to be significantly different ($P<0.0001$). The equation generated for each line was used to calculate the time at which 50% of the protein was remaining (half-life) at each temperature. At 37°C the half-life was determined to be 45 min and at 25°C was determined to be 172 minutes. Intersection of red dashed lines with the black lines represents the half-live of EftM at 37°C (black dashed line) and 25°C (black solid line).

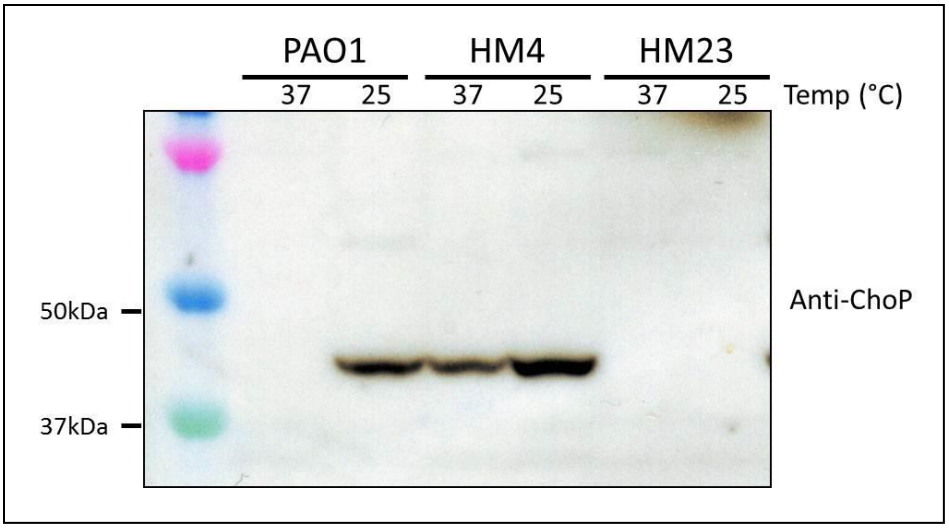

Figure 3.11. PAHM4 and PAHM23 show different EF-Tu modification profiles. Western blot of whole cells lysates from the type strain PAO1 and clinical isolates PAHM4 and PAHM23 blotted using anti-ChoP HAS antibody. The isolate PAHM4 exhibits modification of EF-Tu at both tested temperatures while PAHM23 does not modify EF-Tu at either temperature.

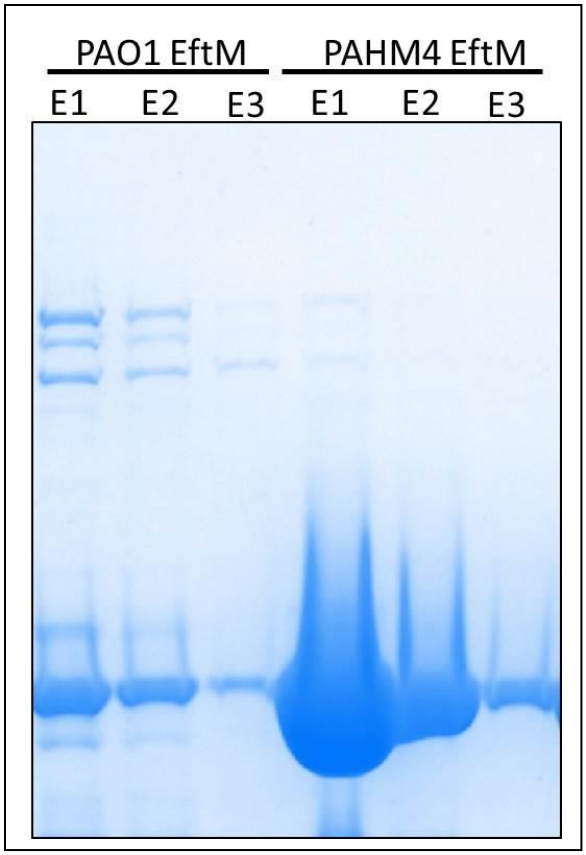

Figure 3.12. Purification of PAO1 and PAHM4 EftM. Purification of PAHM4 yields a much greater amount of purified protein compared to PAO1. Elutions are from the purification of His-tagged EftM expressed from the pCOLDII plasmid in BL21 cells + pG-Tf2. Purifications were done using the same protocol with equal volumes of cultures and were eluted into the same volume. This suggests that PAHM4 EftM may be more stable than wild-type PAO1 EftM.

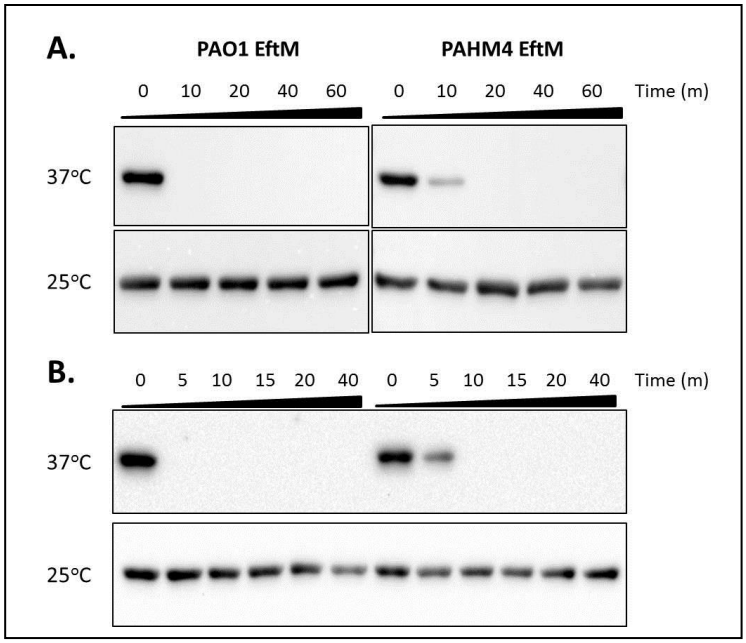

Figure 3.13. PAHM4 EftM methyltransferase activity is sensitive to heat pre-treatment. (A) A Western blot of products from methyltransferase assays using both PAO1 and PAHM4 EftM done at 25°C after a pre-incubation (0 minutes - 60 minutes) at 25°C (lower) or 37°C (upper) and blotted against di/trimethyl lysine. PAHM4 EftM (Right) is more tolerant of heat compared to PAO1 EftM (Left). (B) A repeat of this experiment with a shorter time frame (5 minutes - 40 minutes) shows similar results with PAHM4 EftM exhibiting greater heat tolerance.

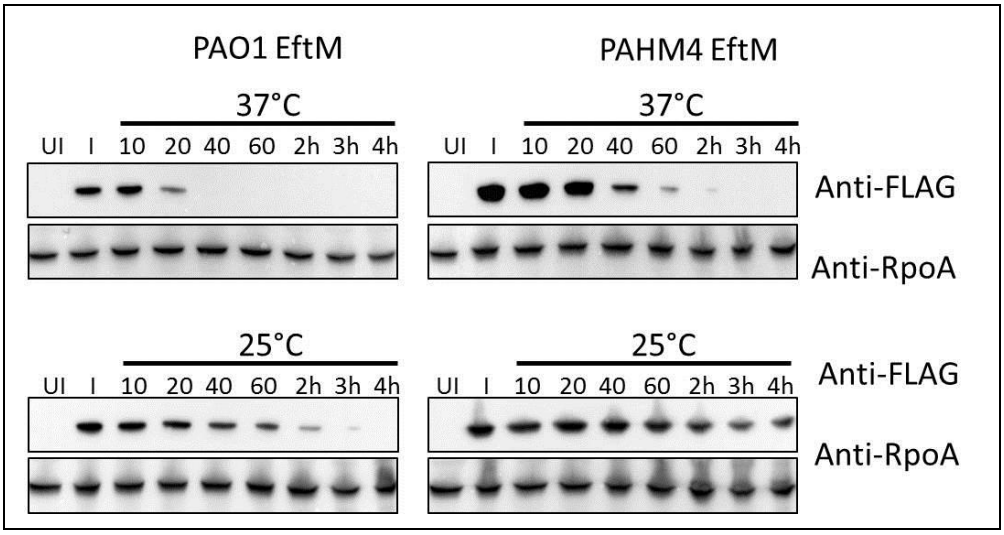

Figure 3.14. PAHM4 EftM has a longer half-life *in vivo* compared to PAO1 EftM. Strain PAO1Δ*eftM* was complemented with *eftM* or PAHM4 *eftM* on a plasmid, pHERD20T, under control of the arabinose-inducible/glucose-repressible P_{BAD} promoter. Production of EftM was induced for 2 hours at 25°C with 2% arabinose [wt/vol] before washing the cells and resuspending in LB + glucose. Cultures were then split and incubated at either 25°C or 37°C and the (A) *in vivo* degradation of EftM was monitored by Western blotting for recombinant FLAG-tagged EftM (28 kDa) and RNA polymerase (37kDa) as a loading control using chemiluminescence.

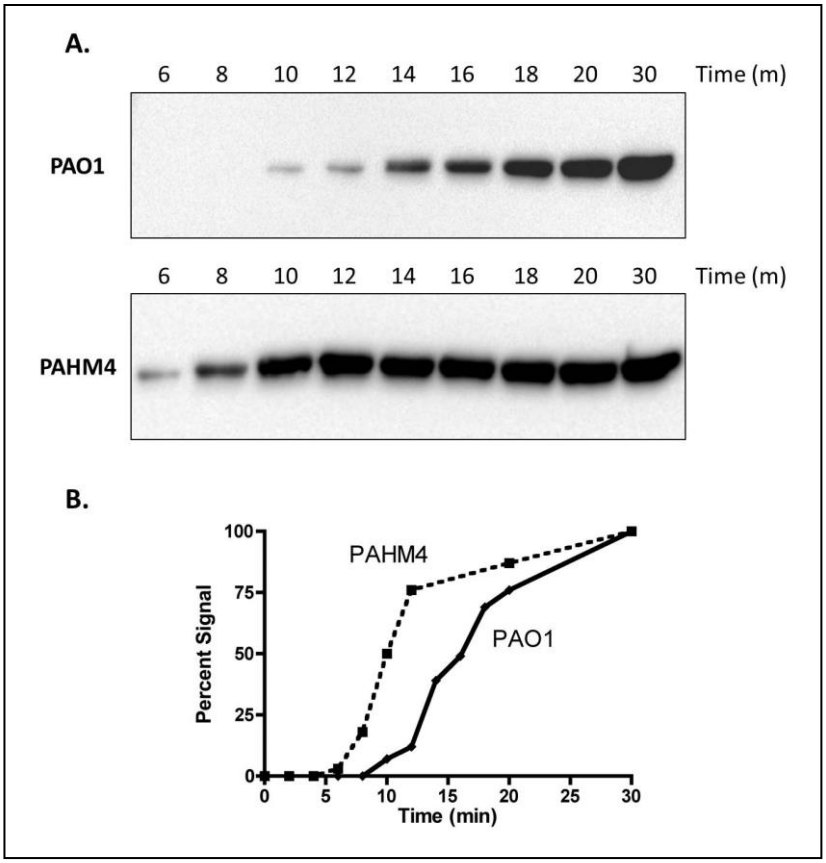

Figure 3.15. PAHM4 EftM methylates EF-Tu more efficiently *in vitro* compared to wild-type EftM. Identical EftM concentrations (500 nM) were used for methyltransferase assays at 25°C. At two minute intervals, aliquots were removed from the reaction and the reaction stopped by the addition of 2x Laemmli buffer and boiling. (A) Samples were used for Western blotting with the anti-di/trimethyl lysine antibody to detect modification of EF-Tu using chemiluminescence. (B) Band intensities were determined using BioRad ImageLab software version 5.1 and plotted against time. Dashed line represents activity of PAHM4 EftM and the solid line PAO1 EftM.

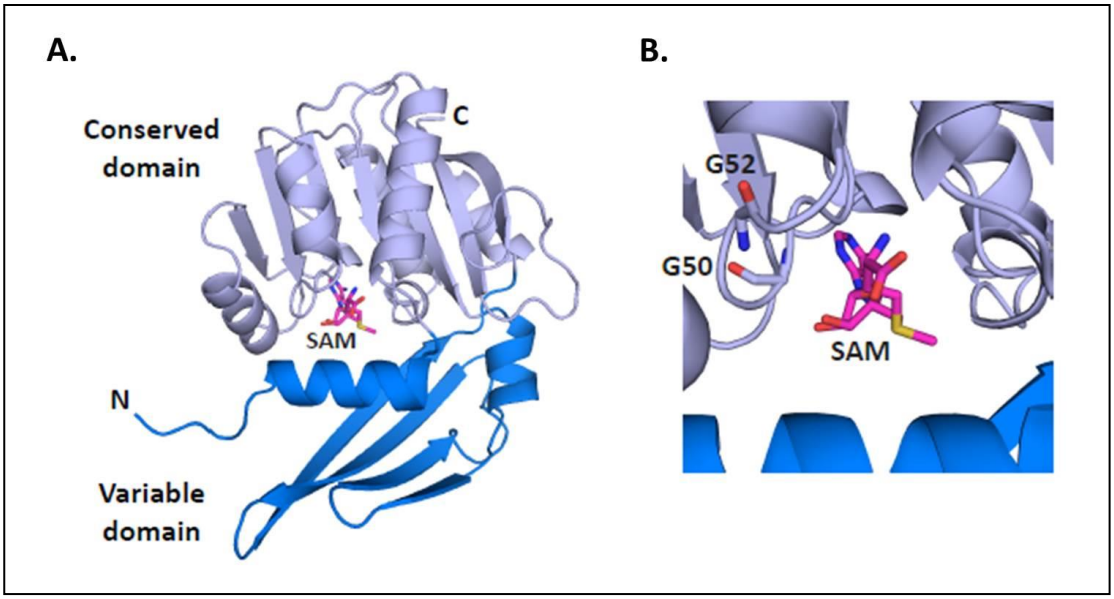

Figure 3.16. EftM shares structural homology with Class I SAM-dependent methyltransferases. Light blue indicates conserved Class I domains and blue indicates variable domains. (A) Tertiary structure of EftM based upon homology to DesVI (pdb 3BXO) with conserved Class I domains (light blue), variable domains (blue) and SAM (pink) indicated (generated with PyMOL). (B) Magnification of the SAM binding region of EftM with residues G50 and G52 of the conserved E/DX**G**XG SAM binding domain highlighted. The model was created by first performing a remote homology prediction search with the EftM amino acid sequence using HHpred. The crystal structure of the identified homologue, DesVI, was then used with MODELLER to thread the EftM sequence onto the known structure. (Jeffrey Meisner)

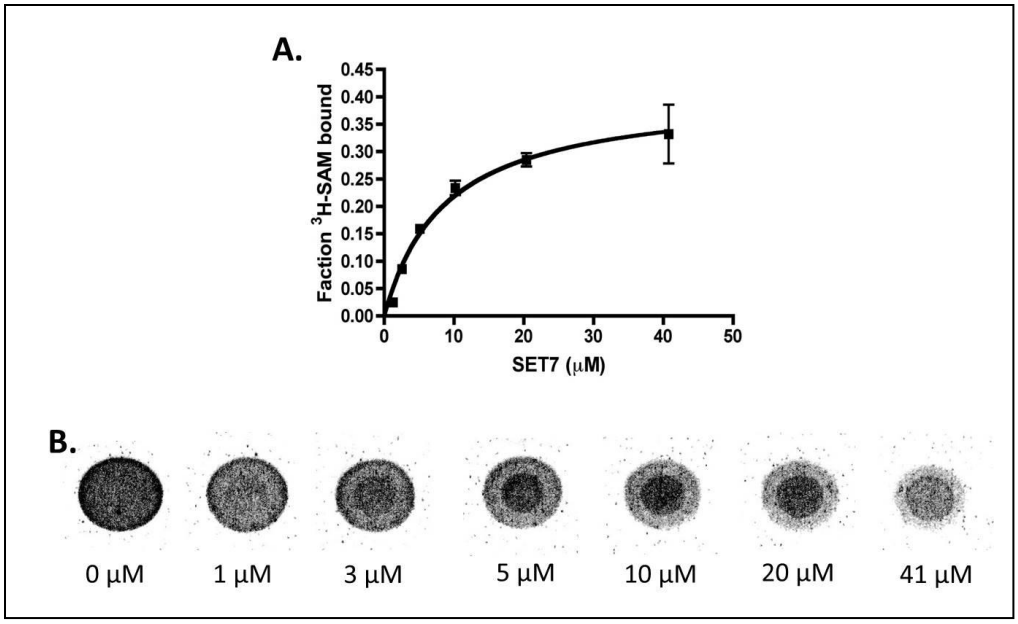

Figure 3.17. Validation of DRaCALA assay using SET7. (A) The fraction bound (F_B) of SET7 to ^{3}[H]-SAM was plotted against SET7 concentration. Non-linear regression analysis for one site binding was used to determine the K_d of SET7-SAM interaction. This was calculated as 9 ± 2 μM with a 95% confidence interval of 4 μM to 13 μM using GraphPad Prism version 4.0c for Mac (GraphPad Software, San Diego, California USA). (B) Representative DRaCALA images used for K_d determination for the interaction of SET7 and SAM. Concentration of SET7 used in each spot is indicated below each image.

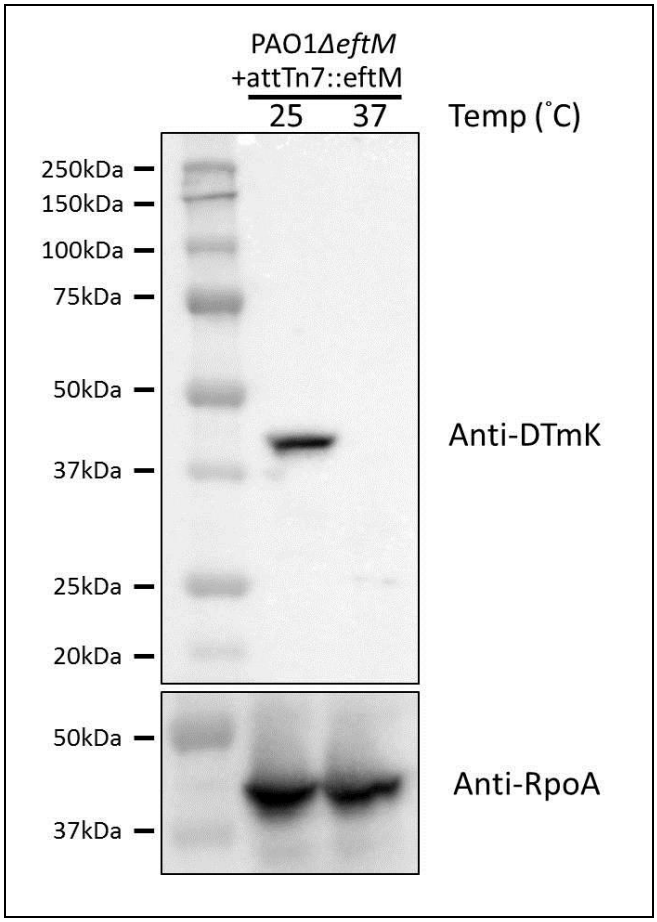

Figure 3.18. A single copy of *eftM* along with the 500 bp upstream sequence of the coding region was introduced into the *P. aeruginosa* PAO1Δ*eftM* chromosome. The complemented strain was grown at both 25°C and 37°C to generate whole cell lysates to be used for Western blotting for di/trimethylation of EF-Tu and anti-RpoA as a loading control. Introduction of a single copy presumably under the control of the native promoter restored the temperature-dependent methylation of EF-Tu.

Table 3.1. Summary of strains, plasmids and primers used in Chapter 3

Strain	Relevant Characteristics or Genotype	Source/Reference
PAO1	Wild-type	(19)
PAO1Δ*eftM*	Partial deletion of *eftM* derived from PAO1	(19)
PAHM4	Non-CF bronchiectasis isolate	(18)
PAHM23 (G50R)	Cystic fibrosis isolate with G50R mutation in *eftM*	(18)
PASP09	PAO1Δ*eftM* attTn7::500bp upstream + PA4178 C-terminal FLAG	This study
BL21	*fhuA2 [lon] ompT gal [dcm]* Δ*hsdS*	NEB
BL21-AI	F^- *ompT* $hsdS_B(r_B^-m_B^-)$ *gal dcm araB::T7RNAP-tetA*	Invitrogen
Top10 *E.coli*	F^- *mcr*A Δ*(mrr-hsd*RMS-*mcr*BC*)* Φ80*lac*ZΔM15 Δ*lac*X74 *rec*A1 *ara*D139 Δ*(ara-leu)*7697 *gal*U *gal*K *rps*L (Str^R) *end*A1 *nup*G	Invitrogen
DH5α Library Efficiency	F^- φ80*lac*ZΔM15 Δ*(lac*ZYA-*arg*F)U169 *rec*A1 *end*A1 *hsd*R17(r_k^-,m_k^+)*pho*A *sup*E55 *thi*-1 *gyr*A96 *rel*A1 λ^-	Invitrogen

Plasmid	Description	Source/Reference
pJPO1	pCOLDII + *eftM* N-terminal 6x-His fusion	This study
pJPO2	pCOLDII + *eftM* G50R N-terminal 6x-His fusion	This study
pJPO4	pDEST14 + *tufB* N-Terminal 6x-His fusion	This study
pJPO5	pDEST14 + *tufB* K5A N-Terminal 6x-His fusion	This study
pJPO6	pHERD20T + *eftM* C-terminal FLAG fusion	This study
pUCP18ApGw(*eftM*)	pUP18ApGw + *eftM* C-terminal FLAG fusion	(19)
pJPO7	pUP18ApGw + PAHM23 (G50R) *eftM* C-terminal FLAG fusion	This study
pJPO9	pHERD20T + PAHM4 *eftM* C-terminal FLAG fusion	This study
pJPO10	pCOLDII + PAHM4 *eftM* N-terminal 6x-His fusion	This study
pSP05	pUC18T-mini-Tn7T-Tp + PAO1 *eftM* FLAG fusion + 500bp upstream	This study

Table 3.1 continued. Summary of strains, plasmids and primers used in Chapter 3

Plasmid	Description	Source/Reference
pG-Tf2	Tetracycline inducible chaperone plasmid containing groES-groEL-tig; Cm^r	Takara
pCOLDII	Cold shock expression vector; Ap^r	Takara
pDEST14	Gateway® compatible arabinose inducible expression vector; Ap^r	Life Technologies
pHERD20T	Arabinose-inducible/glucose repressible P_{BAD}-based shuttle vector; Ap^r	(102)
pENTR/SD/D-TOPO	Gateway® compatible directional cloning entry vector with Shine-Dalgarno sequence; Ap^r	Life Technologies
pTNS3	Tn7 transposase expression vector; GenBank EU215432	(108)
pUC18T-mini-Tn7T-Tp	Broad host-range mini-Tn7 vector for single copy genomic insertion; GenBank DQ493875	(107)

Primer	Sequence	Description
*tufB*F	CACCATGCATCATCATCATCATATGGCTAAAGAAAAATTTGA	(19)
*tufB*R	TTATTCGATGATCTTGGCAACC	(19)
*tufB*F K5A	CACCATGCATCATCATCATCATATGGCTAAAGAAGCATTTGA	(19)
oJPO20	CATCATATGTCCGCCACCGCGCTG	*eftM* Forward NdeI
oJPO21	CTAAAGCTTCTAGCGCTTCACGCAGACGAACAG	*eftM* Reverse HindIII
oJPO120	CATCCATGGCATCCGCCACCGCGCTGTACA	*eftM* Forward NcoI
oJPO121	ATGAAGCTTCTACTTGTCATCGTCATCCTTGTAGTCGCGCTTCACGCAGAC	*eftM* Reverse FLAG HindIII
oJPO18	CACCATGTCCGCCACCGCGCTG	*eftM* Forward Gateway
oJPO19	CTACTTGTCATCGTCATCCTTGTAGTCGCGCTTCACGCAGAC	*eftM* Reverse C-FLAG
oJPO90	CACCATGCATCATCATCATCATATGTCCTCCAACGCG	PAHM4 *eftM* Forward Gateway
oJPO119	CTAAAGCTTCTAGCGCTTGATGCAGGCGAACAG	PAHM4 *eftM* Reverse HindIII
oJPO122	CATCCATGGCATCCTCCAACGCGCTGTACA	PAHM4 *eftM* Gateway Forward
oJPO123	ATGAAGCTTCTACTTGTCATCGTCATCCTTGTAGTCGCGCTTGATGCAGGC	PAHM4 *eftM* Reverse C-FLAG

Table 3.1 continued. Summary of strains, plasmids and primers used in Chapter 3

Primer	Sequence	Description
pTn7R	CACAGCATAACTGGACTGATTTC	(107)
p*glmS*-down	GCACATCGGCGACGTGCTCTC	(107)
pHERD-SF	ATCGCAACTCTCTACTGTTTCT	(102)
pHERD-SR	TGCAAGGCGATTAAGTTGGGT	(102)
SMP21	CACTTCCTCGATTTCGGCTATC	*eftM* RT-qPCR Forward
SMP22	TGCGTTGTAGTGGATCGAATAG	*eftM* RT-qPCR Reverse
SMP48	ACATCGACTACCAGGCGCAG	*eftM* RT-qPCR Forward
SMP49	GAGCATCGGCTGGTTGATGTC	*eftM* RT-qPCR Reverse
piv Forward	CTGCTGAACAACGGCAACTC	(115)
piv Reverse	GTGACGCTCTGGTTGATGGTC	(115)
omlA Forward	AAAATCGACATCCSGCAAGG	(113)
omlaA Reverse	GGTCGCTGTCGTTGAAGAAC	(113)
SMP10	TGGATCCCCAGACCTTCCACGGCAGTTG	PAO1 500 upstream F
SMP45	TGAATTCCTACTTGTCATCGTCATCCTTGTAGTCGCGCTTCACGCAGAC	PAO1 eftM R + FLAG

Chapter 4

Conclusions and future directions

Pseudomonas aeruginosa is a clinically important pathogen which primarily affects immunocompromised individuals. This pathogen is most commonly associated with infections of the respiratory tract. Similar to other respiratory pathogens, it was originally shown that *P. aeruginosa* displayed a phosphorylcholine (ChoP)-like modification on its surface. This modification was located on the traditionally cytoplasmic essential translation factor EF-Tu that was displayed on the extracellular surface.

Studies of other pathogens have shown that the addition of ChoP to their surfaces confers numerous advantages. These advantages include increased adhesion to the respiratory epithelium mediated by ChoP interaction with PAFR (31), resistance to host-derived antimicrobials such as LL-37 (32)**,** global down-regulation of the adaptive immune response (20, 40), and an increased ability to form biofilms (46, 47). These benefits come with the cost of increased killing by sensitivity to serum components such as C-reactive protein (33). Pathways for the addition of ChoP have been identified and studied in other respiratory pathogens such as *S. pneumoniae* and *H. influenzae* (1); however, no homologues for genes in those pathways have been identified in *P. aeruginosa*.

Through our work, we have shown that the ChoP-like modification on *P. aeruginosa* is actually trimethylation of lysine residue 5 of EF-Tu (19). I propose that this modification functions as a molecular mimic of ChoP providing some of the same benefits as ChoP. The presence of ChoP on other respiratory pathogens confers resistance to host derived antimicrobial compounds. To determine if the presence of lysine 5 trimethylated EF-Tu provides a survival advantage in a range of conditions, both PAO1 and PAO1Δ*eftM* will

be tested using the Biolog phenotype microarray. This array has the ability to test for growth or susceptibility to thousands of conditions and compounds.

We also identified the gene, *eftM*, which encodes a novel SAM-dependent methyltransferase that is responsible for the trimethylation of lysine 5 in EF-Tu (19). Trimethylation of proteins is exceedingly rare in prokaryotes (123), so the identification of a gene responsible for trimethylation is itself interesting. Identification of EftM as a SAM-dependent methyltransferase gives us the ability to more fully characterize how the methylation of EF-Tu affects both its canonical function in protein chain elongation as well as its 'moonlighting' roles by performing well controlled *in vitro* assays.

In functioning as a ChoP mimic, we have shown that *P. aeruginosa* uses methylation of EF-Tu to mediate adherence to airway epithelial cells via PAFR. We have also shown that in a murine model of acute pneumonia that *P. aeruginosa*, without the ability to modify EF-Tu, does not colonize the host as well and has decreased virulence as measured by an increased LD_{50} and mean time to death (19). While clearly important for pathogenesis, perhaps the bigger question that remains unanswered is how methylation of lysine 5 in EF-Tu affects its canonical function in protein chain elongation. A recent paper has fully described this canonical role by characterization of the biochemical properties of recombinant EF-Tu from *P. aeruginosa* expressed in *E. coli* (72). This includes the ability of EF-Tu to exchange guanine nucleotides with and without interaction with EF-Ts as well as the ability of EF-Tu to function in protein synthesis. The preparation of EF-Tu in this study was done using *E. coli*; therefore the EF-Tu used

would have been unmethylated at lysine 5 as *E. coli* lacks a homologue to EftM. It would be interesting to determine if trimethylation of EF-Tu affects its ability to function in protein synthesis.

To gain a better understanding of how methylated EF-Tu may function in the cell, we propose a number of experiments both *in vivo* and *in vitro* that can help answer this question. We must first gain an understanding of what proportion of EF-Tu is methylated *in vivo*. This is important because if 100% of the EF-Tu within *P. aeruginosa* is modified, then the likelihood of methylation having an effect on the protein chain elongation is greatly increased. This goal can be achieved with current methods employed in the lab such as the purification of recombinant EF-Tu from *P. aeruginosa* followed by quantitative mass spectrometry analysis to determine the proportions of the various potential EF-Tu methylation subtypes (mono-, di-, and tri-). We can also replace the chromosomal copies of EF-Tu with the unmodifiable K5A version to assess how unmodified EF-Tu changes cellular phenotypes that are associated with methylation. This is assuming that the K5A mutation does not affect the essential function of EF-Tu in protein chain elongation.

Understanding how EftM adds methyl groups will allow us to predict whether or not we can reasonably expect to find mono- and di-methylated intermediates of EF-Tu in *P. aeruginosa*. It will be possible to determine if EftM adds methyl groups in a processive or distributive manner by using the *in vitro* assay that I developed in Chapter 3. The *in vitro* assay can be performed in either a time limiting or SAM limiting fashion and the

products subjected to mass spectrometry analysis. If the enzyme is processive, we would expect that most of the EF-Tu will either be in the unmethylated or trimethylated form with very little of the intermediates present. On the other hand, if it acts in a distributive manner the enzyme would release from the substrate after the addition of each successive methyl group allowing for a build-up of the intermediates.

If we determine that EftM functions by the distributive method of methylation, it is possible that these different EF-Tu methyl intermediates will exhibit different biological functions. One can imagine a similar scenario to what is seen with the methylation of *E. coli* EF-Tu at lysine 56. In that system, the methylation status of EF-Tu is regulated by growth phase such that di-methylated EF-Tu becomes the predominant species during the transition from logarithmic growth to stationary phase (71). The dimethylation of EF-Tu at lysine 56 in stationary phase decreases the rate of GTP hydrolysis which may increase translational accuracy (71). In *P. aeruginosa*, we know that growth temperature affects the methylation status of EF-Tu. Our current Western blot assay prohibits accurate detection of mono- and di-methylated EF-Tu. However, detection of these intermediates is possible through the use of mass spectrometry analysis of purified proteins. The potential also remains that we could generate antibodies to small synthetic peptides with a known methylation status to be used in Western blotting. It is possible that the mono- and dimethyl EF-Tu species exist and play an as yet unknown role.

Based upon all of our experimental results, it appears that there is a delicate balance in the cell as to when trimethylation of EF-Tu occurs. We hypothesize that slight changes to

the steady state levels of EftM determine if there are detectable levels of trimethylated EF-Tu. Our RT-qPCR results indicate that there is no difference in transcript level of EftM at 25°C and 37°C (Figure 3.7). Not only is there no difference in transcript level, compared to our reference gene, there is relatively little transcript which is supported by previously published RNA-Seq and DNA microarray data (114, 115). Low mRNA levels are generally assumed to correlate with lower expression of the encoded protein but this is not always true. To try to determine if there is a difference in the amount of protein produced at the different temperatures, we introduced a FLAG-tagged copy of *eftM* into the chromosome of the PAO1Δ*eftM* with the addition of the 500 bp upstream, which should contain the native promoter. In this construct, we saw restoration of the normal temperature dependent methylation phenotype (Figure 3.17). Currently, we are unable to detect the FLAG-tagged protein, which further supports our evidence of low levels of EftM expression.

If modification of EF-Tu is dependent on slight changes of EftM levels in the cell, it is helpful to understand the properties of EftM. We examined the ability of EftM to methylate EF-Tu at different temperatures and our data suggest that EftM becomes partially unfolded at temperatures above 25°C rendering it unable to methylate EF-Tu (Figure 3.8 and Figure 3.9). Unfolded proteins are generally degraded at a faster rate than stable, properly folded proteins. Our data support that this is the case with EftM when expressed in *P. aeruginosa*. At 37°C, EftM is degraded at a significantly faster rate than at 25°C suggesting that it is less stable at 37°C (Figure 3.10). Interestingly, when PAHM4 EftM is expressed in PAO1Δ*eftM*, it is degraded at a slower rate compared to

wild-type EftM (Figure 3.14). This provides further evidence that there is some intrinsic stability associated with numerous mutations present in PAHM4 EftM. This difference in proteolysis of EftM further supports our hypothesis that small changes in the amount of EftM in *P. aeruginosa* leads to the observable methylation phenotype.

It is possible that unstable EftM is directly degraded by specific proteases. Many proteases have been identified in *P. aeruginosa* and transposon mutants in these proteases exist in both the PAO1 and PA14 mutant libraries. Previous screening of the PA14 library at 25°C would not have identified these genes as important to modification of EF-Tu because the phenotype would only have been seen at 37°C. To identify if specific proteases may be responsible for the degradation of EftM, we can test these transposon mutants for the ability to methylate EF-Tu at 37°C. If efficient degradation of EftM is inhibited by the lack of a specific protease, it is possible that any residual activity of the unstable enzyme will be detected via Western blotting.

Apparent differences in stability and degradation do not preclude the possibility that biochemical properties of these two enzymes are slightly different. It will be necessary to determine the kinetic properties of both PAHM4 and PAO1 EftM at both 25°C and 37°C to determine if, in addition to protein stability, the temperature dependent phenotype can be explained by the enzyme kinetics. We will continue to study these enzymes in an effort to determine what role these kinetic properties play in modification of EF-Tu.

Like many enzymes, methyltransferases are extremely specific for their substrates. For example, in eukaryotes, histone methyltransferases methylate histone tails at very specific lysine residues, which result in either activation or repression of gene expression. These lysine residues can be extremely close to one another such as K4 and K9 of histone H3. In EF-Tu there are three lysine residues which are very close to one another: K3, K5, and K10 (Figure 2.9). Of these residues, only lysine 5 is methylated by EftM. It may be possible that methylation of K5 prevents methylation at these other sites by other unidentified methyltransferases.

To better understand the function of EftM, how it identifies its substrate, and how it interacts with EF-Tu, we plan on determining the crystal structure of this enzyme. Co-crystallization of an EftM-EF-Tu complex will give us insight into how the enzyme recognizes its substrate and how it modifies this portion of EF-Tu. Crystallization may need to be done in the presence of all or some of the cofactors for each enzyme including SAM, aa-tRNA, GDP or GTP. None of the current known structures of EF-Tu show the amino acids where this modification exists. This is presumably because of the inherent disorder of that region which leads to difficulty in structure determination.

EftM is predicted to be a cytoplasmic protein. Our data show that it is a SAM-dependent methyltransferase and SAM is found in the cytoplasm. To accurately show the localization of EftM cellular fractionation studies can be performed; however, currently no specific antibodies to EftM exist. In the absence of specific antibodies, localization can be done by overexpressing the protein fused to a tag such as poly-histidine or FLAG.

One drawback of this approach is that overexpression of proteins can cause artifacts in localization studies. This may be an even greater consideration in the case of EftM since our data suggests the protein is typically expressed at low levels *in vivo*. One well described technique for the determination protein subcellular localization is the use of alkaline phosphatase, PhoA, and β-galactosidase, LacZ, fusions. These two reporter proteins only function when they are present in the correct subcellular compartment. LacZ is only active when present in the cytoplasm and PhoA is only active in the periplasm where the correct disulfide bonds formation can take place. This reporter system could be useful in determining the localization of EftM. However, the generation of EftM specific antibodies from purified recombinant EftM will allow us to directly visualize the protein without the use of tags which may produce unknown and unintended consequences. We can then use these specific antibodies for various microscopy and subcellular fractionation techniques identify the location of EftM within the bacterium.

EF-Tu lacks known signal sequences; however, there are many reports in various microbes of EF-Tu associating with the outer membrane where it can interact with host factors such as fibronectin and factor H (12, 63). The mechanism by which EF-Tu is transported to the membrane in all of these microbes is currently unknown. With current tools, it is possible to test if methylation status affects the membrane association of EF-Tu. We could once again utilize the previously proposed EF-Tu K5A chromosomal replacement strain. If the two chromosomal copies of EF-Tu were replaced with recombinant EF-Tu K5A, it would be possible to perform cellular fractionation

experiments to determine if EF-Tu is still located in the membrane fraction assuming the mutation itself does not affect the canonical function of EF-Tu.

If methylation of the N-terminal peptide by EftM is a more universal signal for cellular export, we may be able to use a computational analysis to identify similar sequences in the *P. aeruginosa* genome. Initial BLAST analysis of the *P. aeruginosa* genome did not return any similar amino acid sequences. However, if the sequence is degenerate and only a few conserved amino acids are necessary for recognition by EftM, this approach may prove to be difficult. We can use recombinant reporter proteins to determine if the trimethylation of the N-terminus is a signal for cellular export. First, we would need to test *in vitro* if EftM is able to recognize and methylate other recombinant proteins that have been engineered to contain the N-terminal region of EF-Tu. If EftM is able to recognize and methylate other proteins with the addition of this peptide, it shows that it could potentially have a more global regulatory role. Once the ability to methylate these recombinant proteins has been demonstrated, we can test to see if methylation has an effect on the localization of these proteins. This could be done by expression of this modifiable recombinant protein in *P. aeruginosa* and either testing for activity of the reporter or through cellular fractionation studies. It would obviously be very exciting and have broad implications if the function of EftM is tied to a novel cellular export system. Even if the methylation of the N-terminus of other proteins does not affect localization, this does not preclude the possibility that it does affect the localization of EF-Tu.

Lastly, through our screening of the PA14 transposon mutant library, we were able to identify *eftM* as one of the genes responsible for the modification of EF-Tu (19). However, we only screened the library for the loss-of-function mutation at 25°C, meaning we would be unable to detect any potential repressors or inhibitors that may be present at 37°C. It would be advantageous for us to rescreen this comprehensive library for any gain-of-function mutations that would be present at 37°C. Many high-throughput methods for screening this library were unsuccessful; however, most of these methods relied heavily on the specificity and affinity of the anti-ChoP antibodies. We now know that the modification is not ChoP but rather trimethylation of a lysine residue. We currently have new antibodies which may be better suited for the high-throughput methods that were previously unsuccessful such as whole cell ELISA. Through replication of the PA14 library, it would be feasible to inoculate a second set of plates to be grown at 37°C to which the cells would bind to the plate. After optimization with the appropriate controls, use of the pan di/trimethyl lysine antibody to detect the presence of methylated EF-Tu may yield positive results.

As screening of this comprehensive library is a large undertaking, it may be easier to use our purified EftM protein as a bait protein to find interacting partners that are present in cells grown at either 25°C or 37°C. Any interacting proteins identified at 25°C could represent other targets for methylation by EftM or accessory proteins that are necessary for EftM to complete its function or direct it to a specific cellular location. Interacting proteins from cells grown at 37°C could be unidentified inhibitory proteins that function to prevent interaction with EF-Tu. Identification of these proteins may provide us with

insight into the nature of the observed temperature dependent phenotype of EF-Tu methylation in *P. aeruginosa*.

In its totality, this project has yielded some very interesting results that could have broad implication for basic biology and applied sciences. We have discovered a novel modification of EF-Tu that is a functional mimic of a known adhesion factor for other respiratory pathogens. Prophylactic treatment of patients with an inhibitor of this adhesin may decrease attachment and colonization by this important pathogen. At a basic biology level, the potential exists that the methylation of EF-Tu affects the essential function of protein chain elongation. If methylation of EF-Tu represents a strategy to avoid the action of antimicrobial agents, inhibition of EftM could prove to be a novel therapeutic target. Further study of both EftM and EF-Tu will provide valuable evidence elucidating the roles of the proteins in their normal bacterial functions as well as pathogenesis.

Appendix I

Adapted from "Analysis of the *Pseudomonas aeruginosa* regulon controlled by the sensor kinase KinB and sigma factor RpoN"

F. Heath Damron, Joshua P. Owings, Yuta Okkotsu, John J. Varga, Jill R. Schurr, Joanna B. Goldberg, Michael J. Schurr, and Hongwei D. Yu

Journal of Bacteriology. 2012 Jan; 194(4)

*Joshua P. Owings performed all mouse studies in this manuscript

Abstract

Alginate overproduction by *Pseudomonas aeruginosa*, also known as mucoidy, is associated with chronic endobronchial infections in cystic fibrosis. Alginate biosynthesis is initiated by the extracytoplasmic function sigma factor (σ^{22}; AlgU/AlgT). In the wild-type (wt) nonmucoid strains, such as PAO1, AlgU is sequestered to the cytoplasmic membrane by the anti-sigma factor MucA that inhibits alginate production. One mechanism underlying the conversion to mucoidy is mutation of *mucA*. However, the mucoid conversion can occur in wt *mucA* strains via the degradation of MucA by activated intramembrane proteases AlgW and/or MucP. Previously, we reported that the deletion of the sensor kinase KinB in PAO1 induces an AlgW-dependent proteolysis of MucA, resulting in alginate overproduction. This type of mucoid induction requires the alternate sigma factor RpoN (σ^{54}). In an acute pneumonia murine infection model, BALB/c mice exhibited increased survival when challenged with the *kinB* mutant relative to survival with PAO1 challenge. These data suggest that KinB regulates virulence factors important for the development of acute pneumonia and conversion to mucoidy (113).

Introduction

P. aeruginosa is a Gram-negative opportunistic pathogen that can infect cystic fibrosis (CF) patients. CF patients initially suffer from recurring acute infections with *P. aeruginosa* which eventually become chronic infections. The bacteria that cause acute and chronic infections in this patient population exhibit different characteristics. Acute infection isolates typically express numerous virulence factors and are relatively

cytotoxic. Once the transition to a chronic infection occurs, the bacteria are generally less cytotoxic and inflammatory. Other changes include a loss of motility, loss of LPS O-antigen, a transition to a biofilm mode of growth, and the expression of alginate.

The overproduction of the exopolysaccharide alginate causes a phenotype known as mucoidy. One of the master regulators of alginate production is the sigma factor σ^{22} also known as AlgU (AlgT). AlgU activates alginate overproduction by regulating the expression of transcription factors (124-126) leading to transcriptional activation of the *algD* biosynthetic operon (127-129). The genes controlled by AlgU and their role in the alginate machinery have been extensively reviewed elsewhere (130).

MucA is an antisigma factor and the primary negative regulator of alginate overproduction. MucA directly sequesters AlgU to the inner membrane (131). Constitutively mucoid CF isolates typically harbor mutations in *mucA* (129), but mutations in the other negative regulators of AlgU, *mucB* and *mucD*, have been identified in mucoid CF isolates (132). If the *mucA* gene is wild-type (wt), MucA must be proteolytically degraded to activate AlgU (133).

The mucoid phenotype can also be regulated via environmental sensing. Environmental nonmucoid strains have the capacity to become mucoid regardless of *mucA* mutation (134). One method used by bacteria to sense the environment is through two-component regulatory systems which are comprised of a cytoplasmic membrane-bound histidine kinase, a sensor, and a response regulator, usually a transcription factor. Phosphorylation

and de-phosphorylation are mechanisms of signal transduction across the inner membrane and can result in changes in gene expression mediated by the response regulator. *P. aeruginosa* strain PAO1 has 63 sensors and 64 response regulators (135). We recently reported that the inactivation of a gene encoding a histidine kinase, KinB, resulted in alginate overproduction (136). In the PAO1 *kinB* strain, the activated protease AlgW degrades MucA (Figure AI.1). Furthermore, regulated proteolysis of MucA is dependent on the cognate response regulator of *kinB*, which is known as AlgB, as well as the *rpoN* gene encoding σ^{54} (136). A CF isolate with the *kinB* mutation has been identified (136). AlgB has been suggested to be an atypical response regulator because AlgB-dependent transcription in alginate regulation does not require phosphorylation (137), and it can be inferred that AlgB would not be phosphorylated in the absence of KinB.

In this study, we analyzed the whole transcriptomes and proteomes of PAO1 *kinB* and PAO1 *kinB* Δ*rpoN* to identify the genes and proteins that are uniquely controlled by KinB and RpoN. Our data indicated that KinB, in concert with RpoN, controls alginate and rhamnolipid expression as well as structural pilus genes and other potentially novel factors. In the *kinB* mutant, RpoN alone represses pyochelin, type IVb pili, antibiotic efflux, and quorumsensing (QS) genes. In light of these data, we hypothesized that KinB may control virulence in *P. aeruginosa*, which was corroborated in an acute murine infection model. Collectively, our data show that KinB is a pleiotropic regulator that through RpoN controls a regulon consisting of approximately 20% of the PAO1 genome and includes the alginate biosynthetic pathway as well as key determinants of virulence.

Methods and Materials

Strains

Bacterial strains used in this study are indicated on Table AI.1.

Murine acute pneumonia model

P. aeruginosa strains were grown on *Pseudomonas* isolation agar (PIA; Becton Dickinson) plates for 24 h at 37°C and suspended in 1x PBS to an OD650 of 1.8. Inocula were diluted 1:1 with 1x PBS to obtain the desired challenge dose in 20 µl. Six- to 8-week-old female BALB/c mice (Harlan Laboratories) were anesthetized by intraperitoneal injection of 0.2 ml of ketamine (6.7 mg/ml) and xylazine (1.3 mg/ml) in 0.9% saline. Anesthetized animals were placed on their backs, and 10 µl inocula were pipetted directly into each nostril (20 µl total). Bacterial doses were verified immediately after infection by serial dilution in 1x PBS–1% bovine serum albumin (BSA) and plating on PIA. All animals were carefully observed for the duration of the trials. The University of Virginia Animal Care and Use Committee approved all procedures used in this work.

Results and Discussion

KinB, RpoN, and AlgU control virulence of *P. aeruginosa* in a murine model

Transcriptomic, proteomic, and phenotypic analyses of the mucoid PAO1 *kinB* strain and nonmucoid PAO1 *kinB* Δ*rpoN* double mutant showed that KinB controls not only alginate but also a wide array of genes and virulence factors. Since sensor kinases monitor the environment and activate responses, KinB may be required for virulence.

Furthermore, other investigators have shown that *kinB* is required for virulence in a zebra fish model (138). To test this hypothesis, an acute pneumonia model was utilized with BALB/c mice infected by the intranasal route. Since the *kinB* mutant is mucoid, PDO300, a mucoid *mucA22* mutant (139) with a wild-type *kinB*, was used for comparison. With a dose of 1 x 10^7 CFU of bacteria, 0% of BALB/c mice survived infection by PAO1 after 40 to 50 hours (Figure AI.2). Similar mortality was observed with the mucoid strain PDO300 (Figure AI.2). However, PAO1 *kinB* did not cause the death of any mice (Figure AI.2). PAO1 *kinB* Δ*rpoN* caused slightly greater mortality than PAO1 *kinB*; however, 75% of the mice survived the infection (Figure AI.2). Interestingly, nonmucoid PAO1 *kinB* Δ*algU* caused a similar rate of mortality as PAO1 (Figure AI.2). Collectively, these data suggest that KinB/RpoN regulates virulence factors and may be required for virulence in acute infection by *P. aeruginosa*.

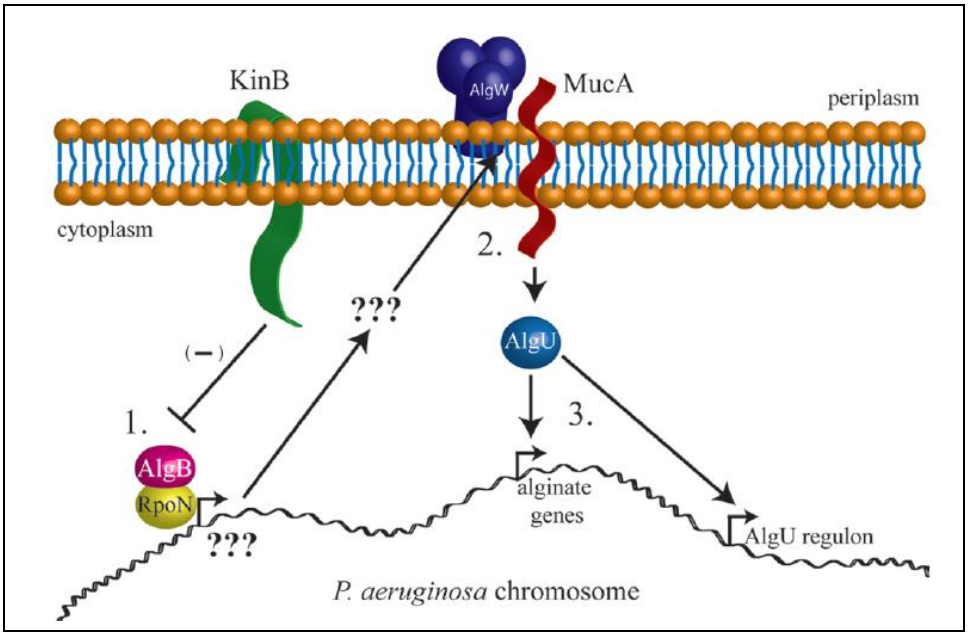

Figure AI.1. *P. aeruginosa* sensor kinase KinB regulation of alginate overproduction. KinB is a sensor kinase that localizes to the inner membrane. KinB is also a negative regulator of alginate overproduction (136). We have previously shown that in the absence of *kinB*, AlgB and RpoN activate expression of unknown genes (step 1) (136). These unknown factors caused AlgW-mediated proteolysis of MucA, resulting in activated AlgU (step 2). AlgU then drives expression of the alginate biosynthetic operon as well as other AlgU regulon genes (step 3). The goal of this study is to determine the genes (indicated as ???) controlled by KinB through RpoN. Adapted from (113) with permission of The American Society for Microbiology.

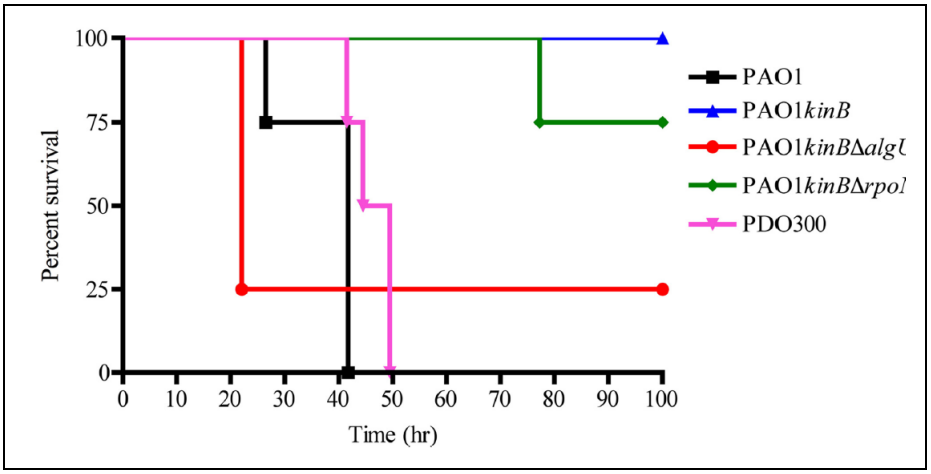

Figure AI.2. Survival of BALB/c challenged with *P. aeruginosa* strains. The percent survival of female BALB/c mice is plotted over time (n = 8 mice per group) with each mouse receiving a comparable dose of 1 x 10^7 CFU via intranasal delivery. Statistical analyses were performed using a log rank test, and all strains were compared to PAO1. *P* values for PAO1 compared to the various strains are as follows: *kinB* strain, 0.01; *kinBΔalgU* strain, 0.6; *kinBΔrpoN* strain, 0.01; PDO300 (*mucA22*) strain, 0.1. Adapted from (113) with permission.

Table AI.1. Bacterial strains used in Appendix I. Adapted from (113) with permission.

Bacterial strains	Phenotype, genotype, description, or sequence [a]	Source
P. aeruginosa		
PAO1	Alg^- Prototroph	P. Phibbs
PAO1*kinB::aacC1*	Alg^+, PAO1 *kinB*:: Gm^r	(136)
PAO1*kinB::aacC1*Δ*algU*	Alg^- , PAO1*kinB::aacC1* in-frame deletion of *algU* (PA0762)	(136)
PAO1*kinB::aacC1*Δ*rpoN*	Alg^- , PAO1*kinB::aacC1* in-frame deletion of *rpoN* (PA4462)	(136)
PDO300	Alg^+, PAO1 *mucA22*	(139)

[a] Alg^-, non-mucoid phenotype and Alg^+, mucoid phenotype

REFERENCES

1. **Weiser JN, Shchepetov M, Chong ST.** 1997. Decoration of lipopolysaccharide with phosphorylcholine: a phase-variable characteristic of *Haemophilus influenzae*. Infection and immunity **65:**943-950.
2. **Fan X, Pericone CD, Lysenko E, Goldfine H, Weiser JN.** 2003. Multiple mechanisms for choline transport and utilization in *Haemophilus influenzae*. Molecular microbiology **50:**537-548.
3. **Sadikot RT, Blackwell TS, Christman JW, Prince AS.** 2005. Pathogen-host interactions in *Pseudomonas aeruginosa* pneumonia. American journal of respiratory and critical care medicine **171:**1209-1223.
4. **Struelens MJ, Schwam V, Deplano A, Baran D.** 1993. Genome macrorestriction analysis of diversity and variability of *Pseudomonas aeruginosa* strains infecting cystic fibrosis patients. Journal of clinical microbiology **31:**2320-2326.
5. **Burns JL, Gibson RL, McNamara S, Yim D, Emerson J, Rosenfeld M, Hiatt P, McCoy K, Castile R, Smith AL, Ramsey BW.** 2001. Longitudinal assessment of *Pseudomonas aeruginosa* in young children with cystic fibrosis. The Journal of infectious diseases **183:**444-452.
6. **Lambert PA.** 2002. Mechanisms of antibiotic resistance in *Pseudomonas aeruginosa*. Journal of the Royal Society of Medicine **95 Suppl 41:**22-26.
7. **Mena A, Smith EE, Burns JL, Speert DP, Moskowitz SM, Perez JL, Oliver A.** 2008. Genetic adaptation of *Pseudomonas aeruginosa* to the airways of cystic

fibrosis patients is catalyzed by hypermutation. Journal of bacteriology **190:**7910-7917.

8. **Gellatly SL, Hancock RE.** 2013. *Pseudomonas aeruginosa*: new insights into pathogenesis and host defenses. Pathogens and disease **67:**159-173.
9. **Clark SE, Weiser JN.** 2013. Microbial modulation of host immunity with the small molecule phosphorylcholine. Infection and immunity **81:**392-401.
10. **Silby MW, Winstanley C, Godfrey SA, Levy SB, Jackson RW.** 2011. *Pseudomonas genomes*: diverse and adaptable. FEMS microbiology reviews **35:**652-680.
11. **Kline KA, Falker S, Dahlberg S, Normark S, Henriques-Normark B.** 2009. Bacterial adhesins in host-microbe interactions. Cell host & microbe **5:**580-592.
12. **Balasubramanian S, Kannan TR, Baseman JB.** 2008. The surface-exposed carboxyl region of *Mycoplasma pneumoniae* elongation factor Tu interacts with fibronectin, p. 3116-3123, Infection and immunity, 2008/04/16 ed, vol. 76.
13. **Pizarro-Cerda J, Cossart P.** 2006. Bacterial adhesion and entry into host cells. Cell **124:**715-727.
14. **Cundell DR, Gerard NP, Gerard C, Idanpaan-Heikkila I, Tuomanen EI.** 1995. *Streptococcus pneumoniae* anchor to activated human cells by the receptor for platelet-activating factor. Nature **377:**435-438.
15. **Schenkein HA, Barbour SE, Berry CR, Kipps B, Tew JG.** 2000. Invasion of human vascular endothelial cells by *Actinobacillus actinomycetemcomitans* via the receptor for platelet-activating factor. Infection and immunity **68:**5416-5419.

16. **Swords WE, Buscher BA, Ver Steeg Ii K, Preston A, Nichols WA, Weiser JN, Gibson BW, Apicella MA.** 2000. Non-typeable *Haemophilus influenzae* adhere to and invade human bronchial epithelial cells via an interaction of lipooligosaccharide with the PAF receptor. Molecular microbiology **37:**13-27.

17. **Serino L, Virji M.** 2002. Genetic and functional analysis of the phosphorylcholine moiety of commensal *Neisseria* lipopolysaccharide. Molecular microbiology **43:**437-448.

18. **Barbier M, Oliver A, Rao J, Hanna SL, Goldberg JB, Alberti S.** 2008. Novel phosphorylcholine-containing protein of *Pseudomonas aeruginosa* chronic infection isolates interacts with airway epithelial cells. The Journal of infectious diseases **197:**465-473.

19. **Barbier M, Owings JP, Martinez-Ramos I, Damron FH, Gomila R, Blazquez J, Goldberg JB, Alberti S.** 2013. Lysine trimethylation of EF-Tu mimics platelet-activating factor to initiate *Pseudomonas aeruginosa* pneumonia. mBio **4:**e00207-00213.

20. **Harnett W, Harnett MM.** 2001. Modulation of the host immune system by phosphorylcholine-containing glycoproteins secreted by parasitic filarial nematodes. Biochimica et biophysica acta **1539:**7-15.

21. **Gould JM, Weiser JN.** 2001. Expression of C-reactive protein in the human respiratory tract. Infection and immunity **69:**1747-1754.

22. **van Zoelen MA, Florquin S, Meijers JC, de Beer R, de Vos AF, de Boer OJ, van der Poll T.** 2008. Platelet-activating factor receptor contributes to host defense against *Pseudomonas aeruginosa* pneumonia but is not essential for the

accompanying inflammatory and procoagulant response. Journal of immunology (Baltimore, Md. : 1950) **180:**3357-3365.

23. **Branger J, Wieland CW, Florquin S, Maris NA, Pater JM, Speelman P, Shimizu T, Ishii S, van der Poll T.** 2004. Platelet-activating factor receptor-deficient mice show an unaltered clearance of nontypeable *Haemophilus influenzae* from their respiratory tract. Shock **22:**543-547.

24. **Tomasz A.** 1981. Surface components of *Streptococcus pneumoniae*. Reviews of infectious diseases **3:**190-211.

25. **Harnett W, Harnett MM.** 1999. Phosphorylcholine: friend or foe of the immune system? Immunology today **20:**125-129.

26. **Kolberg J, Hoiby EA, Jantzen E.** 1997. Detection of the phosphorylcholine epitope in *streptococci, Haemophilus* and pathogenic *Neisseriae* by immunoblotting. Microbial pathogenesis **22:**321-329.

27. **Serino L, Virji M.** 2000. Phosphorylcholine decoration of lipopolysaccharide differentiates commensal *Neisseriae* from pathogenic strains: identification of *licA*-type genes in commensal *Neisseriae*. Molecular microbiology **35:**1550-1559.

28. **Weiser JN, Goldberg JB, Pan N, Wilson L, Virji M.** 1998. The phosphorylcholine epitope undergoes phase variation on a 43-kilodalton protein in *Pseudomonas aeruginosa* and on pili of *Neisseria meningitidis* and *Neisseria gonorrhoeae*. Infection and immunity **66:**4263-4267.

29. **Smani Y, Docobo-Perez F, Lopez-Rojas R, Dominguez-Herrera J, Ibanez-Martinez J, Pachon J.** 2012. Platelet-activating factor receptor initiates contact

of *Acinetobacter baumannii* expressing phosphorylcholine with host cells. The Journal of biological chemistry **287:**26901-26910.

30. **Weiser JN, Lindberg AA, Manning EJ, Hansen EJ, Moxon ER.** 1989. Identification of a chromosomal locus for expression of lipopolysaccharide epitopes in *Haemophilus influenzae*. Infection and immunity **57:**3045-3052.

31. **Pang B, Winn D, Johnson R, Hong W, West-Barnette S, Kock N, Swords WE.** 2008. Lipooligosaccharides containing phosphorylcholine delay pulmonary clearance of nontypeable *Haemophilus influenzae*. Infection and immunity **76:**2037-2043.

32. **Lysenko ES, Gould J, Bals R, Wilson JM, Weiser JN.** 2000. Bacterial phosphorylcholine decreases susceptibility to the antimicrobial peptide LL-37/hCAP18 expressed in the upper respiratory tract. Infection and immunity **68:**1664-1671.

33. **Weiser JN, Pan N, McGowan KL, Musher D, Martin A, Richards J.** 1998. Phosphorylcholine on the lipopolysaccharide of *Haemophilus influenzae* contributes to persistence in the respiratory tract and sensitivity to serum killing mediated by C-reactive protein. The Journal of experimental medicine **187:**631-640.

34. **Casey R, Newcombe J, McFadden J, Bodman-Smith KB.** 2008. The acute-phase reactant C-reactive protein binds to phosphorylcholine-expressing *Neisseria meningitidis* and increases uptake by human phagocytes. Infection and immunity **76:**1298-1304.

35. **Abbas AK, Lichtman AH, Pillai S.** 2007. Cellular and molecular immunology, 6th edition. ed. Saunders Elsevier.

36. **Gould JM, Weiser JN.** 2002. The inhibitory effect of C-reactive protein on bacterial phosphorylcholine platelet-activating factor receptor-mediated adherence is blocked by surfactant. The Journal of infectious diseases **186:**361-371.

37. **Tan Y, Arnold RJ, Luo ZQ.** 2011. *Legionella pneumophila* regulates the small GTPase Rab1 activity by reversible phosphorylcholination. Proceedings of the National Academy of Sciences of the United States of America **108:**21212-21217.

38. **Goody PR, Heller K, Oesterlin LK, Muller MP, Itzen A, Goody RS.** 2012. Reversible phosphocholination of Rab proteins by *Legionella pneumophila* effector proteins. The EMBO journal **31:**1774-1784.

39. **Mukherjee S, Liu X, Arasaki K, McDonough J, Galan JE, Roy CR.** 2011. Modulation of Rab GTPase function by a protein phosphocholine transferase. Nature **477:**103-106.

40. **Lovell TM, Woods RJ, Butlin DJ, Brayley KJ, Manyonda IT, Jarvis J, Howell S, Lowry PJ.** 2007. Identification of a novel mammalian post-translational modification, phosphocholine, on placental secretory polypeptides. Journal of molecular endocrinology **39:**189-198.

41. **Harnett W, Harnett MM.** 1993. Inhibition of murine B cell proliferation and down-regulation of protein kinase C levels by a phosphorylcholine-containing filarial excretory-secretory product. Journal of immunology (Baltimore, Md. : 1950) **151:**4829-4837.

42. **Harnett W, Deehan MR, Houston KM, Harnett MM.** 1999. Immunomodulatory properties of a phosphorylcholine-containing secreted filarial glycoprotein. Parasite immunology **21:**601-608.

43. **Kooyman FN, de Vries E, Ploeger HW, van Putten JP.** 2007. Antibodies elicited by the bovine lungworm, *Dictyocaulus viviparus*, cross-react with platelet-activating factor. Infection and immunity **75:**4456-4462.

44. **Nichols WA, Raetz CRH, Clementz T, Smith AL, Hanson JA, Ketterer MR, Sunshine M, Apicella MA.** 1997. *htrB* of *Haemophilus influenzae*: determination of biochemical activity and effects on virulence and lipooligosaccharide toxicity. Journal of Endotoxin Research **4:**163-172.

45. **Wang X, Moser C, Louboutin JP, Lysenko ES, Weiner DJ, Weiser JN, Wilson JM.** 2002. Toll-like receptor 4 mediates innate immune responses to *Haemophilus influenzae* infection in mouse lung. Journal of immunology (Baltimore, Md. : 1950) **168:**810-815.

46. **West-Barnette S, Rockel A, Swords WE.** 2006. Biofilm growth increases phosphorylcholine content and decreases potency of nontypeable *Haemophilus influenzae* endotoxins. Infection and immunity **74:**1828-1836.

47. **Hong W, Mason K, Jurcisek J, Novotny L, Bakaletz LO, Swords WE.** 2007. Phosphorylcholine decreases early inflammation and promotes the establishment of stable biofilm communities of nontypeable *Haemophilus influenzae* strain 86-028NP in a chinchilla model of otitis media. Infection and immunity **75:**958-965.

48. **Hong W, Pang B, West-Barnette S, Swords WE.** 2007. Phosphorylcholine expression by nontypeable *Haemophilus influenzae* correlates with maturation of biofilm communities *in vitro* and *in vivo*. Journal of bacteriology **189:**8300-8307.

49. **Albelo ST, Domenech CE.** 1997. Carbons from choline present in the phospholipids of *Pseudomonas aeruginosa*. FEMS microbiology letters **156:**271-274.

50. **Berka RM, Vasil ML.** 1982. Phospholipase C (heat-labile hemolysin) of *Pseudomonas aeruginosa*: purification and preliminary characterization. Journal of bacteriology **152:**239-245.

51. **Malek AA, Chen C, Wargo MJ, Beattie GA, Hogan DA.** 2011. Roles of three transporters, CbcXWV, BetT1, and BetT3, in *Pseudomonas aeruginosa* choline uptake for catabolism. Journal of bacteriology **193:**3033-3041.

52. **Massimelli MJ, Beassoni PR, Forrellad MA, Barra JL, Garrido MN, Domenech CE, Lisa AT.** 2005. Identification, cloning, and expression of *Pseudomonas aeruginosa* phosphorylcholine phosphatase gene. Current microbiology **50:**251-256.

53. **Salvano MA, Lisa TA, Domenech CE.** 1989. Choline transport in *Pseudomonas aeruginosa*. Molecular and cellular biochemistry **85:**81-89.

54. **Lucchesi GI, Pallotti C, Lisa AT, Domenech CE.** 1998. Constitutive choline transport in *Pseudomonas aeruginosa*. FEMS microbiology letters **162:**123-126.

55. **Wilderman PJ, Vasil AI, Martin WE, Murphy RC, Vasil ML.** 2002. *Pseudomonas aeruginosa* synthesizes phosphatidylcholine by use of the phosphatidylcholine synthase pathway. Journal of bacteriology **184:**4792-4799.

56. **Voorhees RM, Ramakrishnan V.** 2013. Structural basis of the translational elongation cycle. Annual review of biochemistry **82:**203-236.

57. **Caldas TD, El Yaagoubi A, Richarme G.** 1998. Chaperone properties of bacterial elongation factor EF-Tu. The Journal of biological chemistry **273:**11478-11482.

58. **Wong DK, Lee BY, Horwitz MA, Gibson BW.** 1999. Identification of fur, aconitase, and other proteins expressed by *Mycobacterium tuberculosis* under conditions of low and high concentrations of iron by combined two-dimensional gel electrophoresis and mass spectrometry. Infection and immunity **67:**327-336.

59. **Marques MA, Chitale S, Brennan PJ, Pessolani MC.** 1998. Mapping and identification of the major cell wall-associated components of *Mycobacterium leprae*. Infection and immunity **66:**2625-2631.

60. **Porcella SF, Belland RJ, Judd RC.** 1996. Identification of an EF-Tu protein that is periplasm-associated and processed in *Neisseria gonorrhoeae*. Microbiology (Reading, England) **142 (Pt 9):**2481-2489.

61. **Granato D, Bergonzelli GE, Pridmore RD, Marvin L, Rouvet M, Corthesy-Theulaz IE.** 2004. Cell surface-associated elongation factor Tu mediates the attachment of *Lactobacillus johnsonii* NCC533 (La1) to human intestinal cells and mucins. Infection and immunity **72:**2160-2169.

62. **Schaumburg J, Diekmann O, Hagendorff P, Bergmann S, Rohde M, Hammerschmidt S, Jansch L, Wehland J, Karst U.** 2004. The cell wall subproteome of *Listeria monocytogenes*. Proteomics **4:**2991-3006.

63. **Kunert A, Losse J, Gruszin C, Huhn M, Kaendler K, Mikkat S, Volke D, Hoffmann R, Jokiranta TS, Seeberger H, Moellmann U, Hellwage J, Zipfel PF.** 2007. Immune evasion of the human pathogen *Pseudomonas aeruginosa*: elongation factor Tuf is a factor H and plasminogen binding protein. Journal of immunology (Baltimore, Md. : 1950) **179:**2979-2988.

64. **Barel M, Hovanessian AG, Meibom K, Briand JP, Dupuis M, Charbit A.** 2008. A novel receptor - ligand pathway for entry of *Francisella tularensis* in monocyte-like THP-1 cells: interaction between surface nucleolin and bacterial elongation factor Tu. BMC microbiology **8:**145.

65. **Kraal B, Lippmann C, Kleanthous C.** 1999. Translational regulation by modifications of the elongation factor Tu. Folia microbiologica **44:**131-141.

66. **Villa E, Sengupta J, Trabuco LG, LeBarron J, Baxter WT, Shaikh TR, Grassucci RA, Nissen P, Ehrenberg M, Schulten K, Frank J.** 2009. Ribosome-induced changes in elongation factor Tu conformation control GTP hydrolysis. Proceedings of the National Academy of Sciences of the United States of America **106:**1063-1068.

67. **Cruz JW, Rothenbacher FP, Maehigashi T, Lane WS, Dunham CM, Woychik NA.** 2014. Doc toxin is a kinase that inactivates elongation factor Tu. The Journal of biological chemistry **289:**7788-7798.

68. **Castro-Roa D, Garcia-Pino A, De Gieter S, van Nuland NA, Loris R, Zenkin N.** 2013. The Fic protein Doc uses an inverted substrate to phosphorylate and inactivate EF-Tu. Nature chemical biology **9:**811-817.

69. **Lippmann C, Lindschau C, Vijgenboom E, Schroder W, Bosch L, Erdmann VA.** 1993. Prokaryotic elongation factor Tu is phosphorylated *in vivo*. The Journal of biological chemistry **268:**601-607.

70. **L'Italien JJ, Laursen RA.** 1979. Location of the site of methylation in elongation factor Tu. FEBS letters **107:**359-362.

71. **Van Noort JM, Kraal B, Sinjorgo KM, Persoon NL, Johanns ES, Bosch L.** 1986. Methylation *in vivo* of elongation factor EF-Tu at lysine-56 decreases the rate of tRNA-dependent GTP hydrolysis. European journal of biochemistry / FEBS **160:**557-561.

72. **Palmer SO, Rangel EY, Montalvo AE, Tran AT, Ferguson KC, Bullard JM.** 2013. Cloning and characterization of EF-Tu and EF-Ts from *Pseudomonas aeruginosa*. BioMed research international **2013:**585748.

73. **Martin JL, McMillan FM.** 2002. SAM (dependent) I AM: the *S*-adenosylmethionine-dependent methyltransferase fold. Current opinion in structural biology **12:**783-793.

74. **Wilson GG, Murray NE.** 1991. Restriction and modification systems. Annual review of genetics **25:**585-627.

75. **Garcia-Fontana C, Corral Lugo A, Krell T.** 2014. Specificity of the CheR2 methyltransferase in *Pseudomonas aeruginosa* is directed by a C-terminal pentapeptide in the McpB chemoreceptor. Science signaling **7:**ra34.

76. **Schmidt J, Musken M, Becker T, Magnowska Z, Bertinetti D, Moller S, Zimmermann B, Herberg FW, Jansch L, Haussler S.** 2011. The *Pseudomonas*

aeruginosa chemotaxis methyltransferase CheR1 impacts on bacterial surface sampling. PloS one **6:**e18184.

77. **Schubert HL, Blumenthal RM, Cheng X.** 2003. Many paths to methyltransfer: a chronicle of convergence. Trends in biochemical sciences **28:**329-335.

78. **Cantoni GL.** 1975. Biological methylation: selected aspects. Annual review of biochemistry **44:**435-451.

79. **Bennett BD, Kimball EH, Gao M, Osterhout R, Van Dien SJ, Rabinowitz JD.** 2009. Absolute metabolite concentrations and implied enzyme active site occupancy in *Escherichia coli*. Nature chemical biology **5:**593-599.

80. **Mandsberg LF, Ciofu O, Kirkby N, Christiansen LE, Poulsen HE, Hoiby N.** 2009. Antibiotic resistance in *Pseudomonas aeruginosa* strains with increased mutation frequency due to inactivation of the DNA oxidative repair system. Antimicrobial agents and chemotherapy **53:**2483-2491.

81. **Henrichfreise B, Wiegand I, Pfister W, Wiedemann B.** 2007. Resistance mechanisms of multiresistant *Pseudomonas aeruginosa* strains from Germany and correlation with hypermutation. Antimicrobial agents and chemotherapy **51:**4062-4070.

82. **Choi KH, Kumar A, Schweizer HP.** 2006. A 10-min method for preparation of highly electrocompetent *Pseudomonas aeruginosa* cells: application for DNA fragment transfer between chromosomes and plasmid transformation. Journal of microbiological methods **64:**391-397.

83. **Pospiech A, Neumann B.** 1995. A versatile quick-prep of genomic DNA from Gram-positive bacteria. Trends in genetics : TIG **11:**217-218.

84. **Schweizer HP.** 1991. *Escherichia-Pseudomonas* shuttle vectors derived from pUC18/19. Gene **97:**109-121.

85. **Quenee L, Lamotte D, Polack B.** 2005. Combined *sacB*-based negative selection and *cre-lox* antibiotic marker recycling for efficient gene deletion in *Pseudomonas aeruginosa*. BioTechniques **38:**63-67.

86. **Wargo MJ, Ho TC, Gross MJ, Whittaker LA, Hogan DA.** 2009. GbdR regulates *Pseudomonas aeruginosa plcH* and *pchP* transcription in response to choline catabolites. Infection and immunity **77:**1103-1111.

87. **Smith EE, Buckley DG, Wu Z, Saenphimmachak C, Hoffman LR, D'Argenio DA, Miller SI, Ramsey BW, Speert DP, Moskowitz SM, Burns JL, Kaul R, Olson MV.** 2006. Genetic adaptation by *Pseudomonas aeruginosa* to the airways of cystic fibrosis patients. Proceedings of the National Academy of Sciences of the United States of America **103:**8487-8492.

88. **Filiatrault MJ, Picardo KF, Ngai H, Passador L, Iglewski BH.** 2006. Identification of *Pseudomonas aeruginosa* genes involved in virulence and anaerobic growth. Infection and immunity **74:**4237-4245.

89. **Jacobs MA, Alwood A, Thaipisuttikul I, Spencer D, Haugen E, Ernst S, Will O, Kaul R, Raymond C, Levy R, Chun-Rong L, Guenthner D, Bovee D, Olson MV, Manoil C.** 2003. Comprehensive transposon mutant library of *Pseudomonas aeruginosa*. Proceedings of the National Academy of Sciences of the United States of America **100:**14339-14344.

90. **Liberati NT, Urbach JM, Miyata S, Lee DG, Drenkard E, Wu G, Villanueva J, Wei T, Ausubel FM.** 2006. An ordered, nonredundant library of *Pseudomonas*

aeruginosa strain PA14 transposon insertion mutants. Proceedings of the National Academy of Sciences of the United States of America **103:**2833-2838.

91. **Winsor GL, Lam DK, Fleming L, Lo R, Whiteside MD, Yu NY, Hancock RE, Brinkman FS.** 2011. *Pseudomonas* Genome Database: improved comparative analysis and population genomics capability for *Pseudomonas* genomes. Nucleic acids research **39:**D596-600.

92. **Lathe WC, 3rd, Bork P.** 2001. Evolution of *tuf* genes: ancient duplication, differential loss and gene conversion. FEBS letters **502:**113-116.

93. **Baensch M, Frank R, Kohl J.** 1998. Conservation of the amino-terminal epitope of elongation factor Tu in eubacteria and Archaea. Microbiology (Reading, England) **144 (Pt 8):**2241-2246.

94. **Yang L, Jelsbak L, Marvig RL, Damkiaer S, Workman CT, Rau MH, Hansen SK, Folkesson A, Johansen HK, Ciofu O, Hoiby N, Sommer MO, Molin S.** 2011. Evolutionary dynamics of bacteria in a human host environment. Proceedings of the National Academy of Sciences of the United States of America **108:**7481-7486.

95. **Rau MH, Marvig RL, Ehrlich GD, Molin S, Jelsbak L.** 2012. Deletion and acquisition of genomic content during early stage adaptation of *Pseudomonas aeruginosa* to a human host environment. Environmental microbiology **14:**2200-2211.

96. **Predescu D, Ihida K, Predescu S, Palade GE.** 1996. The vascular distribution of the platelet-activating factor receptor. European journal of cell biology **69:**86-98.

97. **Brocheriou I, Stengel D, Mattsson-Hulten L, Stankova J, Rola-Pleszczynski M, Koskas F, Wiklund O, Le Charpentier Y, Ninio E.** 2000. Expression of platelet-activating factor receptor in human carotid atherosclerotic plaques: relevance to progression of atherosclerosis. Circulation **102:**2569-2575.

98. **Warren MJ, Jennings MP.** 2003. Identification and characterization of *pptA*: a gene involved in the phase-variable expression of phosphorylcholine on pili of *Neisseria meningitidis*. Infection and immunity **71:**6892-6898.

99. **Nyyssola A, Reinikainen T, Leisola M.** 2001. Characterization of glycine sarcosine *N*-methyltransferase and sarcosine dimethylglycine *N*-methyltransferase. Applied and environmental microbiology **67:**2044-2050.

100. **Ben Haj Khalifa A, Moissenet D, Vu Thien H, Khedher M.** 2011. [Virulence factors in *Pseudomonas aeruginosa*: mechanisms and modes of regulation]. Annales de biologie clinique **69:**393-403.

101. **Bertani G.** 1951. Studies on lysogenesis. I. The mode of phage liberation by lysogenic *Escherichia coli*. Journal of bacteriology **62:**293-300.

102. **Qiu D, Damron FH, Mima T, Schweizer HP, Yu HD.** 2008. PBAD-based shuttle vectors for functional analysis of toxic and highly regulated genes in *Pseudomonas* and *Burkholderia spp*. and other bacteria. Applied and environmental microbiology **74:**7422-7426.

103. **Studier FW.** 2005. Protein production by auto-induction in high density shaking cultures. Protein expression and purification **41:**207-234.

104. **Roelofs KG, Wang J, Sintim HO, Lee VT.** 2011. Differential radial capillary action of ligand assay for high-throughput detection of protein-metabolite

interactions. Proceedings of the National Academy of Sciences of the United States of America **108:**15528-15533.

105. **Schneider CA, Rasband WS, Eliceiri KW.** 2012. NIH Image to ImageJ: 25 years of image analysis. Nature methods **9:**671-675.

106. **Davis MR, Jr., Muszynski A, Lollett IV, Pritchett CL, Carlson RW, Goldberg JB.** 2013. Identification of the mutation responsible for the temperature-sensitive lipopolysaccharide O-antigen defect in the *Pseudomonas aeruginosa* cystic fibrosis isolate 2192. Journal of bacteriology **195:**1504-1514.

107. **Choi KH, Schweizer HP.** 2006. mini-Tn7 insertion in bacteria with single attTn7 sites: example *Pseudomonas aeruginosa*. Nature protocols **1:**153-161.

108. **Choi KH, Mima T, Casart Y, Rholl D, Kumar A, Beacham IR, Schweizer HP.** 2008. Genetic tools for select-agent-compliant manipulation of *Burkholderia pseudomallei*. Applied and environmental microbiology **74:**1064-1075.

109. **Elias JE, Gygi SP.** 2007. Target-decoy search strategy for increased confidence in large-scale protein identifications by mass spectrometry. Nat Meth **4:**207-214.

110. **Xu P, Duong DM, Peng J.** 2009. Systematical Optimization of Reverse-Phase Chromatography for Shotgun Proteomics. Journal of Proteome Research **8:**3944-3950.

111. **Seyfried NT, Gozal YM, Donovan LE, Herskowitz JH, Dammer EB, Xia Q, Ku L, Chang J, Duong DM, Rees HD, Cooper DS, Glass JD, Gearing M, Tansey MG, Lah JJ, Feng Y, Levey AI, Peng J.** 2012. Quantitative Analysis of the Detergent-Insoluble Brain Proteome in Frontotemporal Lobar Degeneration Using SILAC Internal Standards. Journal of Proteome Research **11:**2721-2738.

112. **Gozal YM, Seyfried NT, Gearing M, Glass JD, Heilman CJ, Wuu J, Duong DM, Cheng D, Xia Q, Rees HD, Fritz JJ, Cooper DS, Peng J, Levey AI, Lah JJ.** 2011. Aberrant septin 11 is associated with sporadic frontotemporal lobar degeneration. Mol Neurodegener **6:**82.

113. **Damron FH, Owings JP, Okkotsu Y, Varga JJ, Schurr JR, Goldberg JB, Schurr MJ, Yu HD.** 2012. Analysis of the *Pseudomonas aeruginosa* regulon controlled by the sensor kinase KinB and sigma factor RpoN. Journal of bacteriology **194:**1317-1330.

114. **Wurtzel O, Yoder-Himes DR, Han K, Dandekar AA, Edelheit S, Greenberg EP, Sorek R, Lory S.** 2012. The single-nucleotide resolution transcriptome of *Pseudomonas aeruginosa* grown in body temperature. PLoS pathogens **8:**e1002945.

115. **Barbier M, Damron FH, Bielecki P, Suarez-Diez M, Puchalka J, Alberti S, Dos Santos VM, Goldberg JB.** 2014. From the Environment to the Host: Re-Wiring of the Transcriptome of *Pseudomonas aeruginosa* from 22 degrees C to 37 degrees C. PloS one **9:**e89941.

116. **Termine E, Michel GP.** 2009. Transcriptome and secretome analyses of the adaptive response of *Pseudomonas aeruginosa* to suboptimal growth temperature. International microbiology : the official journal of the Spanish Society for Microbiology **12:**7-12.

117. **Soding J, Biegert A, Lupas AN.** 2005. The HHpred interactive server for protein homology detection and structure prediction. Nucleic acids research **33:**W244-248.

118. **Burgie ES, Holden HM.** 2008. Three-dimensional structure of DesVI from *Streptomyces venezuelae*: a sugar *N,N*-dimethyltransferase required for dTDP-desosamine biosynthesis. Biochemistry **47:**3982-3988.

119. **Wilson JR, Jing C, Walker PA, Martin SR, Howell SA, Blackburn GM, Gamblin SJ, Xiao B.** 2002. Crystal structure and functional analysis of the histone methyltransferase SET7/9. Cell **111:**105-115.

120. **Gur E, Biran D, Ron EZ.** 2011. Regulated proteolysis in Gram-negative bacteria--how and when? Nature reviews. Microbiology **9:**839-848.

121. **Battesti A, Gottesman S.** 2013. Roles of adaptor proteins in regulation of bacterial proteolysis. Current opinion in microbiology **16:**140-147.

122. **Salih M, Mytilinaios I, Schofield HK, Lambert RJ.** 2012. Modelling of bacterial growth with shifts in temperature using automated methods with *Listeria monocytogenes* and *Pseudomonas aeruginosa* as examples. International journal of food microbiology **155:**29-35.

123. **Lanouette S, Mongeon V, Figeys D, Couture JF.** 2014. The functional diversity of protein lysine methylation. Molecular systems biology **10:**724.

124. **Goldberg JB, Dahnke T.** 1992. *Pseudomonas aeruginosa* AlgB, which modulates the expression of alginate, is a member of the NtrC subclass of prokaryotic regulators. Molecular microbiology **6:**59-66.

125. **Deretic V, Dikshit R, Konyecsni WM, Chakrabarty AM, Misra TK.** 1989. The *algR* gene, which regulates mucoidy in *Pseudomonas aeruginosa,* belongs to a class of environmentally responsive genes. Journal of bacteriology **171:**1278-1283.

126. **Baynham PJ, Brown AL, Hall LL, Wozniak DJ.** 1999. *Pseudomonas aeruginosa* AlgZ, a ribbon-helix-helix DNA-binding protein, is essential for alginate synthesis and *algD* transcriptional activation. Molecular microbiology **33:**1069-1080.

127. **DeVries CA, Ohman DE.** 1994. Mucoid-to-nonmucoid conversion in alginate-producing *Pseudomonas aeruginosa* often results from spontaneous mutations in *algT*, encoding a putative alternate sigma factor, and shows evidence for autoregulation. Journal of bacteriology **176:**6677-6687.

128. **Hershberger CD, Ye RW, Parsek MR, Xie ZD, Chakrabarty AM.** 1995. The *algT* (*algU*) gene of *Pseudomonas aeruginosa*, a key regulator involved in alginate biosynthesis, encodes an alternative sigma factor (sigma E). Proceedings of the National Academy of Sciences of the United States of America **92:**7941-7945.

129. **Martin DW, Schurr MJ, Mudd MH, Govan JR, Holloway BW, Deretic V.** 1993. Mechanism of conversion to mucoidy in *Pseudomonas aeruginosa* infecting cystic fibrosis patients. Proceedings of the National Academy of Sciences of the United States of America **90:**8377-8381.

130. **Ramsey DM, Wozniak DJ.** 2005. Understanding the control of *Pseudomonas aeruginosa* alginate synthesis and the prospects for management of chronic infections in cystic fibrosis. Molecular microbiology **56:**309-322.

131. **Rowen DW, Deretic V.** 2000. Membrane-to-cytosol redistribution of ECF sigma factor AlgU and conversion to mucoidy in *Pseudomonas aeruginosa* isolates from cystic fibrosis patients. Molecular microbiology **36:**314-327.

132. **Ciofu O, Lee B, Johannesson M, Hermansen NO, Meyer P, Hoiby N, Scandinavian Cystic Fibrosis Study C.** 2008. Investigation of the *algT* operon sequence in mucoid and non-mucoid *Pseudomonas aeruginosa* isolates from 115 Scandinavian patients with cystic fibrosis and in 88 in vitro non-mucoid revertants. Microbiology (Reading, England) **154:**103-113.

133. **Qiu D, Eisinger VM, Rowen DW, Yu HD.** 2007. Regulated proteolysis controls mucoid conversion in *Pseudomonas aeruginosa*. Proceedings of the National Academy of Sciences of the United States of America **104:**8107-8112.

134. **Damron FH, Davis MR, Jr., Withers TR, Ernst RK, Goldberg JB, Yu G, Yu HD.** 2011. Vanadate and triclosan synergistically induce alginate production by *Pseudomonas aeruginosa* strain PAO1. Molecular microbiology **81:**554-570.

135. **Rodrigue A, Quentin Y, Lazdunski A, Mejean V, Foglino M.** 2000. Two-component systems in *Pseudomonas aeruginosa*: why so many? Trends in microbiology **8:**498-504.

136. **Damron FH, Qiu D, Yu HD.** 2009. The *Pseudomonas aeruginosa* sensor kinase KinB negatively controls alginate production through AlgW-dependent MucA proteolysis. Journal of bacteriology **191:**2285-2295.

137. **Ma S, Selvaraj U, Ohman DE, Quarless R, Hassett DJ, Wozniak DJ.** 1998. Phosphorylation-independent activity of the response regulators AlgB and AlgR in promoting alginate biosynthesis in mucoid *Pseudomonas aeruginosa*. Journal of bacteriology **180:**956-968.

138. **Chand NS, Lee JS, Clatworthy AE, Golas AJ, Smith RS, Hung DT.** 2011. The sensor kinase KinB regulates virulence in acute *Pseudomonas aeruginosa* infection. Journal of bacteriology **193:**2989-2999.

139. **Mathee K, Ciofu O, Sternberg C, Lindum PW, Campbell JI, Jensen P, Johnsen AH, Givskov M, Ohman DE, Molin S, Hoiby N, Kharazmi A.** 1999. Mucoid conversion of *Pseudomonas aeruginosa* by hydrogen peroxide: a mechanism for virulence activation in the cystic fibrosis lung. Microbiology (Reading, England) **145 (Pt 6):**1349-1357.